Received: 13 April 2021 | Revised: 16 June 2021 | Accepted: 24 August 2021

DOI: 10.1002/wrna.1692

ADVANCED REVIEW

WIREs RNA WILEY

Alternative polyadenylation: An enigma of transcript length variation in health and disease

Neeraja K. Mohanan[1,2] | **Feba Shaji**[1,3] | **Ganesh R. Koshre**[1,2] | **Rakesh S. Laishram**[1]

[1]Cardiovascular and Diabetes Biology Group, Rajiv Gandhi Centre for Biotechnology, Trivandrum, India

[2]Manipal Academy of Higher Education, Manipal, India

[3]Regional Centre for Biotechnology, Faridabad, India

Correspondence
Rakesh S. Laishram, Cardiovascular and Diabetes Biology Group, Rajiv Gandhi Centre for Biotechnology, Thycaud Post, Poojappura, Trivandrum 695014, India.
Email: laishram@rgcb.res.in

Funding information
DST SWARNAJAYANTI FELLOWSHIP, Grant/Award Number: SB/SJF/2019-20/09; Science and Engineering Research Board, Grant/Award Number: CRG/2019/003230

Edited by: Purusharth Rajyaguru, Associate Editor and Jeff Wilusz, Editor-in-Chief

Abstract

Alternative polyadenylation (APA) is a molecular mechanism during a pre-mRNA processing that involves usage of more than one polyadenylation site (PA-site) generating transcripts of varying length from a single gene. The location of a PA-site affects transcript length and coding potential of an mRNA contributing to both mRNA and protein diversification. This variation in the transcript length affects mRNA stability and translation, mRNA subcellular and tissue localization, and protein function. APA is now considered as an important regulatory mechanism in the pathophysiology of human diseases. An important consequence of the changes in the length of 3′-untranslated region (UTR) from disease-induced APA is altered protein expression. Yet, the relationship between 3′-UTR length and protein expression remains a paradox in a majority of diseases. Here, we review occurrence of APA, mechanism of PA-site selection, and consequences of transcript length variation in different diseases. Emerging evidence reveals coordinated involvement of core RNA processing factors including poly(A) polymerases in the PA-site selection in diseases-associated APAs. Targeting such APA regulators will be therapeutically significant in combating drug resistance in cancer and other complex diseases.

This article is categorized under:

RNA Processing > 3′ End Processing

RNA in Disease and Development > RNA in Disease

Translation > Regulation

KEYWORDS

3′-UTR length, alternative polyadenylation, cancer, cleavage and polyadenylation factors, drug resistance, human diseases, PA-site selection, poly(A) polymerases, Star-PAP

1 | INTRODUCTION

Almost all eukaryotic messenger RNAs (mRNAs) undergo polyadenylation at the 3′-end in two concerted steps—endonucleolytic cleavage followed by addition of a poly(A) tail (PA-tail) in the nucleus (Colgan & Manley, 1997; Neve et al., 2017; Shi & Manley, 2015). Polyadenylation is carried out by poly(A) polymerases (PAPs) in a cleavage and

Neeraja K Mohanan and Feba Shaji authors contributed equally to this work.

polyadenylation (CPA) complex comprised of subunits of CPA specificity factor (CPSF), Cleavage stimulatory factor (CSTF), cleavage factor (CFIm) and (CFIIm), Poly(A) binding protein (PABPN1), and Symplekin as core components (Mandel et al., 2008; J. Zhao et al., 1999). The basic mechanism of 3′-end processing involves recognition of a PA-signal by CPSF subunits, assembly of a CPA complex, endonucleoytic cleavage, and subsequent PA (Neve et al., 2017). List of core CPA factors and their role in the 3′-end processing reaction is detailed in Table 1. Interestingly, over 70% of human genes have multiple polyadenylation sites (PA-sites) at the 3′-UTR that are alternately used for polyadenylation (Derti et al., 2012; Hoque et al., 2013; B. Tian et al., 2005). This alternate usage of PA-sites (known as alternative polyadenylation, APA) generates more than one mRNA isoform with different lengths. The choice of a PA-site is an important determinant of transcript length that can affect both mRNA and protein diversification (Ren et al., 2020; B. Tian & Manley, 2013; Y. Zhang et al., 2021).

When PA-site(s) located upstream of a terminal exon in the coding region or intronic region are used, the APA isoform alters the primary structure of the protein. This type of APA is broadly termed as coding region APA (or CR-APA). CR-APA results in a C-terminally truncated protein that has changed or lost the original protein function (Dafne Campigli Di Giammartino et al., 2011; Neve et al., 2017; B. Tian & Manley, 2017). CR-APA can also affect nuclear-cytoplasmic localization on limited mRNAs (Fischl et al., 2019). On the other hand, when PA-sites located in the terminal exon downstream of the translation termination site are used, the APA isoform alters the transcript length but retains the primary structure of the protein after translation. This type of APA is termed as UTR-APA. The difference in the 3′-UTR length from UTR-APA affects mRNA stability, translation efficiency, mRNA subcellular or tissue localization, and protein interaction and function (Dafne Campigli Di Giammartino et al., 2011; Neve et al., 2017; B. Tian & Manley, 2017). We refer to the PA-site proximal to the transcription start site at the 3′-UTR as "proximal" PA-site and subsequent downstream PA-sites at the 3′-UTR as "distal" PA-site, and the PA-site(s) upstream of the terminal exon (internal PA-sites) are described based on the location of the PA-site (intronic or cds) in the text.

APA is involved in the regulation of a variety of cellular processes including development, tissue specificity, stress response, cellular growth, immune function, and neuronal activity (Chang et al., 2018; Chuvpilo et al., 1999; Flavell et al., 2008; Hollerer et al., 2016; Hu et al., 2017; Lianoglou et al., 2013; Sandberg et al., 2008; H. Zhang et al., 2005). Emerging studies now show role of APA in the pathophysiology of a number of human diseases (Abdel Wahab et al., 1998; Creemers et al., 2016; Mayr & Bartel, 2009; Patel et al., 2019; Riaz et al., 2016; Soetanto et al., 2016; P. Tian et al., 2014). Analysis of occurrence of APA in different human diseases from published literature shows a lopsided report on cancer (>60%) followed far behind by neurological (13%), immunological (5%), and musculoskeletal (5%) diseases (Figure 1a). Significant numbers of studies on APA also exists in hematologic (4%), cardiovascular (3%), endocrine (2%), and others including developmental, aging-related, or genetic diseases (Figure 1). Between the two types of APA, CR-APA is primarily reported in cancer, neurological, endocrine, immunological and muscular diseases, whereas UTR-APA is widespread in most diseases (Figure 1). While APA can increase or decrease a transcript length, PA-site switch in a majority of diseases primarily results in shortening of 3′-UTR (Dickson et al., 2013; Graham et al., 2007; Lembo et al., 2012; Mayr & Bartel, 2009; J. Y. Park et al., 2011; Patel et al., 2019; Riaz et al., 2016; Shell et al., 2005; Soetanto et al., 2016; P. Tian et al., 2014; Xia et al., 2014; Yan et al., 2018). A key consequence of this 3′-UTR shortening is the increase stability of the mRNA and the resultant protein expression. As opposed to this, several mRNAs with longer 3′-UTRs can express higher protein than the shorter APA isoforms in many diseases (Lemmers et al., 2010; L. Li et al., 2014; H. J. Park et al., 2018; Rhinn et al., 2012; Soetanto et al., 2016; Stacey et al., 2011; A. Sudheesh et al., 2019; Thivierge et al., 2018; X. Wang et al., 2015; Zhou et al., 2012). This further complicates our understanding of the effect of 3′-UTR length variation on protein expression. Here, we review occurrence of APA in different human diseases, and molecular mechanism of PA-site selection and consequences of mRNA and protein diversification in disease-associated APA.

2 | IMPLICATION OF DISEASE-INDUCED APA IN GENE EXPRESSION AND PROTEIN FUNCTION

2.1 | Functional and nonfunctional protein variants (protein truncation)

CR-APA generates mRNA isoforms that has lost a part of a coding region. These transcripts translate into truncated protein variants with altered function, loss of function, or aberrant protein directed for degradation (S. H. Lee et al., 2018; I. Singh et al., 2018; X. Zhang et al., 2007). Such truncated proteins can act antagonistically to the original

TABLE 1 Core processing factors and their role in cleavage and polyadenylation reaction

Processing factors	Subunits	Function	References
Cleavage and polyadenylation specificity factor (CPSF)	CPSF160 (CPSF1)	Previously considered as the PA-signal recognition factor. Involved in interaction with CSTF complex (via direct contact CSTF3) for stable CPA complex assembly. Also, functionally interacts with PAP	Keller et al. (1991), Murthy and Manley (1995)
	CPSF100 (CPSF2)	Precise role in the 3′-end processing is unclear, involved in the assembly of CPA complex	Jenny et al. (1994), Kolev et al. (2008)
	CPSF73 (CPSF3)	It is the endonuclease in the CPSF complex, required for cleavage at the PA-site	Kolev et al. (2008), Mandel et al. (2006), Ryan et al. (2004)
	CPSF30 (CPSF4)	Required for recognition of the PA-signal along with WDR33	Chan et al. (2014), Clerici et al. (2018), Shimberg et al. (2016), Y. Sun et al. (2018)
	hFip1	hFip1 binds PAP and directs it toward the PA-site	Kaufmann et al. (2004)
	WDR33	Directly binds the PA-signal on the pre-mRNA 3′-UTR in conjunction with CPSF4	Chan et al. (2014), Clerici et al. (2018), Schönemann et al. (2014), Shi et al. (2009), Y. Sun et al. (2018)
Cleavage stimulation factor (CSTF)	CstF50 (CSTF1)	CSTF1 interacts with the Pol II C-terminal domain coupling 3′-end processing to transcription	McCracken et al. (1997), Takagaki and Manley (1994)
	CstF64 (CSTF2)	Binds downstream U/GU-rich element and cooperates with CPSF complex facilitating assembly of CPA complex	MacDonald et al. (1994), Perez Canadillas and Varani (2003), Takagaki et al. (1992), Takagaki and Manley (1997)
	CstF77 (CSTF3)	CSTF3 bridges CSTF1 and CSTF2 and associates with CPSF1 to cooperate in the CPA complex assembly	Murthy and Manley (1995), Takagaki and Manley (1994)
Cleavage factor Im (CFIm)	CIm25 (CPSF5)	Binds to USE containing U(G/A)UA motif and cooperates with CPSF in the CPA complex assembly	Brown and Gilmartin (2003), Ruegsegger et al. (1996), Q. Yang et al. (2011)
	CFIm68 (CPSF6)	Interacts with CPSF5 and enhances RNA binding of CFIm complex. Also directly interacts with hFip1	Brown and Gilmartin (2003), Q. Yang et al. (2011), Y. Zhu et al. (2018)
	CFIm59 (CPSF7)	Cooperates with CPSF5 for CFIm complex RNA interaction. Like CPSF6, CPSF7 directly interacts with hFip1	Ruegsegger et al. (1996), Y. Zhu et al. (2018)
Cleavage factor IIm (CFIIm)	hPcf11	Links 3′-end cleavage with Pol II transcription termination	West and Proudfoot (2008)
	hClp1	Links CFIm and CPSF within the CPA complex	de Vries et al. (2000)
Poly A binding protein (PABPN1)	—	Binds and stabilizes the PA-tail, and controls PA-tail length	Deo et al. (1999), Kerwitz et al. (2003), Kuhn et al. (2009), Kuhn and Wahle (2004), Wahle (1991)
Poly(A) polymerase (PAP)	—	Adds 200–250 adenosines in template independent manner on nascent mRNA inside the nucleus, also requires for cleavage reaction	Laishram and Anderson (2010), Raabe et al. (1991), Wahle (1991), Wahle et al. (1991)
Symplekin (SYMPK)	—	Acts as a scaffold to assemble the CPA complex	Takagaki and Manley (2000), K. Xiang et al. (2010)

Note: This table shows core CPA factors and their mechanistic function in the general 3′-end cleavage and polyadenylation reaction.

protein (D. C. Di Giammartino et al., 2014; S. H. Lee et al., 2018; Locke et al., 2011; Mueller et al., 2016) or can function entirely different from the full-length protein (Mueller et al., 2016; Sommer et al., 2014). Moreover, CR-APA induced protein truncations can also result in dominant negative proteins that inhibit the function of the full-length protein (Ni & Kuperwasser, 2016; I. Singh et al., 2018).

2.2 | mRNA subcellular localization

Both CR-APA and UTR-APA can affect mRNA localization in the cell including nucleo-cytoplasmic localization or localizations in different subcellular compartments (Ciolli Mattioli et al., 2019; Fischl et al., 2019; Rhinn et al., 2012). For example, while short UTR mRNA isoform of a neuronal gene *BDNF* localizes in soma, longer *BDNF* isoform localizes in dendrites (Baj et al., 2011; Lau et al., 2010). Globally longer mRNA isoforms tend to be in the nucleus than in the cytoplasm. A progressive shift toward shorter UTR isoform from UTR-APA increases the cytoplasmic fraction and translation (Fischl et al., 2019; Neve et al., 2016; Solnestam et al., 2012). The nuclear-cytoplasmic localization of APA isoforms is controlled by nuclear export, and stability difference of APA isoforms in the two subcellular compartments (S. Chen et al., 2019; Neve et al., 2016; Ruepp et al., 2009). However, the *cis*-elements or RNA binding proteins (RBPs) that drive such subcellular targeting are yet to be defined.

2.3 | mRNA tissue specific expression

UTR-APA affects tissue specificities of mRNA isoform expression. For example, a neuronal gene *HTT* encoded shorter UTR mRNA isoform is expressed in testes, muscle and kidney, whereas the longer UTR isoform is enriched in the brain, breast and ovary (Romo et al., 2017). Global study has shown a biased tissue preference of proximal versus distal PA-site usage on distinct human tissues (E. T. Wang et al., 2008; H. Zhang et al., 2005). While neuronal tissues favor longer isoforms, testes or blood prefer shorter isoforms (Lianoglou et al., 2013; Miura et al., 2013; H. Zhang et al., 2005). The actual mechanism of tissue preference of APA isoforms is still unclear and it likely involves *cis*-elements and differential expression of trans-acting APA regulators in different tissues. Testes specific mRNAs largely lacks AAUAAA hexamer canonical PA-signal sequence and requires CSTF2 paralogue CSTF2τ expression for processing (W. Li et al., 2012; Liu et al., 2007; Wallace et al., 1999; Yao et al., 2013; H. Zhang et al., 2005). In the brain, there is prevalence of GU-rich and U-rich sequences downstream of the mRNA PA-site (H. Zhang et al., 2005). However, high nPTB level in the brain can compete with CSTF2τ regulating PA-site choice (Castelo-Branco et al., 2004; H. Zhang et al., 2005). In addition, the presence of U1A protein and the brain specific CSTF2 isoform (CSTF2β) is likely to play an important role in PA-site usage in the brain (Miura et al., 2013; Shankarling et al., 2009; H. Zhang et al., 2005).

2.4 | Protein interaction and function

UTR-APA can also alter interacting partners of the translated protein of an APA isoform affecting the protein function or localization. The long 3′-UTR mRNA isoform of *CDC47* mRNA acts as a scaffold that recruits HUR and SET proteins that results in HUR-SET interaction with CDC47. It then promotes CDC47 translocation to the plasma membrane (Berkovits & Mayr, 2015; W. Ma & Mayr, 2018). However, CDC47 translated from the short UTR mRNA isoform does not assemble HUR-SET complex and is retained in the endoplasmic reticulum. The same mechanism is seen in *CD44*, *ITGA1*, *TSPAN13*, and *TNFRSF13C* mRNAs. In parallel, 3′-UTR length dependent protein interaction is also reported in *BIRC3* mRNA that regulates BIRC3 protein function (S. H. Lee & Mayr, 2019).

2.5 | mRNA stability and translation (protein expression)

UTR-APA widely affects stability and translation of different mRNA isoforms. There is an inverse relationship between 3′-UTR length and resultant protein expression (Creemers et al., 2016; Fu et al., 2018; Liaw et al., 2013; Mayr & Bartel, 2009; Patel et al., 2019; Riaz et al., 2016). Thus, shorter mRNA isoforms have higher protein expression whereas longer isoforms are associated with reduced protein levels (Abdel Wahab et al., 1998; M. Chen et al., 2018; Kreth

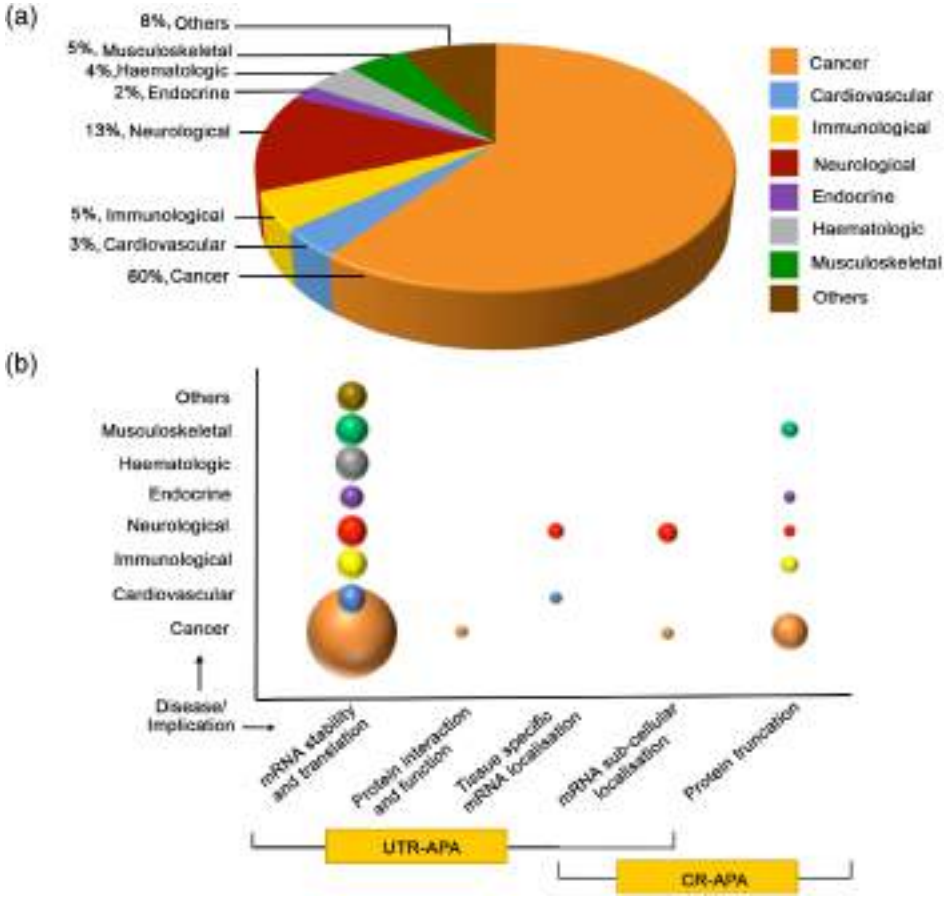

FIGURE 1 Distribution of reports on APA and their implications in different human diseases. (a) Pie chart showing distribution of APA occurrence in various human diseases. Chart was prepared from exhaustive literature search of research articles published in index journals on APA and its relevance in different human diseases. (We considered only research articles for the plot. We have divided human diseases into eight main disease categories as indicated. "Other" diseases include genetic, developmental, and aging-related diseases that are marginally represented in the distribution. We obtained around 250-research article related to APA in different diseases that is distributed unevenly among different disease categories as indicated. (Many reference articles from the pie chart that has no direct citation in the text are omitted from the reference list in the text considering limited space available in the journal). (b) Bubble plot showing distribution of APA occurrence in human diseases with respect to APA implications in gene expression and protein function. We plotted three variables, *x*-axis represents implications of APA in expression or function of disease causing genes, *y*-axis represents human diseases in which APA has been reported; and size of the bubble represents frequency or number of reports pertaining to each category

et al., 2013; S. M. Park et al., 2016; L. Wang, Chen, et al., 2020; Z. Yang & Kaye, 2009). In the contrary, a number of mRNAs with lengthened 3′-UTR are translationally more efficient than the shorter counterparts (Lemmers et al., 2010; L. Li et al., 2014; Patel et al., 2019; Rhinn et al., 2012; A. Sudheesh et al., 2019; Thivierge et al., 2018) indicating a paradox effect of 3′-UTR length on protein expression. Key implications of both CR-APA and UTR-APA on mRNA and proteins in different diseases are detailed in Figure 2.

3 | MECHANISM OF THE PARADOX OF 3′-UTR LENGTH VERSUS PROTEIN EXPRESSION

3′-UTR length influences mRNA abundance, translation, or both mRNA abundance and translation. mRNA 3′-UTR harbors miRNA regulatory sites, *cis*-RNA regulatory elements (AU-rich, U-rich, and GU-rich elements), trans-acting RBPs sites, and other regulatory sequences (such as piRNA region) (Gupta et al., 2014; Halees et al., 2011; J. E. Lee et al., 2010; Majoros & Ohler, 2007; Plass et al., 2017; Roy & Mallick, 2018; Shao et al., 2013; Van Peer et al., 2018). 3′-UTR shortening will result in a loss of these sites evading negative regulation and increase stability (abundance) and

translation efficiency. While miRNA mediated control is widespread, *cis*-elements and loss of destabilizing RBPs also accounts for increased protein expression in a number of mRNAs (Kumar et al., 2014; W. Li et al., 2016; Romo et al., 2017; Shao et al., 2013). Also, a loss of piRNA-miwi-based mRNA elimination pathway from UTR shortening can induce stability of target mRNAs (Roy & Mallick, 2018). Furthermore, a biased proximal PA-site selection, and an increase in miRNA expression can reduce the long to short ratio of APA isoforms increasing the short mRNA abundance (X. Chen et al., 2018; Jenal et al., 2012; Liaw et al., 2013; Masamha et al., 2014). Apart from mRNA abundance, UTR length can directly influence translation by inducing polysome loading on the mRNA. Shorter mRNA isoforms are generally associated with higher polysome compared to the longer isoforms (Fu et al., 2018; X. Jia et al., 2017; Kraynik et al., 2015; Passacantilli et al., 2017) likely mediated through *cis*-elements at the 3′-UTR (S. M. Park et al., 2016).

However, not all shortened 3′-UTR results in increased protein expression (A. R. Gruber et al., 2014). In some cases, UTR-shortening can retain the miRNA targeting sites (Rehfeld et al., 2014). In addition, many mRNAs with longer 3′-UTR isoforms appears refractory to miRNA targeting and expresses more protein (Lemmers et al., 2010; L. Li et al., 2014; A. Sudheesh et al., 2019; Thivierge et al., 2018; X. Wang et al., 2015). The mechanistic paradox of this phenomenon is not fully understood. At least four mechanisms are reported that can explain such contrasting observation: (1) differential PA-tail length addition, (2) positive *cis*-elements and RBPs, (3) indirectly through control of miRNA expression, and (4) in trans through competing endogenous RNA (ceRNA) network. A variant PAP, Star-PAP controls an optimum PA-tail length (~72) addition on the longer APA isoform of target mRNAs, whereas shorter isoforms harbor suboptimal PA-tail length for translation (Mohan et al., 2018; A. Sudheesh et al., 2019). Additionally, 3′-UTR *cis*-element such as AU-rich elements (AREs) can stabilize mRNAs through specific RBP interaction (Hu-proteins; Dormoy-Raclet et al., 2007; Y. Z. Xu et al., 2005; Young et al., 2009). Stimulated HuR expression stabilizes target longer UTR APA isoforms including HuR itself through ARE-mediated stabilization (Al-Ahmadi et al., 2009; Denkert et al., 2006; Heinonen et al., 2005). The same HuR overexpression also down regulates target miRNAs and indirectly increases stability and translation from longer UTR mRNA isoform (Agra Andrieu et al., 2012; Denkert et al., 2006; Young et al., 2012). Likewise, many 3′-UTR lengthened mRNA isoforms are stabilized through distinct RBP interaction (Allen et al., 2013; Rhinn et al., 2012; Shao et al., 2013). Moreover, secondary structural element or RNA folding at the 3′-UTR can render longer UTR isoform refractory to miRNA targeting (Thivierge et al., 2018). Loss of such secondary structural elements can expose hidden destabilizing *cis*-element on 3′-UTR shortening (Begik et al., 2017; Hoffman et al., 2016; Masamha et al., 2016). Recent studies have shown role of ceRNA network in the stabilization and translation efficiency of longer UTR APA isoforms. 3′-UTR shortening can result in a reduction in protein expression in trans through its effect on ceRNA crosstalk (Fan et al., 2020; L. Li et al., 2014; H. J. Park et al., 2018). Here, shortening of cognate ceRNAs have trans-effect on the available targeting miRNA pool. Figure 3 shows mechanism of inverse and direct relationship between UTR length and protein expression.

4 | MECHANISM OF APA IN HUMAN DISEASES

4.1 | Role of *cis*-acting elements on the pre-mRNA UTR in the PA-site selection

The PA-signal sequence and the surrounding *cis*-elements (DSE, USE, and auxiliary upstream and downstream sequences) are critical for the PA-site recognition (Kumar et al., 2019; Laishram, 2014; Neve et al., 2017). Changes in these *cis*-elements or surrounding sequences affect PA-site selection. Point mutations or deletion in the PA-signal can abrogate a proximal PA-site activating downstream aberrant PA-sites (Bennett et al., 2001; Hellquist et al., 2007; Higgs et al., 1983; Orkin et al., 1985). On the other hand, equivalent mutations can also generate a new PA-signal resulting in premature proximal PA (Wiestner et al., 2007). Apart from the polymorphism, several naturally occurring variants of the PA-signal hexamer (AAGAAA, AGUAAA, UAUAAA, AAUAUA, AAUACA, CAUAAA, and AUUAAA) occurs in >30 of the PA-sites in humans (Beaudoing et al., 2000; B. Tian et al., 2005). These variants are functionally weak and largely present at the proximal PA-site. Processing of these sites requires enhanced recruitment of cleavage factors (CSTF2; Beaudoing et al., 2000; Wallace et al., 1999; Yao et al., 2012). Therefore, elevated levels of CSTF2 can promote selection of these variant PA-sites resulting in UTR shortening (H. B. Akman et al., 2015; X. Chen et al., 2018; Shell et al., 2005). In line with this, GUAAU-mediated recruitment of CSTF2 or UGUA-mediated recruitment of CPSF5 promotes variant proximal PA-site selection (X. Chen et al., 2018; Chu et al., 2019; Q. Yang et al., 2011). Concomitantly,

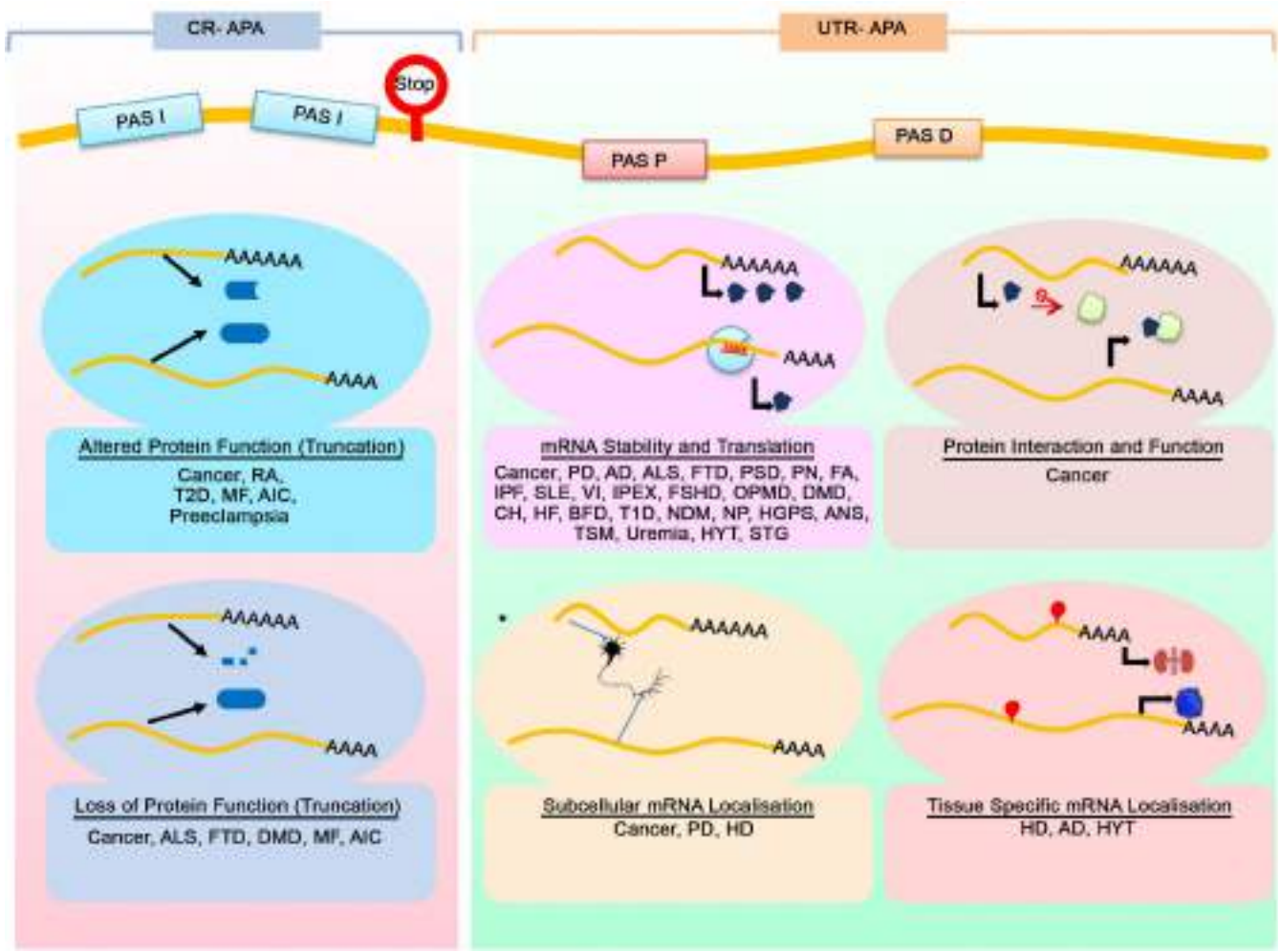

FIGURE 2 A schematic diagram of APA implications on gene expression and protein function in diseases. Two forms of APA (UTR-APA and CR-APA) influences overall expression and properties of translated proteins from the APA isoforms. Overall, APA isoforms can affect (1) mRNA stability and translation (protein expression), (2) mRNA sub-cellular localization, (3) mRNA tissue specific expression, (4) protein interaction and function, and (5) protein truncation resulting into functional or nonfunctional protein variants. Various diseases where these consequences are shown are indicated. (*Changes in subcellular localization has also been shown for CR-APA isoforms but far fewer than that of UTR-APA in cancer; Fischl et al., 2019). Parkinson's disease (PD), psychiatric disorder (PSD), Alzheimer's disease (AD), Huntington's disease (HD), peripheral neuropathy (PN), systemic lupus erythematosus (SLE), viral infection (VI), Immunodysregulation polyendocrinopathy enteropathy X-linked (IPEX), heart failure (HF), cardiac hypertrophy (CH), Oculopharyngeal muscular dystrophy (OPMD), muscle dystrophy (MD), Facioscapulohumeral muscular dystrophy (FSHD), neonatal diabetes mellitus (NDM), type 1 diabetes (T1D), bone fragility disorder (BFD), idiopathic pulmonary fibrosis (IPF), Fanconi's anemia (FA), amyotrophic lateral sclerosis (ALS), frontotemporal dementia (FTD), nasal polyps (NP), Hutchinson–Gilford progeria syndrome (HGPS), Duchenne muscular dystrophy (DMD), muscle fibrosis (MF), type II diabetes (T2D), Wiskott-Aldrich syndrome (WAS), rheumatoid arthritis (RA), autoimmune cholangitis (AIC), muscle wasting (MW), hypertension (HYT), aging and senescence (ANS), α and β thalassemia (TSM), and steroidogenesis (STG)

presence of a multi-allelic T-rich sequence (TRS) (TGTGT) at the 3′-UTR favors distal PA-site selection (Prasad et al., 2013).

4.2 | Role of trans-acting factors in the PA-site selection

Important trans-acting factors that influence PA-site selection includes (1) core CPA factors (2) splicing factors (3) RBPs (4) RNA polymerase and transcription factors and (5) histone modifiers and chromatin remodeling factors. General

factors that regulate PA-site selection is shown in Figure 4 and disease associated APA regulatory proteins are listed in Table 2 along with their mechanism of regulation.

4.3 | Core cleavage and PA factors

Many of the core CPA factors, CPSF subunits (CPSF1, hFIP1), CstF subunits (CSTF2 and CSTF3), CFIm subunits (CPSF5, CPSF6, CPSF7), CFIm subunit hPCF11, PABPN1, and PAPs (PAPα/γ and Star-PAP) are involved in PA-site selection. Among these factors CPSF5, CPSF6, CPSF7, PABPN1, and Star-PAP promotes the distal PA-site selection and their respective cellular depletion results in 3′-UTR shortening (Jenal et al., 2012; S. Kim et al., 2010; W. Li et al., 2017; W. Li et al., 2015; Martin et al., 2012; A. Sudheesh et al., 2019). On the other hand, CPSF1, hFIP1, CSTF2, CSTF3, hPCF11, and PAPα/γ promotes proximal PA-site usage and their respective depletion results in 3′-UTR lengthening

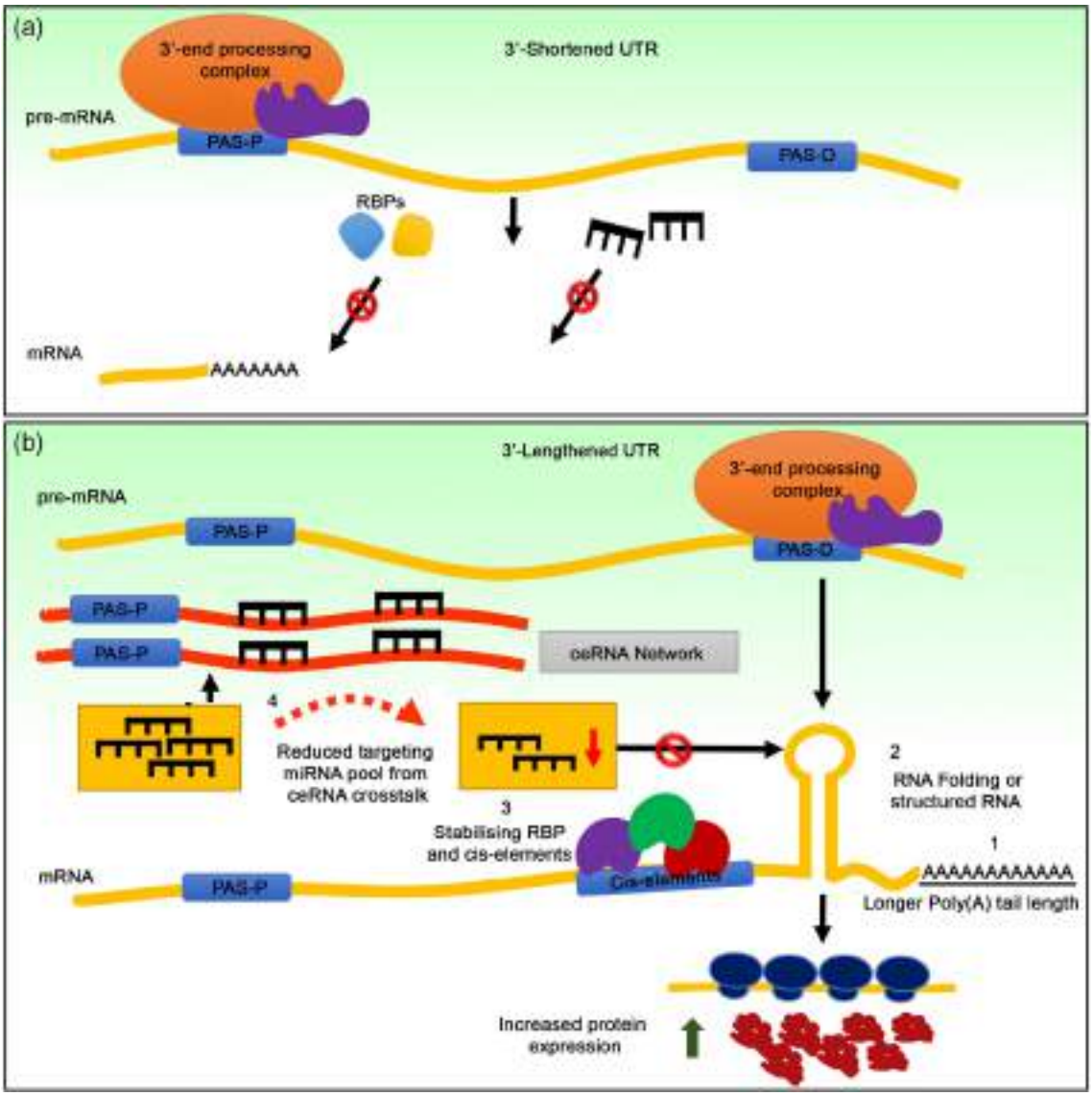

FIGURE 3 Schematics showing mechanism of direct and inverse correlation between UTR length and protein expression of APA isoforms. Widespread mechanism of inverse relation between UTR shortening and protein expression mediated through loss of miRNA targets or destabilizing RBPs is shown in a. how lengthened 3′-UTR mRNA isoform can be translationally more efficient than the shorter mRNA isoforms is shown in B. this involves at least four mechanisms (1) differential PA-tail length addition (optimum versus nonoptimum PA-tail length), (2) presence of RNA secondary structural elements that makes longer isoform refractory to miRNA regulation, (3) presence of stabilizing RBP and or *cis*-elements on the 3′-UTR, and (4) ceRNA cross talk that sequesters targeting miRNAs

(Lackford et al., 2014; W. Li et al., 2017; W. Li et al., 2015; Miles et al., 2016; Van Etten et al., 2017; R. Wang et al., 2019; Yao et al., 2012). However, not all core CPA factors are involved in disease APA. Following are key core CPA factors involved in the determination of PA-site choice in human diseases.

4.3.1 | Cleavage stimulatory factor 64 subunit, CSTF2

As mentioned in the above sections, proximal PA-sites are largely associated with weaker PA-signal sequence and that CSTF2 binding promotes selection of such PA-sites (Beaudoing et al., 2000; Hwang et al., 2016; Takagaki et al., 1996; Yao et al., 2012). Elevated CSTF2 level induces global PA-site switch from distal to proximal PA-site resulting in widespread 3′-UTR shortening and acts as a global regulator of APA (H. B. Akman et al., 2015; X. Chen et al., 2018; Shell et al., 2005; Yao et al., 2012).

4.3.2 | Poly(A) binding protein, PABPN1

PABPN1 is one of the core CPA factors that favors distal PA-site selection, but indirectly by suppressing the usage of weaker proximal PA-sites (de Klerk et al., 2012; Jenal et al., 2012; W. Li et al., 2015). Consequentially, PABPN1 depletion induces PA-site switch from distal to proximal resulting in global 3′-UTR shortening (Creemers et al., 2016; de Klerk et al., 2012; Ichinose et al., 2014; Riaz et al., 2016). Likewise, mutations that render PABPN1 nonfunctional also promote proximal PA-site selection (Abbassi-Daloii et al., 2017; Brais et al., 1998; Raz et al., 2017; Richard et al., 2015).

4.3.3 | Cleavage factor Im, 25 kDa (CPSF5 or NUDT21)

Like PABPN1, CPSF5 promotes distal PA-site selection (A. R. Gruber et al., 2012; S. Kim et al., 2010; Kubo et al., 2006; Martin et al., 2012). CPSF5 down regulation causes global UTR shortening inducing protein expression, whereas CPSF5 ectopic expression elongates 3′-UTR (J. Huang et al., 2018; Masamha et al., 2014; M. Sun et al., 2017; Xiong et al., 2019). The exact mechanism how CPSF5 promotes distal PA-site is unclear and is proposed to occur through two binding sites that sandwich the proximal PA-site on target UTRs. CPSF5 dimer assembly on these two binding sites can skip the proximal PA-site thereby promoting the distal PA-site selection (Martin et al., 2012; Q. Yang et al., 2011).

4.3.4 | Cleavage factor IIm subunit hPCF11

hPCF11 primarily promotes proximal and intronic PA-site selection. And a loss of hPCF11 reduces efficiency of transcription termination and enhances distal PA-site selection on a wide array of target mRNAs (W. Li et al., 2015; Morris et al., 2012; Ogorodnikov et al., 2018; Turner et al., 2020; R. Wang et al., 2019; West & Proudfoot, 2008). In contrast, ubiquitinylation-mediated degradation of hPCF11 can result in 3′-UTR shortening via reduced hPCF11-mediated CFIm recruitment at the distal-PA-site (S. W. Yang et al., 2020).

4.3.5 | Other core CPA factors

CFIm subunits CPSF6 and CPSF7 promote distal PA-site usage (Fang et al., 2020; Sowd et al., 2016), where overexpression of CPSF7 induces distal PA-site selection generating longer transcript, and its depletion results in shorter mRNA (Table 2; Fang et al., 2020). On the other hand, elevated levels of CPSF1 or CSTF3 leads to UTR shortening by promoting proximal PA-site usage (Miles et al., 2016; Van Etten et al., 2017). However, a recent study has shown a distal PA-site preference of CPSF1 on limited mRNAs (S. L. Chen et al., 2021). Moreover, CPSF3, CPSF4, and PAP also contribute to widespread UTR shortening (Morris et al., 2012; Xia et al., 2014; Y. Xiang et al., 2018).

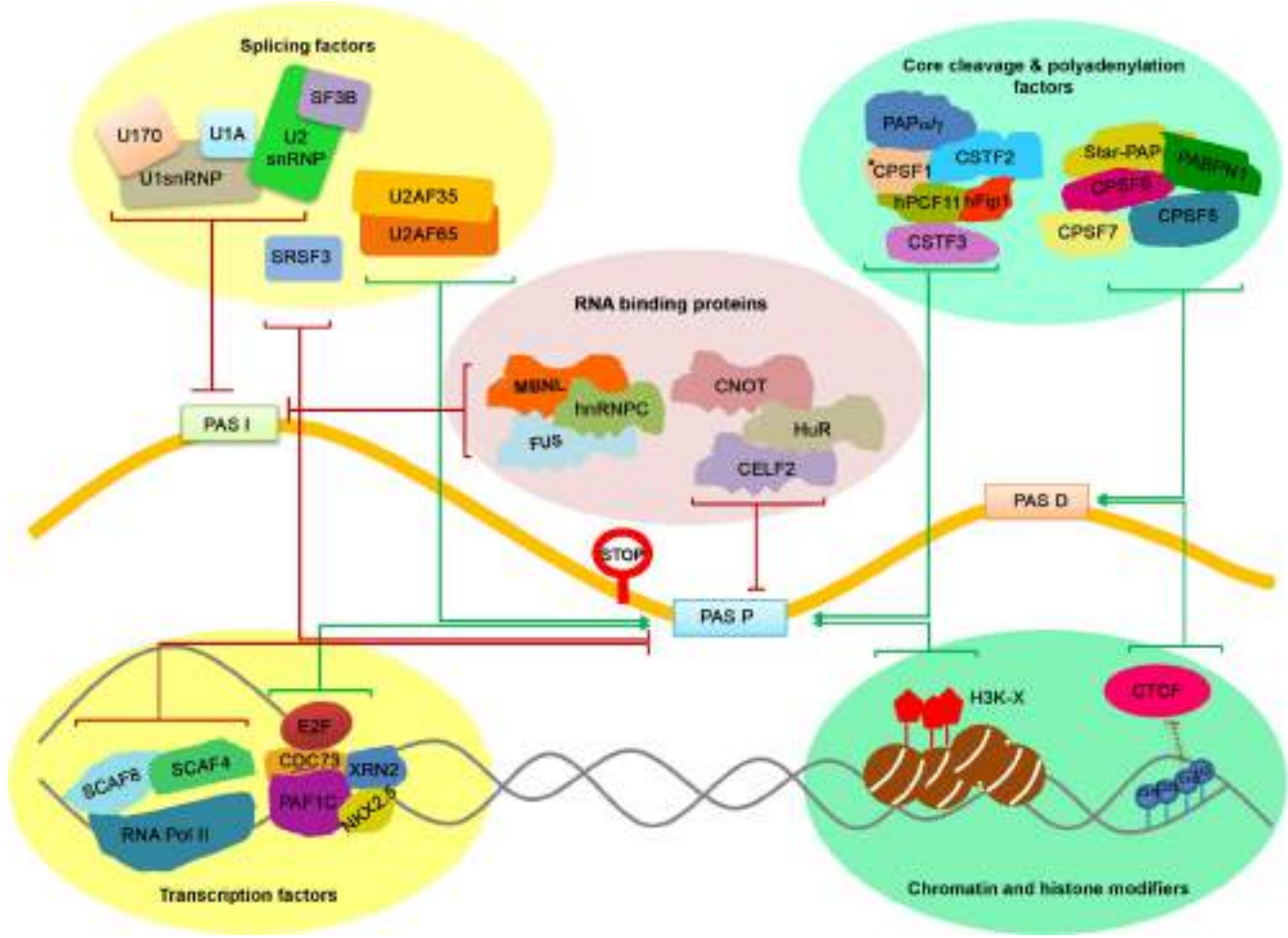

FIGURE 4 A schematic diagram showing various trans-acting factors involved in PA-site selection. Different APA-regulators involved in PA-site determination (core 3′-end processing factors, splicing factors, RNA binding proteins, transcription factors, and chromatin and histone modifiers) and how they influence PA-site usage is indicated. The proximal PA-site (PAS P), distal PA-site (PAS D), and internal PA-sites (PAS I) (intronic or cds) upstream of the terminal exon are as indicated. Factors that favor or inhibit specific PA-site(s) are indicated with green pointed arrow and red blunt arrow lines, respectively. (*A recent study has shown a distal PA-site preference of CPSF1 on limited mRNAs; S. L. Chen et al., 2021)

4.4 | Other APA regulatory proteins in the PA-site selection

4.4.1 | Splicing factors

Splicing factors, U1snRNP and component proteins U1-70K and U1-A, U2snRNP and component protein SF3B, and auxiliary factor U2AF35 and U2AF65, SRSF3 are involved in PA-site recognition (Gunderson et al., 1994; Gunderson et al., 1998; Koga et al., 2014; Kyburz et al., 2006; Lutz et al., 1996; Millevoi et al., 2006; S. M. Park et al., 2016; Shen et al., 2019). However, only a limited number of splicing factors (U1snRNP, U2AF35, and SRSF3) are shown to regulate PA-site selection in disease APA. While U1snRNP inhibit usage of cryptic PA-sites and prevent premature CPA, U2AF35 interact with CPSF7 and promotes proximal PA-site usage (Devany et al., 2016; Oh et al., 2020; S. M. Park et al., 2016). Depletion of U1snRNP results in increased generation of shorter transcripts from the activation of cryptic PA-sites whereas its overexpression prevents such polyadenylaltion (Devany et al., 2016; Kaida et al., 2010). On the other hand, SRSF3 down regulation promotes proximal PA-site selection (Shen et al., 2019).

TABLE 2 List of regulators of PA-site selection in disease APA

CPA factors		Disease	Mechanism of APA	Genes affected	References
Core Cleavage and polyadenylation factor	CPSF1	Cancer (PC)	Increased CPSF1 leads to proximal and upstream PAS usage	*AR-V*, *REEP5, ZNF271P, TUBA1A, MED29* (Genome wide)	[a]S. L. Chen et al. (2021), Liaw et al. (2013), Van Etten et al. (2017)
	CPSF5	Cancers (HCC, LC, BC, GBM, BLC, CRC, CC), IPF, neuropsychiatric diseases	Decrease CPSF5 leads to 3′-UTR shortening	(Genome wide), *PAK1/2, YY1, GNG2/12, GNB1/4, TMEM48, NRAS, TGFA, RAC1, ETS1, GRB2, EPHA2, IGF1R, SET, CCND1, FZD2, GSK3β, MLEC, PPIA, MYC, SMOC1, ACER3, MSRB3, VMA21, TMEM267, RAB3IP, CCT5, UBA5, PTEN, TGFBR1, PSMB2, COL1A1, AKT2, ANXA2, CXXC5, LIMK2, WNT5A, MECP2*	Chu et al. (2019), Gennarino et al. (2015), J. Huang et al. (2018), Mao et al. (2020), Masamha et al. (2014), M. Sun et al. (2017), Tamaddon et al. (2020), Tan et al. (2018), Weng et al. (2019), Xing et al. (2021), Xiong et al. (2019)
	CPSF7	Cancer (HCC)	Increase CPSF7 leads to 3′-UTR lengthening	*WWP2* ATP1B1	Fang et al. (2020)
	PABPN1	Cancer (LGG, NSCLC, BLCA, BRCA, SKCM, GBM, HNSC, KICH, KIRC, KIRP, LIHC, LUAD, LUSC, OV, PRAD, STAD, THCA, CESC), CVD, OPMD	Decrease PABPN1 leads to 3′-UTR shortening	(Genome wide) *ARIH1, ATP1B1, PSMD14, PSME3, MAPKAPK3, TMOD1, VLDLR, PSME3, PSMD14, RAD23A, ATROGIN1, PDRG1*	Creemers et al. (2016), Jenal et al. (2012) Mao et al. (2020), Riaz et al. (2016), Y. Wu et al. (2019), Y. Xiang et al. (2018)
	CSTF2	Cancers (UCB, BLCA, LUSC, LUAD, BRCA, KIRC, UCEC, HNSC) Viral infection, CH	Increase CSTF2 leads to shortened 3′-UTR	(Genome wide) *IQCK, USP9X, RPL13, SNX3, ID2, TOP2A, YMEILI, RAC1, MMP9*	H. B. Akman et al. (2015), X. Chen et al. (2018), Mao et al. (2020), J. Y. Park et al. (2011), Shell et al. (2005), Xia et al. (2014), S. Zhang et al. (2019)
	CSTF3	Cancer (TBNC)	Increase CSTF3 leads to shortened 3′-UTR	*NRAS, cJUN*	Miles et al. (2016)
	hPCF11	Cancer (NB, BC)	Decrease PCF11 level promotes lengthening[b]	Genome wide, *GNB1*	Ogorodnikov et al. (2018), Turner et al. (2020)
Splicing factor	U2AF35 (S34F)	Cancer	Mutation promotes 3′-UTR lengthening	*ATG*	S. M. Park et al. (2016)
	U1snRNA	Cancer	Prevents cryptic polyadenylation	(Genome wide)	Oh et al. (2020)
	SRSF3	Aging-related disease		(Genome wide)	

(Continues)

TABLE 2 (Continued)

CPA factors		Disease	Mechanism of APA	Genes affected	References
			Downregulated SRSF3 leads to 3′-UTR shortening		Muller-McNicoll et al. (2016), Shen et al. (2019)
RNA binding factor	FUS	ALS, FTD	Mutation increases cryptic polyadenylation	(Genome wide)	Jutzi et al. (2020)
	hnRNPC	Metastatic colon cancer	Competes with CstF64, promotes distal PAS	*MTHFDIL*	Fischl et al. (2019)
	CNOT6	Huntington's disease	CNOT6 depletion reduces 3′-UTR lengthening	*HTT, SECISBP2L*	Romo et al. (2017)
	MBNL	Muscular diseases	Loss of MBNL promotes transcript shortening	Genome wide	Batra et al. (2014)
	HuR	Coleorectal cancer	Inhibits usage of PA sites with U-rich region	*COX2*	Agra Andrieu et al. (2012)
	PTBP1	Glioblastoma	Suppresses distal PA-site	Genome wide	A. J. Gruber et al. (2018)
Transcription factors	E2F	Cancer	Increase E2F promotes UTR shortening	*TMEM119, PTGS1,FAM100B*	Elkon et al. (2012)
	Xrn2, Nkx2-5	Congenital heart disease	Decrease Xrn/Nkx2-5 promotes lengthening	*TNNT2, ATP2A2*	Nimura et al. (2016)
	CDC73 PAF1C	Sporadic parathyroid tumors	Decreased CDC73 leads to 3′-UTR lengthening	*INTS6*	Rozenblatt-Rosen et al. (2009)
Chromatin modifier	CTCF	Cancer	CTCF binding promotes proximal PAS usage	*HEATR2, NFYA*, 106 genes	Nanavaty et al. (2020)

Note: List of various trans-acting factors involved in the PA-site selection in disease-associated APA and their mechanistic role in the PA-site usage along with target genes affected.

[a]S. L. Chen et al. (2021) has shown a distal site preference for CPSF1 on limited mRNA.

[b]Ubiquitinylation-mediated hPCF11 degradation causes an opposite effect (S. W. Yang et al., 2020).

4.4.2 | RNA binding proteins

RBPs can influence PA-site selection by inhibiting or promoting recruitment of core processing factors at the PA-site. Important RBPs that affect general PA-site selection include HU protein, NOVA, CELF2, CNOT, FUS, MBNL, hnRNPC, and PTBP1 (Batra et al., 2014; Chatrikhi et al., 2019; Fischl et al., 2019; A. J. Gruber et al., 2018; A. J. Gruber et al., 2016; Jutzi et al., 2020; Licatalosi et al., 2008; Masuda et al., 2015; Romo et al., 2017). However, only a handful of RBPs are associated with disease APA. While MBNL binding close to the PA-site suppresses a PA-site, a distal-binding stimulates the PA-site usage as in the case of neuronal RBP NOVA (Batra et al., 2014; Licatalosi et al., 2008). Also, a depletion of CNOT leads to decrease distal PA-site selection on neuronal mRNAs (Romo et al., 2017). Likewise, mutation in FUS alters interaction with U1snRNP and increases cryptic PA (Jutzi et al., 2020). HU proteins bind and inhibit usage of PA-sites containing U-rich sequence by competing with CSTF2 (Agra Andrieu et al., 2012; Dai et al., 2012; Hall-Pogar et al., 2007; Mansfield & Keene, 2012; H. Zhu et al., 2007). Moreover, heterologous RBP, hnRNPC competes with CSTF2 and blocks CR-APA (Fischl et al., 2019). hnRNPC also promotes proximal PA-site selection of target genes (Fischl et al., 2019; A. J. Gruber et al., 2016). Another RBP, PTBP1 binding suppresses usage of CU-repeat containing distally located PA-sites (A. J. Gruber et al., 2018).

4.4.3 | Transcription factors

3′-end polyadenylation largely occurs co-transcriptionally and hence transcriptional events can influence PA-site choice through RNA polymerase II (Pol II) or associated transcription factors (Fusby et al., 2016; Glover-Cutter et al., 2008; Mapendano et al., 2010; Yonaha & Proudfoot, 2000). Pol II C-terminal domain interacts with CPSF and CSTF1, and hence Pol II elongation or pausing at the PA-site region can influence the PA-site usage by recruitment of CPA factors (Fusby et al., 2016; Glover-Cutter et al., 2008). However, very little is known about role of Pol II or transcription factors in the PA-site selection in disease-associated APA. One of the general elongation factors E2F regulates expression of proximal promoting factors (CSTF2, CSTF3, and CPSF1) thereby influencing proximal PA-site selection (Elkon et al., 2012). E2F also enhances intronic PA-site usage as opposed to the anti-terminator proteins SCAF4/SCAF8 that inhibits premature PA (Gregersen et al., 2019). CDC73, a component of PAF1 transcription factor interacts with CPSF-CSTF complex and promotes proximal PA-site selection. Subsequent depletion of CDC73 result in UTR lengthening (Rozenblatt-Rosen et al., 2009). Similarly, depletion of transcription factors Nkx2-5 and Xrn2 promotes distal PA-site selection (Nimura et al., 2016).

4.4.4 | Histone modifiers and chromatin modulating factors

Emerging studies now show involvement of histone modifications and DNA methylation in the PA-site selection, yet the mechanism is still obscure (Ji et al., 2011; C. Ma et al., 2018; Nanavaty et al., 2020; Spies et al., 2009). It likely involves but not limited to nucleosome occupancy around the PA-site, putative methylation sensitive CPA factors, and chromatin associated proteins that affect CPA complex assembly at the PA-site. While frequently used PA-sites tend to have depleted nucleosome, the downstream sequence of such PA-sites harbors higher nucleosome levels (Huang et al., 2013; Spies et al., 2009). Concomitantly, active histone marks (H3K36 and H3K4me3) occur preferentially at the proximal PA-site in highly expressed genes (Ho et al., 2016; Ji et al., 2011; S. Li et al., 2018; W. Li et al., 2016). Conversely, DNA methylation can function through trans-acting proteins to regulate APA. A chromatin-interacting protein CTCF binding downstream of a proximal PA-site recruits cohesion complex and forms a chromatin loop that enables proximal PA-site selection. DNA methylation at the CTCF binding region prevents CTCF binding and blocks proximal PA-site usage (Nanavaty et al., 2020). In line with this, cells depleted for DNA methyl transferases DNMT1 and DNMT3B show a widespread proximal PA-site usage (Nanavaty et al., 2020). As opposed to this, high DNA methylation at the vicinity of the proximal PA-site can result in 3′-UTR shortening in certain mRNAs where a decrease in methylation promotes distal PA-site usage (C. Ma et al., 2018). Besides, CpG island methylation controls internal PA-site selection that is postulated to act via an unidentified DNA methylation sensitive CPA factor (Cowley et al., 2012). Apart from DNA methylation, RNA methylation (N6-adenosine methylation) influences PA-site selection, a reduction of which leads to increase proximal PA-sites usage (Ke et al., 2015; Shafik et al., 2021).

5 | POLY(A) POLYMERASES IN APA IN HUMAN DISEASES

PAPs are one of the emerging yet underexplored factors that regulate disease-associated APA. Three nuclear PAPs canonical PAPα, PAPγ, and noncanonical Star-PAP regulate APA genome wide (W. Li et al., 2017). While Star-PAP primarily selects the distal PA-site, PAPα and PAPγ targets mostly proximal and intronic PA-sites (W. Li et al., 2017). Depletion of Star-PAP will reduce Star-PAP usage of distal PA-sites thus promoting proximal and intronic PA-sites. Differential expressions of PAPs are known in cancer and in heart diseases that contributes to disease APA (Mohan et al., 2018; A. P. Sudheesh & Laishram, 2017; Topalian et al., 2001; Yu et al., 2017). While Star-PAP is down regulated, PAPγ (a tumourigenic PAP) and PAPα are up regulated in different cancers (Kursun & Kucuk, 2019; Lucchini et al., 1984; Pendurthi et al., 1997; A. P. Sudheesh & Laishram, 2017; Topalian et al., 2001; Yu et al., 2017). The differential expression of PAPs can result in decrease in distal PA-site usage in one hand and increase in proximal PA-site usage leading to overall 3′-UTR shortening. Consistently, PAPα has recently been shown to regulate proximal PA-site selection of *CCND1* mRNA (Komini et al., 2021). Apart from PAPs, core CPA factor CSTF2, PABPN1 or CPSF5 are differentially expressed in different cancers that contribute to PA-site switch (H. B. Akman et al., 2015; Ichinose et al., 2014; Masamha et al., 2014). Interestingly, many of mRNAs that are affected by CSTF2 or PABPN1 are also common with that of Star-PAP or canonical PAP (H. B. Akman et al., 2015; Ichinose et al., 2014; W. Li et al., 2017; Mellman et al., 2008) suggesting a co-ordination of these factors in the regulation of APA. However, it is unclear how PAP controlled APA will coordinate with CSTF2, CPSF5 or PABPN1 controlled APA. A schematic diagram of PAP-mediated APA regulation in different diseases is shown in Figure 5a.

6 | COORDINATED REGULATION OF PROXIMAL AND DISTAL PA-SITE SELECTION FOR GLOBAL UTR LENGTH CONTROL IN DISEASE-ASSOCIATED APA

In the majority of diseases, 3′-UTR shortening occurs by influencing two aspects of PA-site selection, (1) promoting the proximal PA-site, and/or (2) suppressing the distal PA-site usage. This can be achieved by down regulation of APA factors that promote distal PA-site usage (CPSF5, CPSF6, PABPN1, and Star-PAP), and up regulation of proximal PA-site promoting factors (CSTF2, CPSF1, CPSF3, CSTF3, hPCF11 and PAPα/γ; A. R. Gruber et al., 2012; Jenal et al., 2012; W. Li et al., 2017; Miles et al., 2016; Turner et al., 2020; Van Etten et al., 2017; Yao et al., 2012). In cancer, expression of several proximal promoting factors (CPSF1, CPSF3, CSTF2, CSTF3, and hPCF11) are induced whereas the distal PA-site promoting factors (CPSF5, CPSF6, and PABPN1) are down regulated (Chu et al., 2019; Fang et al., 2020; Ichinose et al., 2014; Miles et al., 2016; Sung et al., 2015; Turner et al., 2020; Van Etten et al., 2017; Yi et al., 2016; S. Zhang et al., 2019). For example, in nonsmall lung carcinoma (NSCLC), while elevated CSTF2 level promotes proximal PA-site usage, PABPN1 down regulation suppresses the distal PA-site usage (Ichinose et al., 2014; S. Zhang et al., 2019). In colorectal cancer, there is up regulation of CPSF3, CSTF2, CPSF1, and a parallel down regulation of PABPN1 and hPCF11 that contributes to overall UTR shortening (Mao et al., 2020; Morris et al., 2012). Also, down regulation of PABPN1 or CPSF5 and up regulation of CSFT2 or CPSF1 in hepatocellular carcinoma (HCC) and uterine cancer (UCEC) results in widespread 3′-UTR shortening (Tan et al., 2018; Xia et al., 2014). Similarly, in early hypertrophy, there is increase expression of CSTF2 and a decrease PABPN1 expression that promotes overall proximal PA-site usage (Creemers et al., 2016; J. Y. Park et al., 2011). Thus, a coordinated control of the PA-site choice determines global 3′-UTR length changes during disease progression. A schematic of coordinated control of PA-site selection by proximal and distal promoting APA regulators is shown in Figure 5b. This coordination may not be limited to core processing factors and it can include splicing factors and RBPs as well. For example, in glioblastoma, apart from the loss of CPSF5 that promotes proximal PA-site selection, splicing factor PTBP1 binding suppresses the distal PA-site (A. J. Gruber et al., 2018). It is unclear if the coordinated regulation can affect different PA-sites of a same pre-mRNA, or they act on different pre-mRNAs contributing to overall APA changes. Future studies will also shed light on upstream signals that directs this intricate regulation of PA-site selection and how the two aspects work in concert during disease pathogenesis.

7 | APA IN THE PATHOGENESIS OF DIFFERENT HUMAN DISEASES

7.1 | APA in cancer

While both UTR-APA and CR-APA occurs in cancer, UTR-APA is widespread and primarily regulates cancer progression (Hoffman et al., 2016; Lan & Zhang, 2021; Lembo et al., 2012; Mayr & Bartel, 2009; I. Singh et al., 2018; Q. Wang

et al., 2018; Y. Xiang et al., 2018). UTR-APA is reported in almost all cancer types including breast, bone, lung, blood, colorectal, head and neck, bladder, gastric, prostate, nasopharyngeal, uterine, ovarian, skin, pancreatic, liver, kidney, glioblastoma, lymphoma, germ cell, small intestine, and endocrine cancers (Table 3). Widespread UTR-APA in tumor cells generates transcripts with shorter 3′-UTR resulting in increased expression of important oncogenic proteins and proliferative or metastatic regulators (Table 3). Subsequently, global 3′-UTR shortening is reported in different cancer types including breast, kidney, liver, lung, colon, brain, pancreas, lymph, and blood (Table 3). APA regulation in cancer primarily involves core CPA factors that are differentially expressed (Table 2; Ichinose et al., 2014; Mao et al., 2020; Xia et al., 2014; Y. Xiang et al., 2018; S. Zhang et al., 2019). Analysis of APA factors in different cancers has shown up regulation of ~36 and down regulation of ~8 CPA and RNA processing factors associated with global PA-site switch (Morris et al., 2012; Xia et al., 2014; Y. Xiang et al., 2018). For example, while CSTF2 expression is stimulated in multiple cancers, PABPN1 is down regulated across >17 cancers types that results in global UTR shortening (H. B. Akman et al., 2015; X. Chen et al., 2018; Ichinose et al., 2014; Y. Xiang et al., 2018; S. Zhang et al., 2019).

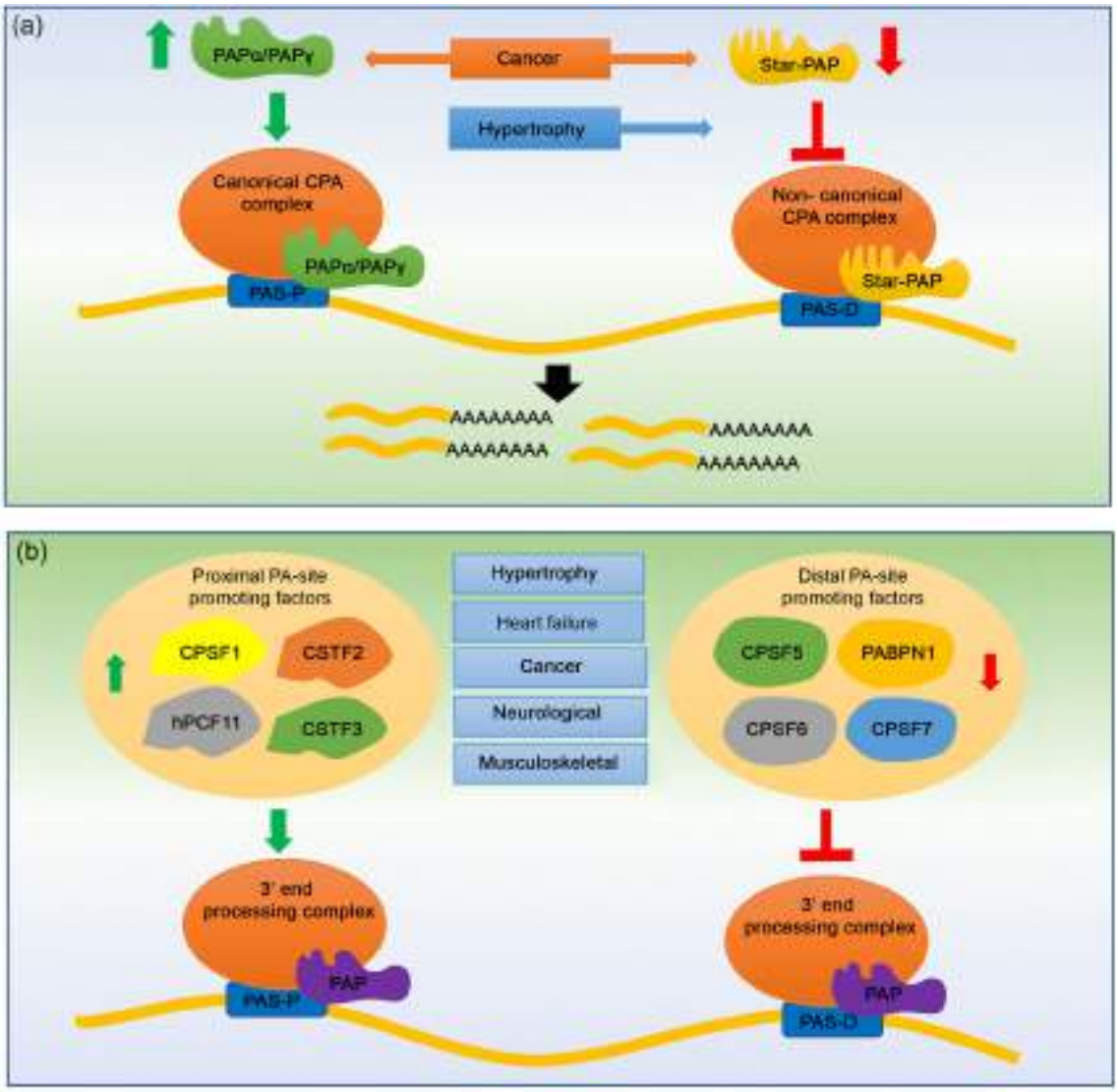

FIGURE 5 Coordinated regulation of PA-site selection by differential expression of core cleavage and polyadenylation factors and PAPs (a) schematic shows factors promoting proximal PA-site selection while coordinately suppressing distal PA-site usage by differential expression of various components of core processing factors in that primarily results in UTR shortening as in the case of majority of human diseases. (b) Role of PAPs in the PA-site selection and APA regulation of cancer and cardiac hypertrophy. Down regulation of Star-PAP during cancer and hypertrophy and up regulation of PAPα/γ in cancer that results in the PA-site switch downstream of disease signals are indicated

UTR-APA not only activates oncogenes, but also renders down regulation of tumor suppressor genes that involves either 3′-UTR-lengthening or shortening (Table 3). Apart from the oncogenic transformation, UTR-APA acts as a critical regulatory mechanism in other processes in cancer progression including proliferation, invasion, migration and metastasis of cancer cells (Andres et al., 2019; Elkon et al., 2012; Oh et al., 2020; L. Wang et al., 2016; Q. Wang et al., 2018). While high invasive cells are associated with preferential 3′-UTR lengthening, low invasive cells show 3′-UTR shortening with respect to nontransformed cells in breast cancer (Fischl et al., 2019; Fu et al., 2011; Turner et al., 2020). This widespread 3′-UTR length changes also regulate tumor growth and metastasis in vivo (Andres et al., 2019; Masamha et al., 2014). On the other hand, the role of CR-APA is limited in cancer that primarily regulates loss of tumor suppressor function promoting cancer cell transformation (S. H. Lee et al., 2018; Rehfeld et al., 2014). CR-APA-induced premature PA can also alter a protein function generating an oncogenic protein or a tumor suppressor protein (Table 3).

7.2 | APA in neurological disorders

Both CR-APA and UTR-APA influences localization and expression of neuronal proteins involved in different neurodegenerative or psychiatric disorders (Alzheimer's disease [AD], Parkinson's disease [PD], Amyotrophic lateral sclerosis [ALS], Frontotemporal dementia [FTD], peripheral neuropathy [PN], and Huntington's disease [HD]) (Table 3). Analysis of APA from RNA-seq data (DaPars) in AD, PD, and ALS show a limited APA shift corresponding to a relatively small number of mRNAs. However, each disease has a subgroup of mRNAs that showed disease-specific APA deregulation (Patel et al., 2019). UTR-APA in *SNCA* (*αSyn*) generates two mRNA isoforms. The longer *αSynL* isoform while induces αSyn protein expression, it is directed toward mitochondria away from the synaptic terminal where it is required for synaptic transmission (Marchese et al., 2017; Rhinn et al., 2012). In PD, APA switch leads to 3′-UTR lengthening (*αSynL)* resulting in accumulation of αSyn protein in the mitochondria (Rhinn et al., 2012). This accumulation can generate toxic soluble oligomers leading to mitochondrial dysfunction (Luth et al., 2014). Alternatively, αSyn relocalization away from synaptic terminal can disrupt synaptic transmission affecting neuronal function and homeostasis contributing to the PD pathogenesis (Rhinn et al., 2012). Similarly, UTR-APA results in mRNA 3′-UTR lengthening of neuronal genes (*LONP* and *NELFA*) that down regulates their expression in PD (Patel et al., 2019). Psychiatric disorders (panic disorder, learning deficit, anxiety and depression) also involve 3′-UTR lengthening of the mRNA for neurotransmitter serotonin transporter (*SERT*) with an addition of ~125-bp from a polymorphism in the proximal PA-site (Gyawali et al., 2010; Hartley et al., 2012; Yoon et al., 2013). This 3′-UTR lengthening of *SERT* is targeted by miR-16 in the brain (Baudry et al., 2010). However, hnRPNK binding stabilizes the longer *SERT* isoform that displaces miR-16 and derepresses their translation to regulate a wide anxiety-related emotional responses (Yoon et al., 2013).

In AD, UTR-APA results in shortened 3′-UTR isoform of mRNA encoding microtubule-associated protein, Tau that undergoes pathological aggregation in the frontal cortex downstream of amyloid β-toxicity (Dickson et al., 2013; Y. Wang et al., 1993). Likewise, UTR-APA reduces long 3′-UTR isoform of *HTT* mRNA increasing relative abundance of *HTT* short isoform in HD motor cortex in the brain (B. Lin et al., 1993; Romo et al., 2017). This APA switch to shorter isoform could increase HTT protein aggregate disrupting normal synaptic transmission in HD (B. Lin et al., 1993; Romo et al., 2017). UTR-APA also results in a prevalence of 3′-UTR shortening in peripheral neuropathic injuries including *Nav1.8* mRNA (Hirai et al., 2017). Likewise, *UBRI*, *VAMP2*, and *CHURC1* mRNAs undergo 3′-UTR shortening, and *COX-2* or *OGDHL* undergo 3′-UTR lengthening in neurodegeneration. While the exact mechanism how this APA regulates neurodegeneration is unclear, it increases CHURC1 and UBRI protein expression and reduces VAMP2 or OGDHL protein expression (Lukiw & Bazan, 1997; Patel et al., 2019). On the other hand, CR-APA regulates neuronal diseases ALS and FTD. CR-APA renders a neuronal growth factor, stathmin-2 (STMN2) nonfunctional by an intronic PA of *STMN2* mRNA, which is critical in the pathogenesis of ALS/FTD (Melamed et al., 2019). Additionally, in ALS, presence of GGGGCC (G4C2) intronic repeats within *C9ORF72* can cause a premature intronic PA that abrogates the encoded protein function (DeJesus-Hernandez et al., 2011; Renton et al., 2011). This is one of the most common genetic causes of ALS/FTD. Interestingly, *C9ORF72* CR-APA associated ALS shows global increased in the proximal PA-site usage among the patients (Prudencio et al., 2015).

7.3 | APA in immunological diseases

Both UTR-APA and CR-APA occurs in immunological diseases (Table 3). More than 1900 mRNAs with tandem 3′-UTR length changes are reported between normal and disease states in immunological disorders (P. Tian et al., 2014). One of

TABLE 3 Occurrence of APA in different cancer types

Disease	Disease Type	Alternatively polyadenylated genes contributing to disease outcome	APA Type	References
CANCER	Colorectal cancer	Pro-tumour(*ABCG2, CCND1, CCND2, COX2, DMKN, FGF2, GPI, IMP1, MACC1, MLEC, NET1, PA2G4, PDXK, POLR2K, PPIA, RAB10, SET, OTUB1*), (Genome wide) Anti-tumour (*P53, DICER, ATP2A2*)	UTR	(Andres et al., 2019; Fischl et al., 2019; Hamaya et al., 2012; Ilm et al., 2016; Y. Lin et al., 2012; Mao et al., 2020; Mayr & Bartel, 2009; Morris et al., 2012; To et al., 2008; Y. Wang et al., 2016; X. Yang et al., 2018; Young & Dixon, 2010)
		Anti-tumour (*PPIE, sVEGFR*) Pro-tumour (*MTHFD1L, NAP1L1*)	CR	(Fischl et al., 2019; Morris et al., 2012; Stagg et al., 2014)
	Breast cancer	Pro-tumour(*ANAPC13, ATP5S, Bcl2, CCNE1, CDC25B, CDC25C, CEP135, CCND2, ANAPC5, AGR2, CCND1, cJUN, CNIH4, DDX5, DVL3, ERBB2, FGF2, IGF2, IMP1, CDK6, SKI, POLR2K, CDC6, IQCK, MGP, MKI67, NRAS, PPIA, PRELID1, RAB10, RAB23, RPL13, SNRNP200, TMEM237, YME1L1, U2SURP, STAT6, SYNCRIP, TGFBR3, TOP2A, TRAM1, TRPS1, USP9X*) (Genome wide) Anti-tumour (*PIK3R1, NDE1, COL1A1, COL1A2, CASP6, DFFA, DFFB, DICER1, PARP1, PNRC1, PHF6, LARP1, CDKN2C, CTNNBIP1, PPM1A, RCAN1, SNX3, TIMP3*)	UTR	(B. H. Akman et al., 2012; H. B. Akman et al., 2015; Begik et al., 2017; Fu et al., 2018; Fu et al., 2011; Ganapathi Sankaran et al., 2019; Gillen et al., 2017; N. Kim et al., 2019; Liaw et al., 2013; Y. Lin et al., 2012; Matoulkova et al., 2017; Mayr & Bartel, 2009; Miles et al., 2016; H. J. Park et al., 2018; Stagg et al., 2014; Tan et al., 2017; X. Wang et al., 2015; Xia et al., 2014; Y. Xiang et al., 2018; Xue et al., 2018; Yan et al., 2018)
		Anti-tumour (*MAGI3, RNF220, FAM70B, ELP5, ERO1A, PHFT1, PRMT2*)	CR	(Elkon et al., 2012; Ni & Kuperwasser, 2016; Turner et al., 2020; Zhong et al., 2011)
	Lung cancer	Pro-tumour(*FGF2, MAP4K4, TMEM237, CCND1, GSK3β, IGF1R, COX-2, AURKA, CAV2, RAB27A, RAD51, NET1, RPL13, WDTC1, TIMELESS, TOP2A, TIMM17A, RPL13, CCND1, CCND2, FGF2, CSNK1D, RAB10, IMP1, CCNE1*) Anti-tumour (*FANCD2*) (Genome wide)	UTR	(Begik et al., 2017; Han et al., 2017; J. Huang et al., 2018; Lembo et al., 2012; Y. Lin et al., 2012; Mayr & Bartel, 2009; Shulman & Elkon, 2019; Xia et al., 2014; Y. Xiang et al., 2018; Xue et al., 2018; S. Zhang et al., 2019)
	Pancreatic cancer	Pro-tumour(*ALDOA, FLNA, PAF1, ENO1, SAT1, CSNK1A1, ZEB1*) (Genome wide) Anti-tumour (*PPP2R2D*)	UTR	(Passacantilli et al., 2017; Venkat et al., 2020)
	Ovarian cancer	Pro-tumour (*BIRC5, HMGA2, IGF2BP1, RPL13, HER-2/neu*) Anti-tumour(*FANCD2*)	UTR	(Begik et al., 2017; Busch et al., 2016; Doherty et al., 1999; Han et al., 2017; X. He et al., 2014; X. J. He et al., 2016)
		Pro-tumour(*ERBB3, HER-2*)	CR	(H. Lee & Maihle, 1998; Scott et al., 1993)
	Bladder cancer	Pro-tumour(*POLH, ANXA2, LIMK2, RAC1*) Anti-tumour(*FANCD2*)	UTR	(X. Chen et al., 2018; Han et al., 2017; Xiong et al., 2019; J. Zhang et al., 2019)
	Prostate cancer	Pro-tumour(*RUNX1, KLK2, KLK3, ECE-1, FGF2*)	UTR	(L. Li et al., 2014; Whyteside et al., 2014; Xue et al., 2018)
	Hepatocellular carcinoma	Pro-tumour(*PSMB2, CXXC5, RAB3IP, TMEM267, UBA5, CCT5, LDH2, LDHA, TEAD2, POLR2K, CCNE1*)	UTR	(M. Li et al., 2020; Y. Lin et al., 2012; M. Sun et al., 2017; Tan et al., 2018; Xue et al., 2018)
		Pro-tumour(*WWP2*)	CR	(Fang et al., 2020)
	Gliobastoma	Pro-tumour(*PAK1, MEF2D, SMOC1, CRTC1, HSBP1, PHC1*) (Genome wide). Anti-tumour (*MGMT*)	UTR	(Chu et al., 2019; Kreth et al., 2013; Shao et al., 2013; Y. Xiang et al., 2018)
	Endocrine cancer	Pro-tumour(*PSMD8,TM9SF3,CD59,ANKH,CIAO1, SRSF5,MRSP16, NDUFA6, RET*) Anti-tumor (*DACT2*)	UTR	(Gartner et al., 2005; Ishizaka et al., 1989; Rehfeld et al., 2014)
		Anti-tumour (*DCC, MAGI1, RIC3, THADA,PDZD2, LRRFIP1*)	CR	(Rehfeld et al., 2014)
	Mantle Cell Lymphoma	Pro-tumour(*CCND1*)	UTR	(Bosch et al., 1994; R. W. Chen et al., 2008; Wiestner et al., 2007)
	Acute Myeloid Leukemia	Pro-tumour(*NFKB1, STAT1, BIRC2, BIRC3, CDKN1B, CREBBP, XIAP, PIK3CB,*) (Genome wide) Anti-tumour(*ATG7*)	UTR	(S. M. Park et al., 2016; Ye et al., 2019)
		Anti-tumour(*TOPO2A, DICER, FOXN3, CARD11, MGA, CHST11, CSF3R*)	CR	(Druhan et al., 2020; Harker et al., 1995; S. H. Lee et al., 2018)
	Renal cell carcinoma	Pro-tumour(*TMCO7, PLXDC2, CSNKD1D, NET1, CCNE1*)	UTR	(Y. Lin et al., 2012; Xia et al., 2014; Y. Xiang et al., 2018; Xue et al., 2018)
	Nasopharyngeal carcinoma	Pro-tumour(*JAG1, EGLN1, WDR5, SMAD3, TIMP3, XRCC5, RAC1, SPAG9, TRIP6, RRAS2, FNDC3B, TRIB1*) (Genome wide) Anti-tumour(*IRF1, PIKR1*)	UTR	(Y. Q. Li et al., 2020; Y. F. Xu et al., 2018)
	Gastric cancer	Pro-tumour(*NET1*)	UTR	(Lai et al., 2015)
	Multiple Myeloma	Pro-tumour(*IKZF1, CUL4A, IQGAP1*) (Genome wide)	CR	(I. Singh et al., 2018)
		Pro-tumour(*CCDN2*)	UTR	(Misiewicz-Krzeminska et al., 2016)
	Cervical cancer	Pro-tumour (*TEAD2*), (Genome wide)	UTR	(M. Li et al., 2020; Y. Xiang et al., 2018; Xing et al., 2021)
	B cell lymphoma	Pro-tumour (*UBE2A*) Anti-tumour(*PIK3AP1*)	UTR	(P. Singh et al., 2009)
	Teratocrcinoma	Anti-tumour(*ZNF143*)	UTR	(Ngondo & Carbon, 2014)
		Pro-tumour(*PDGF*)	CR	(Mosselman et al., 1994)
	Other cancers (MTH, HNSC, ESCC, BCC, PA)	Pro-tumour(*CCNE1*) Anti-tumour(*TP53*) (Genome wide)	UTR	(Stacey et al., 2011; Y. Wu et al., 2019; Xue et al., 2018; Zhou et al., 2012)
		Pro-tumour(*CGRP, FGFR4*) Anti-tumour(*ISO3*)	CR	(Abbass et al., 1997; D. C. Di Giammartino et al., 2014; Mbita et al., 2012; Minvielle et al., 1991)

(Continues)

TABLE 3 (Continued)

Disease	Disease type	Alternatively polyadenylated genes contributing to disease outcome	APA Type	Reference
Cardiovascular diseases	Hypertrophy	*TIA1, CUGBP2, UBE2Z, ANAPC2, CDK1, NQO1, KLF4, LRRC58, UCP3, MEIS1, PPM1K, GSK3b, FAF2, MTUS1 DGKE, ETF1, UTP6, PDZRN3, CTC1,* (Genome wide)	UTR	(J. Y. Park et al., 2011; Soetanto et al., 2016; A. Sudheesh et al., 2019)
	Heart Failure	*PIGK, WEE1, FBRSL1, SERF2* (Genome wide)	UTR	(Creemers et al., 2016)
	Hypertension	*SLC7A1, ATPB1*	UTR	(Prasad et al., 2013; Z. Yang & Kaye, 2009; Z. Yang et al., 2007)
Neurological disorders	Parkinson's disease	*CHURC1, NELFA, SNCA, LONP1*	UTR	(Marchese et al., 2017; Patel et al., 2019; Rhinn et al., 2012)
	Alzheimer's disease	*UBR1, VAMP2, MAPT, COX-2, OGDHL, BIN1*	UTR	(Dickson et al., 2013; Lukiw & Bazan, 1997; Patel et al., 2019)
	Amyotrophic Lateral Sclerosis, Frontotemporal Dementia	*UCHL1, SOD1*	UTR	(Dell'Orco et al., 2021; Patel et al., 2019)
		STMN2, C9ORF72	CR	(DeJesus-Hernandez et al., 2011; Melamed et al., 2019; Prudencio et al., 2015)
	Peripheral Neuropathy	*SCN10A*	UTR	(Hirai et al., 2017)
	Huntigton's disease	*HTT*	UTR	(B. Lin et al., 1993; Romo et al., 2017)
	Psychiatric (Panic disorder, Intellectual deficit, Anxiety and Depression,Autism spectrum disorder)	*MECP2, BDNF, SERT, NRNX1, CNTNAP2, FMR1, DDX6,* (Genome wide)	UTR	(Alcott et al., 2020; Gennarino et al., 2015; Grozdanov et al., 2020; Gyawali et al., 2010; Hartley et al., 2012; Lau et al., 2010; Szkop et al., 2017; Tassone et al., 2011; Yoon et al., 2013)
Immunological diseases	Systemic Lupus Erythematosus	*GIMAP5, IRF5*	UTR	(Cunninghame Graham et al., 2007; Graham et al., 2007; Hellquist et al., 2007)
	Immunodysregulation polyendocrinopathy enteropathy X-linked Syndrome	*FOXP3*	UTR	(Bennett et al., 2001)
	Wiskott-Aldrich Syndrome	*WASP*	UTR	(Andreu et al., 2006)
	Autoimmune Cholangitis	*PKHD1*	CR	(W. Huang et al., 2018)
	Rheumatid Arthritis	*IL6ST (gp130)*	CR	(Sommer et al., 2014)
	Nasal Polyps	(Genome wide)	UTR	(P. Tian et al., 2014)
	Viral infection	(Genome wide)	UTR	(X. Jia et al., 2017; Sowd et al., 2016)
Endocrine diseases	Type I diabetes	*GIMAP5*	UTR	(Shin et al., 2007)
	Type II diabetes	*TCF7L2*	CR	(Locke et al., 2011)
	Neonatal diabetes	*INS*	UTR	(Garin et al., 2010)
	Diabetic nephropathy	*HGRG-14*	UTR	(Abdel Wahab et al., 1998)
	Steroidogenesis	*STAR*	UTR	(D. Zhao et al., 2005)
	Preeclampsia	*FLT1*	CR	(Shibata et al., 2005; Thomas et al., 2007; Vorlova et al., 2011)
Musculoskeletal diseases	Occulopharyngeal Muscular Dystrophy	*ATROGIN1, PSME3, LC3A, AGT5, PSMD14, RAD23A, WIP1,* (Genome wide)	UTR	(Abbassi-Daloii et al., 2017; Calado et al., 2000; Raz et al., 2017; Riaz et al., 2016)
	Facioscapulohumeral Muscular Dystrophy	*DUX4*	UTR	(Lemmers et al., 2010)
	Duchenne Muscular Dystrophy	*DMD*	CR	(Rani et al., 2020)
	Muscle Fibrosis	*PDGFR*	CR	(Mueller et al., 2016)
Other diseases	Aging and Senescence	(Genome wide) *RAS2, MDM2, HN1,HMGA2*	UTR	(M. Chen et al., 2018; Q. Jia et al., 2019; Y. Sun et al., 2020; L. Wang, Chen, et al., 2020)
	Uremia	(Genome wide)	UTR	(Sui et al., 2016)
	Pulmonary fibrosis	*COL1A1, FN, VMA21, TGFBR1, WNT5A, FZD2* (Genome wide)	UTR	(Weng et al., 2019)
	Genetic (Thalassemia, Fabry Disease, Thrombophillia, Fanconi Anemia, Bone fragility disorder, Cryptorchidism)	*HBA, HBB, GLA, FANCD2, BMP1* (Genome wide)	UTR	(Fahiminiya et al., 2015; Ge et al., 2021; Han et al., 2017; Higgs et al., 1983; Orkin et al., 1985; Rund et al., 1992; Yasuda et al., 2003)

Note: Occurrence of APA in different disease types and associated list of genes affected under each disease types along with references. Genome wide APA in different disease types is also indicated. Expansions of gene names are listed in the Supporting Information Box A. UTR-APA mRNAs with lengthened mRNA under pathological condition that are denoted in blue while mRNAs that are shortened are indicated in red. CR-APA mRNAs that are truncated are indicated in green, while inhibitions of CR-APA on mRNAs that leads to longer proteins under pathological condition are indicated in pink. BCC, basal cell carcinoma; ESCC, esophageal squamous cell cancer; HNSC, head and neck squamous cell carcinoma; MTH, medullary thyroid carcinoma; PA, pituitary adenoma.

the common autoimmune disorders, systemic lupus erythematosus (SLE) involves an increased IFN-α expression that is regulated by transcription factor IRF5. Polymorphism in the proximal PA-signal (AAU-"A/G"-AA) at the *IRF5* mRNA causes UTR-APA generating two *IRF5* isoforms. While the presence of "A" variant (AAU-A-AA) causes proximal PA-site usage, the presence of "G" variant (AAU-G-AA) abrogates the proximal PA-site generating the longer UTR isoform. The "A" variant PA-signal is associated with the high risk SLE and results in shorter isoform that enhances IRF5 protein level. This will up-regulate IFN-α and IFN-inducible genes that modify the immune response in a manner that predisposes to SLE (Cunninghame Graham et al., 2007; Graham et al., 2007). UTR-APA also results in 3′-UTR shortening during immune response against viral infections (X. Jia et al., 2017; Sowd et al., 2016). However, in Immunodysregulation polyendocrinopathy enteropathy X-linked (IPEX) syndrome, a polymorphism in the PA-signal (AAUAAA>AAUGAA) abrogates the proximal PA-site in the *FOXP3* mRNA that regulates development and function of regulatory T cells (Bennett et al., 2001). This UTR-APA activates downstream PA-sites on *FOXP3* generating a longer translationally inefficient *FOXP3* mRNA. This results in reduced FOXP3 expression leading to defective regulatory T cells and compromised suppression of autoreactive T cells (Bennett et al., 2001). On the other hand, CR-APA regulates other immunological diseases such as rheumatoid arthritis and autoimmune cholangitis where intronic mutations shorten transcripts of disease-causing genes (*gp-130*, *PKHD1*) generating toxic protein isoforms (W. Huang et al., 2018; Sommer et al., 2014). Moreover, a complex mutation involving regions of the terminal intron and exon of *WASP* mRNA in Wiskott–Aldritch syndrome (WAS) generates two aberrant transcript isoforms of different 3′-UTR length terminating at two alternate PA-sites. Both UTR-APA isoforms encodes an abnormal protein that impairs WASP protein function in WAS patient (Andreu et al., 2006).

7.4 | APA in cardiovascular diseases

Genome wide UTR-APA results in changes in the 3′-UTR length in cardiac hypertrophy (CH) and failing human heart (Creemers et al., 2016; J. Y. Park et al., 2011; Soetanto et al., 2016). 3′-UTR shortening leads to increased expression of a large number of regulators in CH and heart failure (Table 3; Creemers et al., 2016). Nevertheless, many of the anti-hypertrophy regulators that exhibit 3′-UTR shortening are also down regulated from the shortening (Table 3) (Soetanto et al., 2016; A. Sudheesh et al., 2019). Star-PAP regulates distal-PA-site selection through an association with a co-regulator RBM10 in CH (Mohan et al., 2018; A. Sudheesh et al., 2019). Down-regulation of Star-PAP and/or RBM10 during CH will indirectly stimulate proximal PA-site usage promoting global 3′-UTR shortening (W. Li et al., 2017; Mohan et al., 2018; A. Sudheesh et al., 2019). This 3′-UTR shortening induces expression of pro-hypertrophy regulators in one hand and decrease expression of several Star-PAP target anti-hypertrophy regulators (Mohan et al., 2018; Soetanto et al., 2016; A. Sudheesh et al., 2019). In addition to Star-PAP, CSTF2 and PABPN1 are also differentially expressed in early hypertrophy and heart failure that regulates PA-site usage. However, in the failing human heart, there is equal shift toward both proximal and distal PA-sites indicating involvement of more than one factor that controls APA in the human heart (Creemers et al., 2016; Soetanto et al., 2016). Likewise, UTR-APA can generate longer 3′-UTR isoform of an amino acid transporter SLC7A1 reducing SLC7A1 expression in hypertension (Z. Yang & Kaye, 2009; Z. Yang et al., 2007). Besides the expression changes, UTR-APA can influence mRNA tissue specific localization and regulate arterial pressure in the heart (Prasad et al., 2013). However, we do not find any examples of CR-APA in cardiovascular diseases.

7.5 | APA musculoskeletal diseases

Various muscular and skeletal diseases are associated with both UTR-APA and CR-APA (Table 3). Oculopharyngeal muscular dystrophy (OPMD) is caused by a triple repeat (GCG) mutation in PABPN1 that forms a nonfunctional insoluble nuclear aggregate of PABPN1 (Brais et al., 1998; Calado et al., 2000; Raz et al., 2011). This depletes functional soluble PABPN1 level causing widespread APA switch from distal to proximal PA-sites (Anvar et al., 2013; de Klerk et al., 2012; Jenal et al., 2012; Schroder et al., 2011). In addition, the same mutation causes CR-APA events in ~17% of the APA mRNAs that favors intronic PA-sites in majority of these transcripts (Abbassi-Daloii et al., 2017; Raz et al., 2017). Similar reduction of PABPN1 in muscle dystrophy induces cytoplasmic localized ubiquitin ligase Atrogin-1 expression from 3′-UTR shortening of *ATROGIN1* mRNA. Up-regulation Atrogin-1 along with deregulation of other proteasomal genes will induce muscle atrophy by altering protein homeostasis (Riaz et al., 2016). However, in

Facioscapulohumoral muscular dystrophy, UTR-APA induces regulator protein, DUX4 expression from 3′-UTR lengthening (Lemmers et al., 2010). On the other hand, in muscle fibrosis and dystrophy, mRNAs of key regulators (*PDGFRα* or *DMD)* undergoes intronic PA generating truncated nonfunctional proteins (Mueller et al., 2016; Rani et al., 2020).

7.6 | APA in endocrine, hematological, and other diseases

Both CR-APA and UTR-APA regulates important genes in various endocrine diseases (Table 3). In neonatal diabetes, diabetic neuropathy, or steroidogenesis, UTR-APA causes 3′-UTR lengthening (*INS*, *HGRG-14*, and *STAR*) that down regulates their protein expression. This involves abrogation of proximal PA-site by polymorphism generating an unstable longer transcript under disease condition (Abdel Wahab et al., 1998; Garin et al., 2010; D. Zhao et al., 2005). However, type I diabetes involves 3′-UTR shortening that regulates autoantibody generation against β-cell islet proteins (Shin et al., 2007). On the other hand, CR-APA (*TCF7L2* mRNA) is associated with risk of type II diabetes (Locke et al., 2011). Alternatively, inhibition of CR-APA by U1snRNP of *sFLT1* mRNA is linked with preeclampsia (Shibata et al., 2005; Thomas et al., 2007; Vorlova et al., 2011).

In hematological disorder (α- and β-thalassemia), point mutations in the canonical PA-signal (AAUAAA to AAUA AG in *HBA* and AAUAAA to AACAAA in *HBB* mRNAs) abrogate proximal PA-site and activate downstream aberrant PA-sites. Similarly, deletion in the AAUAAA hexamer (terminal -AUAAA- in *HBB* and -AA- in *HBA* mRNAs respectively) promotes usage of aberrant downstream PA-sites. This generates translationally inefficient longer *HBA* and *HBB* transcripts compromising their protein expression in thalassemia (Higgs et al., 1983; Orkin et al., 1985; Prior et al., 2007; Rund et al., 1992). Similar 3′-UTR lengthening occurs in bone fragility disorder in children that down regulates BMP1 expression (Fahiminiya et al., 2015). On the other hand, 3′-UTR lengthening is reported in tissue aging and senescence that regulates important senescent and aging-related mRNAs (*MDM2* and *E3 ligase*; M. Chen et al., 2018; L. Wang, Chen, et al., 2020; Zheng et al., 2018). Analogous to this, UTR-APA regulates expression of key genes in pulmonary fibrosis, and genetic diseases such as Fanconi Anemia, Thrombophillia, and Fabry disease (Gehring et al., 2001; Weng et al., 2019; Yasuda et al., 2003).

8 | APA IN DRUG RESISTANCE IN CANCER THERAPY: A FUTURE PERSPECTIVE

Recent studies indicate potential application of APA in diagnosis, prognosis, and treatment of human diseases. APA signatures are now considered superior to many traditional clinical markers (Ji & Tian, 2009; Ogorodnikov et al., 2018; Xia et al., 2014; Y. Zhang et al., 2020). Several studies have indicated therapeutic advantage of APA that is targetable through CRISPR/Cas9 molecular editing system to alter or silence of aberrant PA-sites (Niu et al., 2016; Xie et al., 2014). Recently, these aspects of APA are reviewed extensively (Nourse et al., 2020; Ren et al., 2020) and hence we have not expanded further on this aspect in this review. An interesting area of APA with an immense therapeutic potential yet underexplored is in combating drug resistance in cancer and other complex diseases. Drug resistance is a stumbling block in cancer therapeutics where the resistance generally appears near to the end of treatment regime (Housman et al., 2014). The relapse from this resistance can be worse than that of original cancer. Emerging studies now indicate crucial contribution of APA changes in the appearance of tumor drug resistance. Apparently, 3′-UTR shortening promote drug resistance, whereas 3′-UTR lengthening induce sensitivity to drug treatment to a cancer cell (Hegi et al., 2005; Kreth et al., 2013; Passacantilli et al., 2017). For example, treatment of pancreatic ductal adenocarcinoma with gemcitabine affects global transcription and translation in cancer cells. Yet, a key metastatic regulator ZEB1 is induced by UTR shortening of *ZEB1* mRNA and contributing to drug resistance (Passacantilli et al., 2017). On the other hand, APA-induced 3′-UTR lengthening of *MGMT* mRNA increases sensitivity to Temezolomide treatment in glioblastoma (Hegi et al., 2005; Kreth et al., 2013). Furthermore, increase expression of *SLC9A1*, *CCSAP*, *NUP98*, *and PLD* from UTR-APA contributes to drug resistance in triple negative breast cancer (TNBC) when administered with paclitaxel (L. Wang, Lang, et al., 2020). Similarly, NSCLC cisplatin resistance or colon cancer Mitoxantron resistance is conferred by UTR shortening of *POLH* and *ABCG2* mRNAs (To et al., 2009; J. Zhang et al., 2019). Consistently, increased expression of proximal PA-site promoting factors (CSTF2) is observed in drug resistant cancers (Tan et al., 2017). PA-site selection is primarily mediated by differential expression of core CPA factors that include CSTF, CFIm and PABPN1 (H. B. Akman et al., 2015; Ichinose et al., 2014; Mao et al., 2020; Masamha et al., 2014; Miles

et al., 2016; Van Etten et al., 2017; S. Zhang et al., 2019). Moreover, depletion of proximal PA-site promoting CPA factors (CSTF2 or CPSF) can reverse widespread UTR shortening in cancer cells (H. B. Akman et al., 2015; S. L. Chen et al., 2021; Van Etten et al., 2017). Therefore, targeting this PA-site selection has tremendous therapeutic potential for combating drug resistance in a cancer treatment regime. This can be achieved through potent molecular inhibitors (chemical based or small RNA based) of APA regulators as adjuvant to the current antitumor drug regime. Molecular inhibitors of PA complex (cordycepin), small molecule HuR inhibitor (KH-3, MS-444), or CPSF inhibitor (JTE-607) are already known to have antitumor activity on different cancers (Imesch et al., 2011; Lang et al., 2017; Ross et al., 2020; X. Wu et al., 2020). Therefore, a combinatorial therapy of targeting APA-regulators in addition to the established anticancer drugs will be a way forward for successful cancer therapeutics.

9 | CONCLUDING REMARKS

This review highlights a widespread occurrence of APA in human diseases and role of APA switch as an important regulatory mechanism in disease pathogenesis. Examination of a disease-associated APA requires an overall understanding involving at least three aspects of APA of global or disease-specific genes. This includes (1) mechanism of PA site selection and pathological signal that drives this choice, (2) consequences of PA-site choice on transcript length, and (3) implication of transcript length variation on expression and function of regulator proteins in disease pathogenesis. Many APA regulators including core CPA factors cooperatively determine the PA-site choice-giving rise to a disease-specific APA profile. However, the upstream pathological signal that drives this coordinated control remains to be elucidated. Notably, studies have shown regulation of PA-site selection by genomic imprinting (Cowley et al., 2012; Wood et al., 2008). Considering the uniqueness in the disease-specific APA profiles, it is tempting to think that PA-site choice itself can be imprinted. Such case would show a potential disease-specific familial APA profile. While such finding will revolutionize the concept of hereditary diseases, it is still a theoretical perspective that needs further exploration. Moreover, APA basically leads to variation in the transcript length of disease causing genes. Nevertheless, most diseases have an associated global change in the transcript length indicating a wide network of APA regulation in the cell. This is particularly important considering the paradoxical effect of 3′-UTR length on resultant protein expression. A global APA switch appears to involve a large number of aberrant APA changes that likely contributes to the discrepancy. Understanding these molecular aspects is critical for examining application potential of APA in prognostication, diagnosis, and therapeutics of various diseases. This understanding will also help in finding suitable molecular targets that regulates any of the three aspects of disease-associated APA.

ACKNOWLEDGMENT

The authors thank Fiona Ukken (University of Maryland, USA) and RSL Lab members for carefully reading the manuscript. This work is supported by Swarnajayanti Fellowship (SB/SJF/2019-20/09) from the Department of Science and Technology, and SERB grant (CRG/2019/003230) to Rakesh S. Laishram. Neeraja K Mohanan is supported by Senior Research Fellowship from University Grant Commission, Feba Shaji by Junior Research Fellowship from the Council of Scientific Industrial and Research, India and Ganesh R. Koshre is supported by Senior Research Fellowship from Department of Biotechnology, India.

CONFLICT OF INTEREST

The authors declare no conflict of interest.

AUTHOR CONTRIBUTIONS

Neeraja K Mohanan: Conceptualization (equal); investigation (equal); methodology (equal); writing – original draft (equal); writing – review and editing (equal). **Feba Shaji:** Conceptualization (equal); investigation (equal); methodology (equal); writing – original draft (equal); writing – review and editing (equal). **Ganesh Koshre:** Writing – review and editing (supporting). **Rakesh Laishram:** Conceptualization (lead); formal analysis (lead); funding acquisition (lead); investigation (lead); methodology (lead); supervision (lead); validation (lead); writing – original draft (lead); writing – review and editing (lead).

DATA AVAILABILITY STATEMENT

Data sharing not applicable - no new data generated.

ORCID

Rakesh S. Laishram https://orcid.org/0000-0003-4124-0468

RELATED WIREs ARTICLES

Means to an end: mechanisms of alternative polyadenylation of messenger RNA precursors

REFERENCES

Abbass, S. A., Asa, S. L., & Ezzat, S. (1997). Altered expression of fibroblast growth factor receptors in human pituitary adenomas. *The Journal of Clinical Endocrinology and Metabolism*, *82*(4), 1160–1166. https://doi.org/10.1210/jcem.82.4.3896

Abbassi-Daloii, T., Yousefi, S., de Klerk, E., Grossouw, L., Riaz, M., t Hoen, P. A. C., & Raz, V. (2017). An alanine expanded PABPN1 causes increased utilization of intronic polyadenylation sites. *npj Aging and Mechanisms of Disease*, *3*, 6. https://doi.org/10.1038/s41514-017-0007-x

Abdel Wahab, N., Gibbs, J., & Mason, R. M. (1998). Regulation of gene expression by alternative polyadenylation and mRNA instability in hyperglycaemic mesangial cells. *The Biochemical Journal*, *336*(Pt 2), 405–411. https://doi.org/10.1042/bj3360405

Agra Andrieu, N., Motiño, O., Mayoral, R., Llorente Izquierdo, C., Fernández-Alvarez, A., Boscá, L., Casado, M., & Martín-Sanz, P. (2012). Cyclooxygenase-2 Is a Target of MicroRNA-16 in Human Hepatoma Cells. *PLoS ONE*, *7*(11), e50935. https://doi.org/10.1371/journal.pone.0050935

Akman, B. H., Can, T., & Erson-Bensan, A. E. (2012). Estrogen-induced upregulation and 3′-UTR shortening of CDC6. *Nucleic Acids Research*, *40*(21), 10679–10688. https://doi.org/10.1093/nar/gks855

Akman, H. B., Oyken, M., Tuncer, T., Can, T., & Erson-Bensan, A. E. (2015). 3′UTR shortening and EGF signaling: Implications for breast cancer. *Human Molecular Genetics*, *24*(24), 6910–6920. https://doi.org/10.1093/hmg/ddv391

Al-Ahmadi, W., Al-Ghamdi, M., Al-Haj, L., Al-Saif, M., & Khabar, K. S. (2009). Alternative polyadenylation variants of the RNA binding protein, HuR: Abundance, role of AU-rich elements and auto-regulation. *Nucleic Acids Research*, *37*(11), 3612–3624. https://doi.org/10.1093/nar/gkp223

Alcott, C. E., Yalamanchili, H. K., Ji, P., van der Heijden, M. E., Saltzman, A., Elrod, N., Lin, A., Leng, M., Bhatt, B., Hao, S., Wang, Q., Saliba, A., Tang, J., Malovannaya, A., Wagner, E. J., Liu, Z., & Zoghbi, H. Y. (2020). Partial loss of CFIm25 causes learning deficits and aberrant neuronal alternative polyadenylation. *eLife*, *9*, e50895. https://doi.org/10.7554/eLife.50895

Allen, M., Bird, C., Feng, W., Liu, G., Li, W., Perrone-Bizzozero, N. I., & Feng, Y. (2013). HuD promotes BDNF expression in brain neurons via selective stabilization of the BDNF long 3′UTR mRNA. *PLoS One*, *8*(1), e55718. https://doi.org/10.1371/journal.pone.0055718

Andres, S. F., Williams, K. N., Plesset, J. B., Headd, J. J., Mizuno, R., Chatterji, P., Lento, A. A., Klein-Szanto, A. J., Mick, R., Hamilton, K. E., & Rustgi, A. K. (2019). IMP1 3′ UTR shortening enhances metastatic burden in colorectal cancer. *Carcinogenesis*, *40*(4), 569–579. https://doi.org/10.1093/carcin/bgy153

Andreu, N., Garcia-Rodriguez, M., Volpini, V., Frecha, C., Molina, I. J., Fontan, G., & Fillat, C. (2006). A novel Wiskott-Aldrich syndrome protein (WASP) complex mutation identified in a WAS patient results in an aberrant product at the C-terminus from two transcripts with unusual polyA signals. *Journal of Human Genetics*, *51*(2), 92–97. https://doi.org/10.1007/s10038-005-0328-7

Anvar, S. Y., Raz, Y., Verway, N., van der Sluijs, B., Venema, A., Goeman, J. J., Vissing, J., van der Maarel, S. M., 't Hoen, P. A., van Engelen, B. G., & Raz, V. (2013). A decline in PABPN1 induces progressive muscle weakness in oculopharyngeal muscle dystrophy and in muscle aging. *Aging (Albany NY)*, *5*(6), 412–426. https://doi.org/10.18632/aging.100567

Baj, G., Leone, E., Chao, M. V., & Tongiorgi, E. (2011). Spatial segregation of BDNF transcripts enables BDNF to differentially shape distinct dendritic compartments. *Proceedings of the National Academy of Sciences of the United States of America*, *108*(40), 16813–16818. https://doi.org/10.1073/pnas.1014168108

Batra, R., Charizanis, K., Manchanda, M., Mohan, A., Li, M., Finn, D. J., Goodwin, M., Zhang, C., Sobczak, K., Thornton, C. A., & Swanson, M. S. (2014). Loss of MBNL leads to disruption of developmentally regulated alternative polyadenylation in RNA-mediated disease. *Molecular Cell*, *56*(2), 311–322. https://doi.org/10.1016/j.molcel.2014.08.027

Baudry, A., Mouillet-Richard, S., Schneider, B., Launay, J. M., & Kellermann, O. (2010). miR-16 targets the serotonin transporter: A new facet for adaptive responses to antidepressants. *Science*, *329*(5998), 1537–1541. https://doi.org/10.1126/science.1193692

Beaudoing, E., Freier, S., Wyatt, J. R., Claverie, J. M., & Gautheret, D. (2000). Patterns of variant polyadenylation signal usage in human genes. *Genome Research*, *10*(7), 1001–1010.

Begik, O., Oyken, M., Cinkilli Alican, T., Can, T., & Erson-Bensan, A. E. (2017). Alternative polyadenylation patterns for novel gene discovery and classification in cancer. *Neoplasia*, *19*(7), 574–582. https://doi.org/10.1016/j.neo.2017.04.008

Bennett, C. L., Brunkow, M. E., Ramsdell, F., O'Briant, K. C., Zhu, Q., Fuleihan, R. L., Shigeoka, A.O., & Chance, P. F. (2001). A rare polyadenylation signal mutation of the FOXP3 gene (AAUAAA→AAUGAA) leads to the IPEX syndrome. *Immunogenetics*, *53*(6), 435–439. https://doi.org/10.1007/s002510100358

Berkovits, B. D., & Mayr, C. (2015). Alternative 3′ UTRs act as scaffolds to regulate membrane protein localization. *Nature*, *522*(7556), 363–367. https://doi.org/10.1038/nature14321

Bosch, F., Jares, P., Campo, E., Lopez-Guillermo, A., Piris, M. A., Villamor, N., Tassies, D., Jaffe, E. S., Montserrat, E., & Rozman, C. (1994). PRAD-1/cyclin D1 gene overexpression in chronic lymphoproliferative disorders: A highly specific marker of mantle cell lymphoma. *Blood*, *84*(8), 2726–2732.

Brais, B., Bouchard, J. P., Xie, Y. G., Rochefort, D. L., Chretien, N., Tome, F. M., Lafrenière, R., Rommens, J. M, Uyama, E., Nohira, O., Blumen, S., Korczyn, A. D., Heutink, P., Mathieu, J., Duranceau, A., Codère, F., Fardeau, M., & Rouleau, G. A. (1998). Short GCG expansions in the PABP2 gene cause oculopharyngeal muscular dystrophy. *Nature Genetics*, *18*(2), 164–167. https://doi.org/10.1038/ng0298-164

Brown, K. M., & Gilmartin, G. M. (2003). A mechanism for the regulation of pre-mRNA 3′ processing by human cleavage factor Im. *Molecular Cell*, *12*(6), 1467–1476.

Busch, B., Bley, N., Muller, S., Glass, M., Misiak, D., Lederer, M., Vetter, M., Strauß, H. G., Thomssen, C., & Huttelmaier, S. (2016). The oncogenic triangle of HMGA2, LIN28B and IGF2BP1 antagonizes tumor-suppressive actions of the let-7 family. *Nucleic Acids Research*, *44*(8), 3845–3864. https://doi.org/10.1093/nar/gkw099

Calado, A., Tome, F. M., Brais, B., Rouleau, G. A., Kuhn, U., Wahle, E., & Carmo-Fonseca, M. (2000). Nuclear inclusions in oculopharyngeal muscular dystrophy consist of poly(A) binding protein 2 aggregates which sequester poly(A) RNA. *Human Molecular Genetics*, *9*(15), 2321–2328. https://doi.org/10.1093/oxfordjournals.hmg.a018924

Castelo-Branco, P., Furger, A., Wollerton, M., Smith, C., Moreira, A., & Proudfoot, N. (2004). Polypyrimidine tract binding protein modulates efficiency of polyadenylation. *Molecular and Cellular Biology*, *24*(10), 4174–4183. https://doi.org/10.1128/MCB.24.10.4174-4183.2004

Chan, S. L., Huppertz, I., Yao, C., Weng, L., Moresco, J. J., Yates, J. R., 3rd, Ule, J., Manley, J. L., & Shi, Y. (2014). CPSF30 and Wdr33 directly bind to AAUAAA in mammalian mRNA 3′ processing. *Genes & Development*, *28*(21), 2370–2380. https://doi.org/10.1101/gad.250993.114

Chang, J. Y., Yu, W. H., Juan, H. F., & Huang, H. C. (2018). Dynamics of alternative polyadenylation in human preimplantation embryos. *Biochemical and Biophysical Research Communications*, *504*(4), 727–733. https://doi.org/10.1016/j.bbrc.2018.09.027

Chatrikhi, R., Mallory, M. J., Gazzara, M. R., Agosto, L. M., Zhu, W. S., Litterman, A. J., Ansel, K. M., & Lynch, K. W. (2019). RNA binding protein CELF2 regulates signal-induced alternative polyadenylation by competing with enhancers of the polyadenylation machinery. *Cell Reports*, *28*(11), 2795–2806 e2793. https://doi.org/10.1016/j.celrep.2019.08.022

Chen, M., Lyu, G., Han, M., Nie, H., Shen, T., Chen, W., Niu, Y., Song, Y., Li, X., Li, H., Chen, X., Wang, Z., Xia, Z., Li, W., Tian, X., Ding, C., Gu, J., Zheng, Y., Liu, X., … Ni, T. (2018). 3′ UTR lengthening as a novel mechanism in regulating cellular senescence. *Genome Research*, *28*(3), 285–294. https://doi.org/10.1101/gr.224451.117

Chen, R. W., Bemis, L. T., Amato, C. M., Myint, H., Tran, H., Birks, D. K., Eckhardt, S. G., & Robinson, W. A. (2008). Truncation in CCND1 mRNA alters miR-16-1 regulation in mantle cell lymphoma. *Blood*, *112*(3), 822–829. https://doi.org/10.1182/blood-2008-03-142182

Chen, S., Wang, R., Zheng, D., Zhang, H., Chang, X., Wang, K., Li, W., Fan, J., Tian, B., & Cheng, H. (2019). The mRNA export receptor NXF1 coordinates transcriptional dynamics, alternative polyadenylation, and mRNA export. *Molecular Cell*, *74*(1), 118–131 e117. https://doi.org/10.1016/j.molcel.2019.01.026

Chen, S. L., Zhu, Z. X., Yang, X., Liu, L. L., He, Y. F., Yang, M. M., Guan, X. Y., Wang, X., & Yun, J. P. (2021). Cleavage and polyadenylation specific factor 1 promotes tumor progression via alternative polyadenylation and splicing in hepatocellular carcinoma. *Frontiers in Cell and Development Biology*, *9*, 616835. https://doi.org/10.3389/fcell.2021.616835

Chen, X., Zhang, J. X., Luo, J. H., Wu, S., Yuan, G. J., Ma, N. F., … Xie, D. (2018). CSTF2-induced shortening of the RAC1 3′UTR promotes the pathogenesis of urothelial carcinoma of the bladder. *Cancer Research*, *78*(20), 5848–5862. https://doi.org/10.1158/0008-5472.CAN-18-0822

Chu, Y., Elrod, N., Wang, C., Li, L., Chen, T., Routh, A., Xia, Z., Li, W., Wagner, E. J., & Ji, P. (2019). Nudt21 regulates the alternative polyadenylation of Pak1 and is predictive in the prognosis of glioblastoma patients. *Oncogene*, *38*(21), 4154–4168. https://doi.org/10.1038/s41388-019-0714-9

Chuvpilo, S., Zimmer, M., Kerstan, A., Glockner, J., Avots, A., Escher, C., Fischer, C., Inashkina, I., Jankevics, E., Berberich-Siebelt, F., Schmitt, E., & Serfling, E. (1999). Alternative polyadenylation events contribute to the induction of NF-ATc in effector T cells. *Immunity*, *10*(2), 261–269. https://doi.org/10.1016/s1074-7613(00)80026-6

Ciolli Mattioli, C., Rom, A., Franke, V., Imami, K., Arrey, G., Terne, M., Woehler, A., Akalin, A., Ulitsky, I., & Chekulaeva, M. (2019). Alternative 3′ UTRs direct localization of functionally diverse protein isoforms in neuronal compartments. *Nucleic Acids Research*, *47*(5), 2560–2573. https://doi.org/10.1093/nar/gky1270

Clerici, M., Faini, M., Muckenfuss, L. M., Aebersold, R., & Jinek, M. (2018). Structural basis of AAUAAA polyadenylation signal recognition by the human CPSF complex. *Nature Structural & Molecular Biology*, *25*(2), 135–138. https://doi.org/10.1038/s41594-017-0020-6

Colgan, D. F., & Manley, J. L. (1997). Mechanism and regulation of mRNA polyadenylation. *Genes & Development*, *11*(21), 2755–2766.

Cowley, M., Wood, A. J., Bohm, S., Schulz, R., & Oakey, R. J. (2012). Epigenetic control of alternative mRNA processing at the imprinted Herc3/Nap1l5 locus. *Nucleic Acids Research*, *40*(18), 8917–8926. https://doi.org/10.1093/nar/gks654

Creemers, E. E., Bawazeer, A., Ugalde, A. P., van Deutekom, H. W., van der Made, I., de Groot, N. E., Adriaens, M. E., Cook, S. A, Bezzina, C. R., Hubner, N., van der Velden, J., Elkon, R., Agami, R., & Pinto, Y. M. (2016). Genome-wide polyadenylation maps reveal dynamic mRNA 3′-end formation in the failing human heart. *Circulation Research*, *118*(3), 433–438. https://doi.org/10.1161/CIRCRESAHA.115.307082

Cunninghame Graham, D. S., Manku, H., Wagner, S., Reid, J., Timms, K., Gutin, A., Lanchbury, J. S., & Vyse, T. J. (2007). Association of IRF5 in UKSLE families identifies a variant involved in polyadenylation. *Human Molecular Genetics*, *16*(6), 579–591. https://doi.org/10.1093/hmg/ddl469

Dai, W., Zhang, G., & Makeyev, E. V. (2012). RNA-binding protein HuR autoregulates its expression by promoting alternative polyadenylation site usage. *Nucleic Acids Research*, *40*(2), 787–800. https://doi.org/10.1093/nar/gkr783

de Klerk, E., Venema, A., Anvar, S. Y., Goeman, J. J., Hu, O., Trollet, C., Dickson, G., den Dunnen, J. T., van der Maarel, S. M., Raz, V., & t Hoen, P. A. (2012). Poly(A) binding protein nuclear 1 levels affect alternative polyadenylation. *Nucleic Acids Research*, *40*(18), 9089–9101. https://doi.org/10.1093/nar/gks655

de Vries, H., Ruegsegger, U., Hubner, W., Friedlein, A., Langen, H., & Keller, W. (2000). Human pre-mRNA cleavage factor II(m) contains homologs of yeast proteins and bridges two other cleavage factors. *The EMBO Journal*, *19*(21), 5895–5904. https://doi.org/10.1093/emboj/19.21.5895

DeJesus-Hernandez, M., Mackenzie, I. R., Boeve, B. F., Boxer, A. L., Baker, M., Rutherford, N. J., Nicholson, A. M., Finch, N. C. A., Flynn, H., Adamson, J., Kouri, N., Wojtas, A., Sengdy, P., Hsiung, G. Y. R., Karydas, A., Seeley, W. W., Josephs, K. A., Coppola, G., Geschwind, D. H., … Rademakers, R. (2011). Expanded GGGGCC hexanucleotide repeat in noncoding region of C9ORF72 causes chromosome 9p-linked FTD and ALS. *Neuron*, *72*(2), 245–256. https://doi.org/10.1016/j.neuron.2011.09.011

Dell'Orco, M., Sardone, V., Gardiner, A. S., Pansarasa, O., Bordoni, M., Perrone-Bizzozero, N. I., & Cereda, C. (2021). HuD regulates SOD1 expression during oxidative stress in differentiated neuroblastoma cells and sporadic ALS motor cortex. *Neurobiology of Disease*, *148*, 105211. https://doi.org/10.1016/j.nbd.2020.105211

Denkert, C., Koch, I., von Keyserlingk, N., Noske, A., Niesporek, S., Dietel, M., & Weichert, W. (2006). Expression of the ELAV-like protein HuR in human colon cancer: Association with tumor stage and cyclooxygenase-2. *Modern Pathology*, *19*(9), 1261–1269. https://doi.org/10.1038/modpathol.3800645

Deo, R. C., Bonanno, J. B., Sonenberg, N., & Burley, S. K. (1999). Recognition of polyadenylate RNA by the poly(A)-binding protein. *Cell*, *98*(6), 835–845. https://doi.org/10.1016/s0092-8674(00)81517-2

Derti, A., Garrett-Engele, P., Macisaac, K. D., Stevens, R. C., Sriram, S., Chen, R., Rohl, C. A., Johnson, J. M., & Babak, T. (2012). A quantitative atlas of polyadenylation in five mammals. *Genome Research*, *22*(6), 1173–1183. https://doi.org/10.1101/gr.132563.111

Devany, E., Park, J. Y., Murphy, M. R., Zakusilo, G., Baquero, J., Zhang, X., Hoque, M., Tian, B., & Kleiman, F. E. (2016). Intronic cleavage and polyadenylation regulates gene expression during DNA damage response through U1 snRNA. *Cell Discov*, *2*, 16013. https://doi.org/10.1038/celldisc.2016.13

Di Giammartino, D. C., Li, W., Ogami, K., Yashinskie, J. J., Hoque, M., Tian, B., & Manley, J. L. (2014). RBBP6 isoforms regulate the human polyadenylation machinery and modulate expression of mRNAs with AU-rich 3′ UTRs. *Genes & Development*, *28*(20), 2248–2260. https://doi.org/10.1101/gad.245787.114

Di Giammartino, D. C., Nishida, K., & Manley, J. L. (2011). Mechanisms and consequences of alternative polyadenylation. *Molecular Cell*, *43*(6), 853–866.

Dickson, J. R., Kruse, C., Montagna, D. R., Finsen, B., & Wolfe, M. S. (2013). Alternative polyadenylation and miR-34 family members regulate tau expression. *Journal of Neurochemistry*, *127*(6), 739–749. https://doi.org/10.1111/jnc.12437

Doherty, J. K., Bond, C. T., Hua, W., Adelman, J. P., & Clinton, G. M. (1999). An alternative HER-2/neu transcript of 8 kb has an extended 3′UTR and displays increased stability in SKOV-3 ovarian carcinoma cells. *Gynecologic Oncology*, *74*(3), 408–415. https://doi.org/10.1006/gyno.1999.5467

Dormoy-Raclet, V., Menard, I., Clair, E., Kurban, G., Mazroui, R., Di Marco, S., von Roretz, C., Pause, A., & Gallouzi, I. E. (2007). The RNA-binding protein HuR promotes cell migration and cell invasion by stabilizing the beta-actin mRNA in a U-rich-element-dependent manner. *Molecular and Cellular Biology*, *27*(15), 5365–5380. https://doi.org/10.1128/MCB.00113-07

Druhan, L. J., Lance, A., Hamilton, A., Steuerwald, N. M., Tjaden, E., & Avalos, B. R. (2020). Altered splicing and intronic polyadenylation of CSF3R via a cryptic exon in acute myeloid leukemia. *Leukemia Research*, *92*, 106349. https://doi.org/10.1016/j.leukres.2020.106349

Elkon, R., Drost, J., van Haaften, G., Jenal, M., Schrier, M., Oude Vrielink, J. A., & Agami, R. (2012). E2F mediates enhanced alternative polyadenylation in proliferation. *Genome Biology*, *13*(7), R59. https://doi.org/10.1186/gb-2012-13-7-r59

Fahiminiya, S., Al-Jallad, H., Majewski, J., Palomo, T., Moffatt, P., Roschger, P., Klaushofer, K., Glorieux, F. H., & Rauch, F. (2015). A polyadenylation site variant causes transcript-specific BMP1 deficiency and frequent fractures in children. *Human Molecular Genetics*, *24*(2), 516–524. https://doi.org/10.1093/hmg/ddu471

Fan, Z., Kim, S., Bai, Y., Diergaarde, B., & Park, H. J. (2020). 3′-UTR shortening contributes to subtype-specific cancer growth by breaking stable ceRNA crosstalk of housekeeping genes. *Frontiers in Bioengineering and Biotechnology*, *8*, 334. https://doi.org/10.3389/fbioe.2020.00334

Fang, S., Zhang, D., Weng, W., Lv, X., Zheng, L., Chen, M., Fan, X., Mao, J., Mao, C., Ye, Y., Xu, M., & Ji, J. (2020). CPSF7 regulates liver cancer growth and metastasis by facilitating WWP2-FL and targeting the WWP2/PTEN/AKT signaling pathway. *Biochimica et Biophysica Acta—Molecular Cell Research*, *1867*(2), 118624. https://doi.org/10.1016/j.bbamcr.2019.118624

Fischl, H., Neve, J., Wang, Z., Patel, R., Louey, A., Tian, B., & Furger, A. (2019). hnRNPC regulates cancer-specific alternative cleavage and polyadenylation profiles. *Nucleic Acids Research*, *47*(14), 7580–7591. https://doi.org/10.1093/nar/gkz461

Flavell, S. W., Kim, T. K., Gray, J. M., Harmin, D. A., Hemberg, M., Hong, E. J., Markenscoff-Papadimitriou, E., Bear, D. M., & Greenberg, M. E. (2008). Genome-wide analysis of MEF2 transcriptional program reveals synaptic target genes and neuronal activity-dependent polyadenylation site selection. *Neuron*, *60*(6), 1022–1038. https://doi.org/10.1016/j.neuron.2008.11.029

Fu, Y., Chen, L., Chen, C., Ge, Y., Kang, M., Song, Z., Li, J., Feng, Y., Huo, Z., He, G., Hou, M., Chen, S., & Xu, A. (2018). Crosstalk between alternative polyadenylation and miRNAs in the regulation of protein translational efficiency. *Genome Research*, *28*(11), 1656–1663. https://doi.org/10.1101/gr.231506.117

Fu, Y., Sun, Y., Li, Y., Li, J., Rao, X., Chen, C., & Xu, A. (2011). Differential genome-wide profiling of tandem 3′ UTRs among human breast cancer and normal cells by high-throughput sequencing. *Genome Research*, *21*(5), 741–747. https://doi.org/10.1101/gr.115295.110

Fusby, B., Kim, S., Erickson, B., Kim, H., Peterson, M. L., & Bentley, D. L. (2016). Coordination of RNA polymerase II pausing and 3′ end processing factor recruitment with alternative polyadenylation. *Molecular and Cellular Biology*, *36*(2), 295–303. https://doi.org/10.1128/MCB.00898-15

Ganapathi Sankaran, D., Stemm-Wolf, A. J., & Pearson, C. G. (2019). CEP135 isoform dysregulation promotes centrosome amplification in breast cancer cells. *Molecular Biology of the Cell*, *30*(10), 1230–1244. https://doi.org/10.1091/mbc.E18-10-0674

Garin, I., Edghill, E. L., Akerman, I., Rubio-Cabezas, O., Rica, I., Locke, J. M., Maestro, M. A., Alshaikh, A., Bundak, R., del Castillo, G., Deeb, A., Deiss, D., Fernandez, J. M., Godbole, K., Hussain, K., O'Connell, M., Klupa, T., Kolouskova, S., Mohsin, F., ... Hattersley, A. T. (2010). Recessive mutations in the INS gene result in neonatal diabetes through reduced insulin biosynthesis. *Proceedings of the National Academy of Sciences of the United States of America*, *107*(7), 3105–3110. https://doi.org/10.1073/pnas.0910533107

Gartner, W., Mineva, I., Daneva, T., Baumgartner-Parzer, S., Niederle, B., Vierhapper, H., Weissel, M., & Wagner, L. (2005). A newly identified RET proto-oncogene polymorphism is found in a high number of endocrine tumor patients. *Human Genetics*, *117*(2–3), 143–153. https://doi.org/10.1007/s00439-005-1280-5

Ge, W., Chen, M., Tian, W., Chen, J., Zhao, Y., Xian, H., Chen, J., & Xu, Y. (2021). Global 3'UTR shortening and down-regulation of repeated element related piRNA play crucial roles in boys with cryptorchidism. *Genomics*, *113*(2), 633–645. https://doi.org/10.1016/j.ygeno.2021.01.006

Gehring, N. H., Frede, U., Neu-Yilik, G., Hundsdoerfer, P., Vetter, B., Hentze, M. W., & Kulozik, A. E. (2001). Increased efficiency of mRNA 3′ end formation: A new genetic mechanism contributing to hereditary thrombophilia. *Nature Genetics*, *28*(4), 389–392. https://doi.org/10.1038/ng578

Gennarino, V. A., Alcott, C. E., Chen, C. A., Chaudhury, A., Gillentine, M. A., Rosenfeld, J. A., Parikh, S., Wheless, J. W., Roeder, E. R., Horovitz, D. D. G., Roney, E. K., Smith, J. L., Cheung, S. W., Li, W., Neilson, J. R., Schaaf, C. P., & Zoghbi, H. Y. (2015). NUDT21-spanning CNVs lead to neuropsychiatric disease and altered MeCP2 abundance via alternative polyadenylation. *eLife*, *4*, e10782. https://doi.org/10.7554/eLife.10782

Gillen, A. E., Brechbuhl, H. M., Yamamoto, T. M., Kline, E., Pillai, M. M., Hesselberth, J. R., & Kabos, P. (2017). Alternative polyadenylation of PRELID1 regulates mitochondrial ROS signaling and cancer outcomes. *Molecular Cancer Research*, *15*(12), 1741–1751. https://doi.org/10.1158/1541-7786.MCR-17-0010

Glover-Cutter, K., Kim, S., Espinosa, J., & Bentley, D. L. (2008). RNA polymerase II pauses and associates with pre-mRNA processing factors at both ends of genes. *Nature Structural & Molecular Biology*, *15*(1), 71–78. doi:nsmb1352 [pii]. https://doi.org/10.1038/nsmb1352

Graham, R. R., Kyogoku, C., Sigurdsson, S., Vlasova, I. A., Davies, L. R. L., Baechler, E. C., Plenge, R. M., Koeuth, T., Ortmann, W. A., Hom, G., Bauer, J. W., Gillett, C., Burtt, N., Cunninghame Graham, D. S., Onofrio, R., Petri, M., Gunnarsson, I., Svenungsson, E., Ronnblom, L., ... Altshuler, D. (2007). Three functional variants of IFN regulatory factor 5 (IRF5) define risk and protective haplotypes for human lupus. *Proceedings of the National Academy of Sciences*, *104*(16), 6758–6763. https://doi.org/10.1073/pnas.0701266104

Gregersen, L. H., Mitter, R., Ugalde, A. P., Nojima, T., Proudfoot, N. J., Agami, R., Stewart, A., & Svejstrup, J. Q. (2019). SCAF4 and SCAF8, mRNA anti-terminator proteins. *Cell*, *177*(7), 1797–1813 e1718. https://doi.org/10.1016/j.cell.2019.04.038

Grozdanov, P. N., Masoumzadeh, E., Kalscheuer, V. M., Bienvenu, T., Billuart, P., Delrue, M. A., Latham, M. P., & MacDonald, C. C. (2020). A missense mutation in the CSTF2 gene that impairs the function of the RNA recognition motif and causes defects in 3′ end processing is associated with intellectual disability in humans. *Nucleic Acids Research*, *48*(17), 9804–9821. https://doi.org/10.1093/nar/gkaa689

Gruber, A. J., Schmidt, R., Ghosh, S., Martin, G., Gruber, A. R., van Nimwegen, E., & Zavolan, M. (2018). Discovery of physiological and cancer-related regulators of 3′ UTR processing with KAPAC. *Genome Biology*, *19*(1), 44. https://doi.org/10.1186/s13059-018-1415-3

Gruber, A. J., Schmidt, R., Gruber, A. R., Martin, G., Ghosh, S., Belmadani, M., Keller, W., & Zavolan, M. (2016). A comprehensive analysis of 3′ end sequencing data sets reveals novel polyadenylation signals and the repressive role of heterogeneous ribonucleoprotein C on cleavage and polyadenylation. *Genome Research*, *26*(8), 1145–1159. https://doi.org/10.1101/gr.202432.115

Gruber, A. R., Martin, G., Keller, W., & Zavolan, M. (2012). Cleavage factor Im is a key regulator of 3′ UTR length. *RNA Biology*, *9*(12), 1405–1412. https://doi.org/10.4161/rna.22570

Gruber, A. R., Martin, G., Muller, P., Schmidt, A., Gruber, A. J., Gumienny, R., Mittal, N., Jayachandran, R., Pieters, J., Keller, W., van Nimwegen, E., & Zavolan, M. (2014). Global 3′ UTR shortening has a limited effect on protein abundance in proliferating T cells. *Nature Communications*, *5*, 5465. https://doi.org/10.1038/ncomms6465

Gunderson, S. I., Beyer, K., Martin, G., Keller, W., Boelens, W. C., & Mattaj, L. W. (1994). The human U1A snRNP protein regulates polyadenylation via a direct interaction with poly(A) polymerase. *Cell*, *76*(3), 531–541.

Gunderson, S. I., Polycarpou-Schwarz, M., & Mattaj, I. W. (1998). U1 snRNP inhibits pre-mRNA polyadenylation through a direct interaction between U1 70K and poly(A) polymerase. *Molecular Cell*, *1*(2), 255–264.

Gupta, I., Clauder-Munster, S., Klaus, B., Jarvelin, A. I., Aiyar, R. S., Benes, V., Wilkening, S., Huber, W., Pelechano, V., & Steinmetz, L. M. (2014). Alternative polyadenylation diversifies post-transcriptional regulation by selective RNA-protein interactions. *Molecular Systems Biology*, *10*, 719. https://doi.org/10.1002/msb.135068

Gyawali, S., Subaran, R., Weissman, M. M., Hershkowitz, D., McKenna, M. C., Talati, A., Fyer, A. J., Wickramaratne, P., Adams, P. B., Hodge, S. E., Schmidt, C. J., Bannon, M. J., & Glatt, C. E. (2010). Association of a polyadenylation polymorphism in the serotonin transporter and panic disorder. *Biological Psychiatry*, *67*(4), 331–338. https://doi.org/10.1016/j.biopsych.2009.10.015

Halees, A. S., Hitti, E., Al-Saif, M., Mahmoud, L., Vlasova-St Louis, I. A., Beisang, D. J., Bohjanen, P. R., & Khabar, K. (2011). Global assessment of GU-rich regulatory content and function in the human transcriptome. *RNA Biology*, *8*(4), 681–691. https://doi.org/10.4161/rna.8.4.16283

Hall-Pogar, T., Liang, S., Hague, L. K., & Lutz, C. S. (2007). Specific trans-acting proteins interact with auxiliary RNA polyadenylation elements in the COX-2 3'-UTR. *RNA*, *13*(7), 1103–1115. https://doi.org/10.1261/rna.577707

Hamaya, Y., Kuriyama, S., Takai, T., Yoshida, K., Yamada, T., Sugimoto, M., Osawa, S., Sugimoto, K., Miyajima, H., & Kanaoka, S. (2012). A distinct expression pattern of the long 3′-untranslated region dicer mRNA and its implications for posttranscriptional regulation in colorectal cancer. *Clinical and Translational Gastroenterology*, *3*, e17. https://doi.org/10.1038/ctg.2012.12

Han, B., Shen, Y., Zhang, P., Jayabal, P., Che, R., Zhang, J., Yu, H., & Fei, P. (2017). Overlooked FANCD2 variant encodes a promising, portent tumor suppressor, and alternative polyadenylation contributes to its expression. *Oncotarget*, *8*(14), 22490–22500. https://doi.org/10.18632/oncotarget.14989

Harker, W. G., Slade, D. L., Parr, R. L., & Holguin, M. H. (1995). Selective use of an alternative stop codon and polyadenylation signal within intron sequences leads to a truncated topoisomerase II alpha messenger RNA and protein in human HL-60 leukemia cells selected for resistance to mitoxantrone. *Cancer Research*, *55*(21), 4962–4971.

Hartley, C. A., McKenna, M. C., Salman, R., Holmes, A., Casey, B. J., Phelps, E. A., & Glatt, C. E. (2012). Serotonin transporter polyadenylation polymorphism modulates the retention of fear extinction memory. *Proceedings of the National Academy of Sciences of the United States of America*, *109*(14), 5493–5498. https://doi.org/10.1073/pnas.1202044109

He, X., Yang, J., Zhang, Q., Cui, H., & Zhang, Y. (2014). Shortening of the 3′ untranslated region: An important mechanism leading to overexpression of HMGA2 in serous ovarian cancer. *Chinese Medical Journal*, *127*(3), 494–499.

He, X. J., Zhang, Q., Ma, L. P., Li, N., Chang, X. H., & Zhang, Y. J. (2016). Aberrant alternative polyadenylation is responsible for Survivin up-regulation in ovarian cancer. *Chinese Medical Journal*, *129*(10), 1140–1146. https://doi.org/10.4103/0366-6999.181965

Hegi, M. E., Diserens, A. C., Gorlia, T., Hamou, M. F., de Tribolet, N., Weller, M., Kros, J. M., Hainfellner, J. A., Mason, W., Mariani, L., Bromberg, J. E. C., Hau, P., Mirimanoff, R. O., Cairncross, J. G., Janzer, R. C., & Stupp, R. (2005). MGMT gene silencing and benefit from temozolomide in glioblastoma. *The New England Journal of Medicine*, *352*(10), 997–1003. https://doi.org/10.1056/NEJMoa043331

Heinonen, M., Bono, P., Narko, K., Chang, S. H., Lundin, J., Joensuu, H., Furneaux, H., Hla, T., Haglund, C., & Ristimaki, A. (2005). Cytoplasmic HuR expression is a prognostic factor in invasive ductal breast carcinoma. *Cancer Research*, *65*(6), 2157–2161. https://doi.org/10.1158/0008-5472.CAN-04-3765

Hellquist, A., Zucchelli, M., Kivinen, K., Saarialho-Kere, U., Koskenmies, S., Widen, E., Julkunen, H., Wong, A., Karjalainen-Lindsberg, M. L., Skoog, T., Vendelin, J., Cunninghame-Graham, D. S., Vyse, T. J., Kere, J., & Lindgren, C. M. (2007). The human GIMAP5 gene has a common polyadenylation polymorphism increasing risk to systemic lupus erythematosus. *Journal of Medical Genetics*, *44*(5), 314–321. https://doi.org/10.1136/jmg.2006.046185

Higgs, D. R., Goodbourn, S. E., Lamb, J., Clegg, J. B., Weatherall, D. J., & Proudfoot, N. J. (1983). Alpha-thalassaemia caused by a polyadenylation signal mutation. *Nature*, *306*(5941), 398–400.

Hirai, T., Mulpuri, Y., Cheng, Y., Xia, Z., Li, W., Ruangsri, S., Spigelman, I., & Nishimura, I. (2017). Aberrant plasticity of peripheral sensory axons in a painful neuropathy. *Scientific Reports*, *7*(1), 3407. https://doi.org/10.1038/s41598-017-03390-9

Ho, T. H., Kapur, P., Joseph, R. W., Serie, D. J., Eckel-Passow, J. E., Tong, P., Wang, J., Castle, E. P., Stanton, M. L., Cheville, J. C., Jonasch, E., Brugarolas, J., & Parker, A. S. (2016). Loss of histone H3 lysine 36 trimethylation is associated with an increased risk of renal cell carcinoma-specific death. *Modern Pathology*, *29*(1), 34–42. https://doi.org/10.1038/modpathol.2015.123

Hoffman, Y., Bublik, D. R., Ugalde, A. P., Elkon, R., Biniashvili, T., Agami, R., Oren, M., & Pilpel, Y. (2016). 3′UTR shortening potentiates MicroRNA-based repression of pro-differentiation genes in proliferating human cells. *PLoS Genetics*, *12*(2), e1005879. https://doi.org/10.1371/journal.pgen.1005879

Hollerer, I., Curk, T., Haase, B., Benes, V., Hauer, C., Neu-Yilik, G., Bhuvanagiri, M., Hentze, M. W., & Kulozik, A. E. (2016). The differential expression of alternatively polyadenylated transcripts is a common stress-induced response mechanism that modulates mammalian mRNA expression in a quantitative and qualitative fashion. *RNA*, *22*(9), 1441–1453. https://doi.org/10.1261/rna.055657.115

Hoque, M., Ji, Z., Zheng, D., Luo, W., Li, W., You, B., Park, J. Y., Yehia, G., & Tian, B. (2013). Analysis of alternative cleavage and polyadenylation by 3′ region extraction and deep sequencing. *Nature Methods*, *10*(2), 133–139. https://doi.org/10.1038/nmeth.2288

Housman, G., Byler, S., Heerboth, S., Lapinska, K., Longacre, M., Snyder, N., & Sarkar, S. (2014). Drug resistance in cancer: An overview. *Cancers (Basel)*, *6*(3), 1769–1792. https://doi.org/10.3390/cancers6031769

Hu, W., Li, S., Park, J. Y., Boppana, S., Ni, T., Li, M., Zhu, J., Tian, B., Xie, Z., & Xiang, M. (2017). Dynamic landscape of alternative polyadenylation during retinal development. *Cellular and Molecular Life Sciences*, *74*(9), 1721–1739. https://doi.org/10.1007/s00018-016-2429-1

Huang, H., Chen, J., Liu, H., & Sun, X. (2013). The nucleosome regulates the usage of polyadenylation sites in the human genome. *BMC Genomics*, *14*, 912. https://doi.org/10.1186/1471-2164-14-912

Huang, J., Weng, T., Ko, J., Chen, N. Y., Xiang, Y., Volcik, K., Han, L., Blackburn, M. R., & Lu, X. (2018). Suppression of cleavage factor Im 25 promotes the proliferation of lung cancer cells through alternative polyadenylation. *Biochemical and Biophysical Research Communications*, *503*(2), 856–862. https://doi.org/10.1016/j.bbrc.2018.06.087

Huang, W., Rainbow, D. B., Wu, Y., Adams, D., Shivakumar, P., Kottyan, L., Karns, R., Aronow, B., Bezerra, J., Gershwin, M. E., Peterson, L. B., Wicker, L. S., & Ridgway, W. M. (2018). A novel Pkhd1 mutation interacts with the nonobese diabetic genetic background to cause autoimmune cholangitis. *Journal of Immunology*, *200*(1), 147–162. https://doi.org/10.4049/jimmunol.1701087

Hwang, H. W., Park, C. Y., Goodarzi, H., Fak, J. J., Mele, A., Moore, M. J., Saito, Y., & Darnell, R. B. (2016). PAPERCLIP identifies MicroRNA targets and a role of CstF64/64tau in promoting non-canonical poly(A) site usage. *Cell Reports*, *15*(2), 423–435. https://doi.org/10.1016/j.celrep.2016.03.023

Ichinose, J., Watanabe, K., Sano, A., Nagase, T., Nakajima, J., Fukayama, M., Yatomi, Y., Ohishi, N., & Takai, D. (2014). Alternative polyadenylation is associated with lower expression of PABPN1 and poor prognosis in non-small cell lung cancer. *Cancer Science*, *105*(9), 1135–1141. https://doi.org/10.1111/cas.12472

Ilm, K., Fuchs, S., Mudduluru, G., & Stein, U. (2016). MACC1 is post-transcriptionally regulated by miR-218 in colorectal cancer. *Oncotarget*, *7*(33), 53443–53458. https://doi.org/10.18632/oncotarget.10803

Imesch, P., Hornung, R., Fink, D., & Fedier, A. (2011). Cordycepin (3′-deoxyadenosine), an inhibitor of mRNA polyadenylation, suppresses proliferation and activates apoptosis in human epithelial endometriotic cells in vitro. *Gynecologic and Obstetric Investigation*, *72*(1), 43–49. https://doi.org/10.1159/000322395

Ishizaka, Y., Itoh, F., Tahira, T., Ikeda, I., Ogura, T., Sugimura, T., & Nagao, M. (1989). Presence of aberrant transcripts of ret proto-oncogene in a human papillary thyroid carcinoma cell line. *Japanese Journal of Cancer Research*, *80*(12), 1149–1152. https://doi.org/10.1111/j.1349-7006.1989.tb01645.x

Jenal, M., Elkon, R., Loayza-Puch, F., van Haaften, G., Kuhn, U., Menzies, F. M., Oude Vrielink, J. A., Bos, A. J., Drost, J., Rooijers, K., Rubinsztein, D. C., & Agami, R. (2012). The poly(A)-binding protein nuclear 1 suppresses alternative cleavage and polyadenylation sites. *Cell*, *149*(3), 538–553. https://doi.org/10.1016/j.cell.2012.03.022

Jenny, A., Hauri, H. P., & Keller, W. (1994). Characterization of cleavage and polyadenylation specificity factor and cloning of its 100-kilodalton subunit. *Molecular and Cellular Biology*, *14*(12), 8183–8190. https://doi.org/10.1128/mcb.14.12.8183-8190.1994

Ji, Z., Luo, W., Li, W., Hoque, M., Pan, Z., Zhao, Y., & Tian, B. (2011). Transcriptional activity regulates alternative cleavage and polyadenylation. *Molecular Systems Biology*, *7*, 534. https://doi.org/10.1038/msb.2011.69

Ji, Z., & Tian, B. (2009). Reprogramming of 3′ untranslated regions of mRNAs by alternative polyadenylation in generation of pluripotent stem cells from different cell types. *PLoS One*, *4*(12), e8419. https://doi.org/10.1371/journal.pone.0008419

Jia, Q., Nie, H., Yu, P., Xie, B., Wang, C., Yang, F., Wei, G., & Ni, T. (2019). HNRNPA1-mediated 3′ UTR length changes of HN1 contributes to cancer- and senescence-associated phenotypes. *Aging (Albany NY)*, *11*(13), 4407–4437. https://doi.org/10.18632/aging.102060

Jia, X., Yuan, S., Wang, Y., Fu, Y., Ge, Y., Ge, Y., Lan, X., Feng, Y., Qiu, F., Li, P., Chen, S., & Xu, A. (2017). The role of alternative polyadenylation in the antiviral innate immune response. *Nature Communications*, *8*, 14605. https://doi.org/10.1038/ncomms14605

Jutzi, D., Campagne, S., Schmidt, R., Reber, S., Mechtersheimer, J., Gypas, F., Schweingruber, C., Colombo, M., von Schroetter, C., Loughlin, F. E., Devoy, A., Hedlund, E., Zavolan, M., Allain, F. H. T., & Ruepp, M. D. (2020). Aberrant interaction of FUS with the U1 snRNA provides a molecular mechanism of FUS induced amyotrophic lateral sclerosis. *Nature Communications*, *11*(1), 6341. https://doi.org/10.1038/s41467-020-20191-3

Kaida, D., Berg, M. G., Younis, I., Kasim, M., Singh, L. N., Wan, L., & Dreyfuss, G. (2010). U1 snRNP protects pre-mRNAs from premature cleavage and polyadenylation. *Nature*, *468*(7324), 664–668. https://doi.org/10.1038/nature09479nature09479

Kaufmann, I., Martin, G., Friedlein, A., Langen, H., & Keller, W. (2004). Human Fip1 is a subunit of CPSF that binds to U-rich RNA elements and stimulates poly(A) polymerase. *The EMBO Journal*, *23*(3), 616–626. https://doi.org/10.1038/sj.emboj.76000707600070

Ke, S., Alemu, E. A., Mertens, C., Gantman, E. C., Fak, J. J., Mele, A., Haripal, B., Zucker-Scharff, I., Moore, M. J., Park, C. Y., Vågbø, C. B., Kusśnierczyk, A., Klungland, A., Darnell, J. E., Jr., & Darnell, R. B. (2015). A majority of m6A residues are in the last exons, allowing the potential for 3′ UTR regulation. *Genes & Development*, *29*(19), 2037–2053. https://doi.org/10.1101/gad.269415.115

Keller, W., Bienroth, S., Lang, K. M., & Christofori, G. (1991). Cleavage and polyadenylation factor CPF specifically interacts with the pre-mRNA 3′ processing signal AAUAAA. *The EMBO Journal*, *10*(13), 4241–4249.

Kerwitz, Y., Kuhn, U., Lilie, H., Knoth, A., Scheuermann, T., Friedrich, H., Schwarz, E., & Wahle, E. (2003). Stimulation of poly(A) polymerase through a direct interaction with the nuclear poly(A) binding protein allosterically regulated by RNA. *The EMBO Journal*, *22*(14), 3705–3714.

Kim, N., Chung, W., Eum, H. H., Lee, H. O., & Park, W. Y. (2019). Alternative polyadenylation of single cells delineates cell types and serves as a prognostic marker in early stage breast cancer. *PLoS One*, *14*(5), e0217196. https://doi.org/10.1371/journal.pone.0217196

Kim, S., Yamamoto, J., Chen, Y., Aida, M., Wada, T., Handa, H., & Yamaguchi, Y. (2010). Evidence that cleavage factor Im is a heterotetrameric protein complex controlling alternative polyadenylation. *Genes to Cells*, *15*(9), 1003–1013. https://doi.org/10.1111/j.1365-2443.2010.01436.x

Koga, M., Satoh, T., Takasaki, I., Kawamura, Y., Yoshida, M., & Kaida, D. (2014). U2 snRNP is required for expression of the 3′ end of genes. *PLoS One*, *9*(5), e98015. https://doi.org/10.1371/journal.pone.0098015

Kolev, N. G., Yario, T. A., Benson, E., & Steitz, J. A. (2008). Conserved motifs in both CPSF73 and CPSF100 are required to assemble the active endonuclease for histone mRNA 3′-end maturation. *EMBO Reports*, *9*(10), 1013–1018. https://doi.org/10.1038/embor.2008.146

Komini, C., Theohari, I., Lambrianidou, A., Nakopoulou, L., & Trangas, T. (2021). PAPOLA contributes to cyclin D1 mRNA alternative polyadenylation and promotes breast cancer cells proliferation. *Journal of Cell Science*, *134*(7), jcs252304. https://doi.org/10.1242/jcs.252304

Kraynik, S. M., Gabanic, A., Anthony, S. R., Kelley, M., Paulding, W. R., Roessler, A., McGuinness, M., & Tranter, M. (2015). The stress-induced heat shock protein 70.3 expression is regulated by a dual-component mechanism involving alternative polyadenylation and HuR. *Biochimica et Biophysica Acta*, *1849*(6), 688–696. https://doi.org/10.1016/j.bbagrm.2015.02.004

Kreth, S., Limbeck, E., Hinske, L. C., Schutz, S. V., Thon, N., Hoefig, K., Egensperger, R., & Kreth, F. W. (2013). In human glioblastomas transcript elongation by alternative polyadenylation and miRNA targeting is a potent mechanism of MGMT silencing. *Acta Neuropathologica*, *125*(5), 671–681. https://doi.org/10.1007/s00401-013-1081-1

Kubo, T., Wada, T., Yamaguchi, Y., Shimizu, A., & Handa, H. (2006). Knock-down of 25 kDa subunit of cleavage factor Im in Hela cells alters alternative polyadenylation within 3′-UTRs. *Nucleic Acids Research*, *34*(21), 6264–6271. https://doi.org/10.1093/nar/gkl794

Kuhn, U., Gundel, M., Knoth, A., Kerwitz, Y., Rudel, S., & Wahle, E. (2009). Poly(A) tail length is controlled by the nuclear poly(A)-binding protein regulating the interaction between poly(A) polymerase and the cleavage and polyadenylation specificity factor. *The Journal of Biological Chemistry*, *284*(34), 22803–22814. https://doi.org/10.1074/jbc.M109.018226M109.018226

Kuhn, U., & Wahle, E. (2004). Structure and function of poly(A) binding proteins. *Biochimica et Biophysica Acta*, *1678*(2–3), 67–84. https://doi.org/10.1016/j.bbaexp.2004.03.008S016747810400079X

Kumar, A., Clerici, M., Muckenfuss, L. M., Passmore, L. A., & Jinek, M. (2019). Mechanistic insights into mRNA 3′-end processing. *Current Opinion in Structural Biology*, *59*, 143–150. https://doi.org/10.1016/j.sbi.2019.08.001

Kumar, A., Varendi, K., Peranen, J., & Andressoo, J. O. (2014). Tristetraprolin is a novel regulator of BDNF. *Springerplus*, *3*, 502. https://doi.org/10.1186/2193-1801-3-502

Kursun, D., & Kucuk, C. (2019). Systematic analysis of the frequently amplified 2p15-p16.1 locus reveals PAPOLG as a potential proto-oncogene in follicular and transformed follicular lymphoma. *Turkish Journal of Biology*, *43*, 124–132. https://doi.org/10.3906/biy-1810-2

Kyburz, A., Friedlein, A., Langen, H., & Keller, W. (2006). Direct interactions between subunits of CPSF and the U2 snRNP contribute to the coupling of pre-mRNA 3′ end processing and splicing. *Molecular Cell*, *23*(2), 195–205. https://doi.org/10.1016/j.molcel.2006.05.037

Lackford, B., Yao, C., Charles, G. M., Weng, L., Zheng, X., Choi, E. A., Xie, X., Wan, J., Xing, Y., Freudenberg, J. M., Yang, P., Jothi, R., Hu, G., & Shi, Y. (2014). Fip1 regulates mRNA alternative polyadenylation to promote stem cell self-renewal. *The EMBO Journal*, *33*(8), 878–889. https://doi.org/10.1002/embj.201386537

Lai, D. P., Tan, S., Kang, Y. N., Wu, J., Ooi, H. S., Chen, J., Shen, T. T., Qi, Y., Zhang, X., Guo, Y., Zhu, T., Liu, B., Shao, Z., & Zhao, X. (2015). Genome-wide profiling of polyadenylation sites reveals a link between selective polyadenylation and cancer metastasis. *Human Molecular Genetics*, *24*(12), 3410–3417. https://doi.org/10.1093/hmg/ddv089

Laishram, R. S. (2014). Poly(A) polymerase (PAP) diversity in gene expression—Star-PAP vs canonical PAP. *FEBS Letters*, *588*(14), 2185–2197. https://doi.org/10.1016/j.febslet.2014.05.029

Laishram, R. S., & Anderson, R. A. (2010). The poly A polymerase Star-PAP controls 3′-end cleavage by promoting CPSF interaction and specificity toward the pre-mRNA. *The EMBO Journal*, *29*(24), 4132–4145. https://doi.org/10.1038/emboj.2010.287

Lan, Y. L., & Zhang, J. (2021). Modulation of untranslated region alternative polyadenylation in glioma tumorigenesis. *Biomedicine & Pharmacotherapy*, *137*, 111416. https://doi.org/10.1016/j.biopha.2021.111416

Lang, M., Berry, D., Passecker, K., Mesteri, I., Bhuju, S., Ebner, F., Sedlyarov, V., Evstatiev, R., Dammann, K., Loy, A., Kuzyk, O., Kovarik, P., Khare, V., Beibel, M., Roma, G., Meisner-Kober, N., & Gasche, C. (2017). HuR small-molecule inhibitor elicits differential effects in adenomatosis polyposis and colorectal carcinogenesis. *Cancer Research*, *77*(9), 2424–2438. https://doi.org/10.1158/0008-5472.CAN-15-1726

Lau, A. G., Irier, H. A., Gu, J., Tian, D., Ku, L., Liu, G., Xia, M., Fritsch, B., Zheng, J. Q., Dingledine, R., Xu, B., Lu, B., & Feng, Y. (2010). Distinct 3′UTRs differentially regulate activity-dependent translation of brain-derived neurotrophic factor (BDNF). *Proceedings of the National Academy of Sciences of the United States of America*, *107*(36), 15945–15950. https://doi.org/10.1073/pnas.1002929107

Lee, H., & Maihle, N. J. (1998). Isolation and characterization of four alternate c-erbB3 transcripts expressed in ovarian carcinoma-derived cell lines and normal human tissues. *Oncogene*, *16*(25), 3243–3252. https://doi.org/10.1038/sj.onc.1201866

Lee, J. E., Lee, J. Y., Wilusz, J., Tian, B., & Wilusz, C. J. (2010). Systematic analysis of cis-elements in unstable mRNAs demonstrates that CUGBP1 is a key regulator of mRNA decay in muscle cells. *PLoS One*, *5*(6), e11201. https://doi.org/10.1371/journal.pone.0011201

Lee, S. H., & Mayr, C. (2019). Gain of additional BIRC3 protein functions through 3′-UTR-mediated protein complex formation. *Molecular Cell*, *74*(4), 701–712 e709. https://doi.org/10.1016/j.molcel.2019.03.006

Lee, S. H., Singh, I., Tisdale, S., Abdel-Wahab, O., Leslie, C. S., & Mayr, C. (2018). Widespread intronic polyadenylation inactivates tumour suppressor genes in leukaemia. *Nature*, *561*(7721), 127–131. https://doi.org/10.1038/s41586-018-0465-8

Lembo, A., Di Cunto, F., & Provero, P. (2012). Shortening of 3′UTRs correlates with poor prognosis in breast and lung cancer. *PLoS One*, *7*(2), e31129. https://doi.org/10.1371/journal.pone.0031129

Lemmers, R. J., van der Vliet, P. J., Klooster, R., Sacconi, S., Camano, P., Dauwerse, J. G., Snider, L., Straasheijm, K. R., van Ommen, G. J., Padberg, G. W., Miller, D. G., Tapscott, S. J., Tawil, R., Frants, R. R., & van der Maarel, S. M. (2010). A unifying genetic model for facioscapulohumeral muscular dystrophy. *Science*, *329*(5999), 1650–1653. https://doi.org/10.1126/science.1189044

Li, L., Wang, D., Xue, M., Mi, X., Liang, Y., & Wang, P. (2014). 3′UTR shortening identifies high-risk cancers with targeted dysregulation of the ceRNA network. *Scientific Reports*, *4*, 5406. https://doi.org/10.1038/srep05406

Li, M., Pan, X., Zeng, T., Zhang, Y. H., Feng, K., Chen, L., Huang, T., & Cai, Y. D. (2020). Alternative polyadenylation modification patterns reveal essential posttranscription regulatory mechanisms of tumorigenesis in multiple tumor types. *BioMed Research International*, *2020*, 6384120. https://doi.org/10.1155/2020/6384120

Li, S., Shen, L., & Chen, K. N. (2018). Association between H3K4 methylation and cancer prognosis: A meta-analysis. *Thoracic Cancer*, *9*(7), 794–799. https://doi.org/10.1111/1759-7714.12647

Li, W., Li, W., Laishram, R. S., Hoque, M., Ji, Z., Tian, B., & Anderson, R. A. (2017). Distinct regulation of alternative polyadenylation and gene expression by nuclear poly(A) polymerases. *Nucleic Acids Research*, *45*(15), 8930–8942. https://doi.org/10.1093/nar/gkx560

Li, W., Park, J. Y., Zheng, D., Hoque, M., Yehia, G., & Tian, B. (2016). Alternative cleavage and polyadenylation in spermatogenesis connects chromatin regulation with post-transcriptional control. *BMC Biology*, *14*, 6. https://doi.org/10.1186/s12915-016-0229-6

Li, W., Yeh, H. J., Shankarling, G. S., Ji, Z., Tian, B., & MacDonald, C. C. (2012). The tauCstF-64 polyadenylation protein controls genome expression in testis. *PLoS One*, *7*(10), e48373. https://doi.org/10.1371/journal.pone.0048373

Li, W., You, B., Hoque, M., Zheng, D., Luo, W., Ji, Z., Park, J. Y., Gunderson, S. I., Kalsotra, A., Manley, J. L., & Tian, B. (2015). Systematic profiling of poly(A)+ transcripts modulated by core 3′ end processing and splicing factors reveals regulatory rules of alternative cleavage and polyadenylation. *PLoS Genetics*, *11*(4), e1005166. https://doi.org/10.1371/journal.pgen.1005166

Li, Y. Q., Chen, Y., Xu, Y. F., He, Q. M., Yang, X. J., Li, Y. Q., Hong, X. H., Huang, S. Y., Tang, L. L., & Liu, N. (2020). FNDC3B 3′-UTR shortening escapes from microRNA-mediated gene repression and promotes nasopharyngeal carcinoma progression. *Cancer Science*, *111*(6), 1991–2003. https://doi.org/10.1111/cas.14394

Lianoglou, S., Garg, V., Yang, J. L., Leslie, C. S., & Mayr, C. (2013). Ubiquitously transcribed genes use alternative polyadenylation to achieve tissue-specific expression. *Genes & Development*, *27*(21), 2380–2396. https://doi.org/10.1101/gad.229328.113

Liaw, H. H., Lin, C. C., Juan, H. F., & Huang, H. C. (2013). Differential microRNA regulation correlates with alternative polyadenylation pattern between breast cancer and normal cells. *PLoS One*, *8*(2), e56958. https://doi.org/10.1371/journal.pone.0056958

Licatalosi, D. D., Mele, A., Fak, J. J., Ule, J., Kayikci, M., Chi, S. W., Clark, T. A., Schweitzer, A. C., Blume, J. E., Wang, X., Darnell, J. C., & Darnell, R. B. (2008). HITS-CLIP yields genome-wide insights into brain alternative RNA processing. *Nature*, *456*(7221), 464–469. https://doi.org/10.1038/nature07488

Lin, B., Rommens, J. M., Graham, R. K., Kalchman, M., MacDonald, H., Nasir, J., Delaney, A., Goldberg, Y. P., & Hayden, M. R. (1993). Differential 3′ polyadenylation of the Huntington disease gene results in two mRNA species with variable tissue expression. *Human Molecular Genetics*, *2*(10), 1541–1545. https://doi.org/10.1093/hmg/2.10.1541

Lin, Y., Li, Z., Ozsolak, F., Kim, S. W., Arango-Argoty, G., Liu, T. T., Tenenbaum, S. A., Bailey, T., Monaghan, A. P., Milos, P. M., & John, B. (2012). An in-depth map of polyadenylation sites in cancer. *Nucleic Acids Research*, *40*(17), 8460–8471. https://doi.org/10.1093/nar/gks637

Liu, D., Brockman, J. M., Dass, B., Hutchins, L. N., Singh, P., McCarrey, J. R., MacDonald, C. C., & Graber, J. H. (2007). Systematic variation in mRNA 3′-processing signals during mouse spermatogenesis. *Nucleic Acids Research*, *35*(1), 234–246. https://doi.org/10.1093/nar/gkl919

Locke, J. M., Da Silva Xavier, G., Rutter, G. A., & Harries, L. W. (2011). An alternative polyadenylation signal in TCF7L2 generates isoforms that inhibit T cell factor/lymphoid-enhancer factor (TCF/LEF)-dependent target genes. *Diabetologia*, *54*(12), 3078–3082. https://doi.org/10.1007/s00125-011-2290-6

Lucchini, R., Vezzoni, P., Giardini, R., Vezzoni, M. A., Raineri, M., & Clerici, L. (1984). Poly(A) polymerase distribution in normal and malignant lymphoid cells. *Tumori*, *70*(2), 141–146.

Lukiw, W. J., & Bazan, N. G. (1997). Cyclooxygenase 2 RNA message abundance, stability, and hypervariability in sporadic Alzheimer neocortex. *Journal of Neuroscience Research*, *50*(6), 937–945. https://doi.org/10.1002/(SICI)1097-4547(19971215)50:6<937::AID-JNR4>3.0.CO;2-E

Luth, E. S., Stavrovskaya, I. G., Bartels, T., Kristal, B. S., & Selkoe, D. J. (2014). Soluble, prefibrillar alpha-synuclein oligomers promote complex I-dependent, Ca2+−induced mitochondrial dysfunction. *The Journal of Biological Chemistry*, *289*(31), 21490–21507. https://doi.org/10.1074/jbc.M113.545749

Lutz, C. S., Murthy, K. G., Schek, N., O'Connor, J. P., Manley, J. L., & Alwine, J. C. (1996). Interaction between the U1 snRNP-A protein and the 160-kD subunit of cleavage-polyadenylation specificity factor increases polyadenylation efficiency in vitro. *Genes & Development*, *10*(3), 325–337.

Ma, C., Wang, Z., Nepal, M., Hokutan, K., Zhang, J., Yu, H., & Fei, P. (2018). DNA methylation at the vicinity of the proximal polyadenylation site in FANCD2 gene involves human malignancy. *Cell Cycle*, *17*(17), 2204–2206. https://doi.org/10.1080/15384101.2018.1516983

Ma, W., & Mayr, C. (2018). A membraneless organelle associated with the endoplasmic reticulum enables 3′UTR-mediated protein-protein interactions. *Cell*, *175*(6), 1492–1506 e1419. https://doi.org/10.1016/j.cell.2018.10.007

MacDonald, C. C., Wilusz, J., & Shenk, T. (1994). The 64-kilodalton subunit of the CstF polyadenylation factor binds to pre-mRNAs downstream of the cleavage site and influences cleavage site location. *Molecular and Cellular Biology*, *14*(10), 6647–6654.

Majoros, W. H., & Ohler, U. (2007). Spatial preferences of microRNA targets in 3′ untranslated regions. *BMC Genomics*, *8*, 152. https://doi.org/10.1186/1471-2164-8-152

Mandel, C. R., Bai, Y., & Tong, L. (2008). Protein factors in pre-mRNA 3′-end processing. *Cellular and Molecular Life Sciences*, *65*(7–8), 1099–1122. https://doi.org/10.1007/s00018-007-7474-3

Mandel, C. R., Kaneko, S., Zhang, H., Gebauer, D., Vethantham, V., Manley, J. L., & Tong, L. (2006). Polyadenylation factor CPSF-73 is the pre-mRNA 3′-end-processing endonuclease. *Nature*, *444*(7121), 953–956. https://doi.org/10.1038/nature05363

Mansfield, K. D., & Keene, J. D. (2012). Neuron-specific ELAV/Hu proteins suppress HuR mRNA during neuronal differentiation by alternative polyadenylation. *Nucleic Acids Research*, *40*(6), 2734–2746. https://doi.org/10.1093/nar/gkr1114

Mao, Z., Zhao, H., Qin, Y., Wei, J., Sun, J., Zhang, W., & Kang, Y. (2020). Post-transcriptional dysregulation of microRNA and alternative polyadenylation in colorectal cancer. *Frontiers in Genetics*, *11*, 64. https://doi.org/10.3389/fgene.2020.00064

Mapendano, C. K., Lykke-Andersen, S., Kjems, J., Bertrand, E., & Jensen, T. H. (2010). Crosstalk between mRNA 3′ end processing and transcription initiation. *Molecular Cell*, *40*(3), 410–422. https://doi.org/10.1016/j.molcel.2010.10.012

Marchese, D., Botta-Orfila, T., Cirillo, D., Rodriguez, J. A., Livi, C. M., Fernandez-Santiago, R., Ezquerra, M., Martí, M. J., Bechara, E., Tartaglia, G. G., & Catalan, M. S. A. R. (2017). Discovering the 3′ UTR-mediated regulation of alpha-synuclein. *Nucleic Acids Research*, *45*(22), 12888–12903. https://doi.org/10.1093/nar/gkx1048

Martin, G., Gruber, A. R., Keller, W., & Zavolan, M. (2012). Genome-wide analysis of pre-mRNA 3′ end processing reveals a decisive role of human cleavage factor I in the regulation of 3′ UTR length. *Cell Reports*, *1*(6), 753–763. https://doi.org/10.1016/j.celrep.2012.05.003S2211-1247(12)00127-1

Masamha, C. P., Xia, Z., Peart, N., Collum, S., Li, W., Wagner, E. J., & Shyu, A. B. (2016). CFIm25 regulates glutaminase alternative terminal exon definition to modulate miR-23 function. *RNA*, *22*(6), 830–838. https://doi.org/10.1261/rna.055939.116

Masamha, C. P., Xia, Z., Yang, J., Albrecht, T. R., Li, M., Shyu, A. B., Li, W., & Wagner, E. J. (2014). CFIm25 links alternative polyadenylation to glioblastoma tumour suppression. *Nature*, *510*(7505), 412–416. https://doi.org/10.1038/nature13261

Masuda, A., Takeda, J., Okuno, T., Okamoto, T., Ohkawara, B., Ito, M., Ishigaki, S., Sobue, G., & Ohno, K. (2015). Position-specific binding of FUS to nascent RNA regulates mRNA length. *Genes & Development*, *29*(10), 1045–1057. https://doi.org/10.1101/gad.255737.114

Matoulkova, E., Sommerova, L., Pastorek, M., Vojtesek, B., & Hrstka, R. (2017). Regulation of AGR2 expression via 3′UTR shortening. *Experimental Cell Research*, *356*(1), 40–47. https://doi.org/10.1016/j.yexcr.2017.04.011

Mayr, C., & Bartel, D. P. (2009). Widespread shortening of 3′UTRs by alternative cleavage and polyadenylation activates oncogenes in cancer cells. *Cell*, *138*(4), 673–684. https://doi.org/10.1016/j.cell.2009.06.016

Mbita, Z., Meyer, M., Skepu, A., Hosie, M., Rees, J., & Dlamini, Z. (2012). De-regulation of the RBBP6 isoform 3/DWNN in human cancers. *Molecular and Cellular Biochemistry*, *362*(1–2), 249–262. https://doi.org/10.1007/s11010-011-1150-5

McCracken, S., Fong, N., Yankulov, K., Ballantyne, S., Pan, G., Greenblatt, J., Patterson, S. D., Wickens, M., & Bentley, D. L. (1997). The C-terminal domain of RNA polymerase II couples mRNA processing to transcription. *Nature*, *385*(6614), 357–361. https://doi.org/10.1038/385357a0

Melamed, Z., López-Erauskin, J., Baughn, M. W., Zhang, O., Drenner, K., Sun, Y., Freyermuth, F., McMahon, M. A., Beccari, M. S., Artates, J. W., Ohkubo, T., Rodriguez, M., Lin, N., Wu, D., Bennett, C. F., Rigo, F., Da Cruz, S., Ravits, J., Lagier-Tourenne, C., & Cleveland, D. W. (2019). Premature polyadenylation-mediated loss of stathmin-2 is a hallmark of TDP-43-dependent neurodegeneration. *Nature Neuroscience*, *22*(2), 180–190. https://doi.org/10.1038/s41593-018-0293-z

Mellman, D. L., Gonzales, M. L., Song, C., Barlow, C. A., Wang, P., Kendziorski, C., & Anderson, R. A. (2008). A PtdIns4,5P2-regulated nuclear poly(A) polymerase controls expression of select mRNAs. *Nature*, *451*(7181), 1013–1017. https://doi.org/10.1038/nature06666

Miles, W. O., Lembo, A., Volorio, A., Brachtel, E., Tian, B., Sgroi, D., Provero, P., & Dyson, N. (2016). Alternative polyadenylation in triple-negative breast tumors allows NRAS and c-JUN to bypass PUMILIO posttranscriptional regulation. *Cancer Research*, *76*, 7231–7241.

Millevoi, S., Loulergue, C., Dettwiler, S., Karaa, S. Z., Keller, W., Antoniou, M., & Vagner, S. (2006). An interaction between U2AF 65 and CF I(m) links the splicing and 3′ end processing machineries. *The EMBO Journal*, *25*(20), 4854–4864. https://doi.org/10.1038/sj.emboj.7601331

Minvielle, S., Giscard-Dartevelle, S., Cohen, R., Taboulet, J., Labye, F., Jullienne, A., Rivaille, P., Milhaud, G., Moukhtar, M. S., & Lasmoles, F. (1991). A novel calcitonin carboxyl-terminal peptide produced in medullary thyroid carcinoma by alternative RNA processing of the calcitonin/calcitonin gene-related peptide gene. *The Journal of Biological Chemistry*, *266*(36), 24627–24631.

Misiewicz-Krzeminska, I., Sarasquete, M. E., Vicente-Duenas, C., Krzeminski, P., Wiktorska, K., Corchete, L. A., Quwaider, D., Rojas, E. A., Corral, R., Martín, A. A., Escalante, F., Bárez, A., García, J. L., Sánchez-García, I., García-Sanz, R., San Miguel, J. F., & Gutierrez, N. C. (2016). Post-transcriptional modifications contribute to the upregulation of cyclin D2 in multiple myeloma. *Clinical Cancer Research*, *22*(1), 207–217. https://doi.org/10.1158/1078-0432.CCR-14-2796

Miura, P., Shenker, S., Andreu-Agullo, C., Westholm, J. O., & Lai, E. C. (2013). Widespread and extensive lengthening of 3′ UTRs in the mammalian brain. *Genome Research*, *23*(5), 812–825. https://doi.org/10.1101/gr.146886.112

Mohan, N., Kumar, V., Kandala, D. T., Kartha, C. C., & Laishram, R. S. (2018). A splicing-independent function of RBM10 controls specific 3′ UTR processing to regulate cardiac hypertrophy. *Cell Reports*, *24*(13), 3539–3553. https://doi.org/10.1016/j.celrep.2018.08.077

Morris, A. R., Bos, A., Diosdado, B., Rooijers, K., Elkon, R., Bolijn, A. S., Carvalho, B., Meijer, G. A., & Agami, R. (2012). Alternative cleavage and polyadenylation during colorectal cancer development. *Clinical Cancer Research*, *18*(19), 5256–5266. https://doi.org/10.1158/1078-0432.CCR-12-05431078-0432.CCR-12-0543

Mosselman, S., Claesson-Welsh, L., Kamphuis, J. S., & van Zoelen, E. J. (1994). Developmentally regulated expression of two novel platelet-derived growth factor alpha-receptor transcripts in human teratocarcinoma cells. *Cancer Research*, *54*(1), 220–225.

Mueller, A. A., van Velthoven, C. T., Fukumoto, K. D., Cheung, T. H., & Rando, T. A. (2016). Intronic polyadenylation of PDGFRalpha in resident stem cells attenuates muscle fibrosis. *Nature*, *540*(7632), 276–279. https://doi.org/10.1038/nature20160

Muller-McNicoll, M., Botti, V., de Jesus Domingues, A. M., Brandl, H., Schwich, O. D., Steiner, M. C., Curk, T., Poser, I., Zarnack, K., & Neugebauer, K. M. (2016). SR proteins are NXF1 adaptors that link alternative RNA processing to mRNA export. *Genes & Development*, *30*(5), 553–566. https://doi.org/10.1101/gad.276477.115

Murthy, K. G., & Manley, J. L. (1995). The 160-kD subunit of human cleavage-polyadenylation specificity factor coordinates pre-mRNA 3′-end formation. *Genes & Development*, *9*(21), 2672–2683.

Nanavaty, V., Abrash, E. W., Hong, C., Park, S., Fink, E. E., Li, Z., Sweet, T. J., Bhasin, J. M., Singuri, S., Lee, B. H., Hwang, T. H., & Ting, A. H. (2020). DNA methylation regulates alternative polyadenylation via CTCF and the Cohesin complex. *Molecular Cell*, *78*(4), 752–764. https://doi.org/10.1016/j.molcel.2020.03.024

Neve, J., Burger, K., Li, W., Hoque, M., Patel, R., Tian, B., Gullerova, M., & Furger, A. (2016). Subcellular RNA profiling links splicing and nuclear DICER1 to alternative cleavage and polyadenylation. *Genome Research*, *26*(1), 24–35. https://doi.org/10.1101/gr.193995.115

Neve, J., Patel, R., Wang, Z., Louey, A., & Furger, A. M. (2017). Cleavage and polyadenylation: Ending the message expands gene regulation. *RNA Biology*, *14*(7), 865–890. https://doi.org/10.1080/15476286.2017.1306171

Ngondo, R. P., & Carbon, P. (2014). ZNF143 is regulated through alternative 3′UTR isoforms. *Biochimie*, *104*, 137–146. https://doi.org/10.1016/j.biochi.2014.06.008

Ni, T. K., & Kuperwasser, C. (2016). Premature polyadenylation of MAGI3 produces a dominantly-acting oncogene in human breast cancer. *eLife*, *5*, e14730. https://doi.org/10.7554/eLife.14730

Nimura, K., Yamamoto, M., Takeichi, M., Saga, K., Takaoka, K., Kawamura, N., Nitta, H., Nagano, H., Ishino, S., Tanaka, T., Schwartz, R. J., Aburatani, H., & Kaneda, Y. (2016). Regulation of alternative polyadenylation by Nkx2-5 and Xrn2 during mouse heart development. *eLife*, *5*, e16030. https://doi.org/10.7554/eLife.16030

Niu, X., He, W., Song, B., Ou, Z., Fan, D., Chen, Y., Fan, Y., & Sun, X. (2016). Combining single strand oligodeoxynucleotides and CRISPR/Cas9 to correct gene mutations in beta-thalassemia-induced pluripotent stem cells. *The Journal of Biological Chemistry*, *291*(32), 16576–16585. https://doi.org/10.1074/jbc.M116.719237

Nourse, J., Spada, S., & Danckwardt, S. (2020). Emerging roles of RNA 3′-end cleavage and polyadenylation in pathogenesis, diagnosis and therapy of human disorders. *Biomolecules*, *10*(6), 915. https://doi.org/10.3390/biom10060915

Ogorodnikov, A., Levin, M., Tattikota, S., Tokalov, S., Hoque, M., Scherzinger, D., Marini, F., Poetsch, A., Binder, H., Macher-Göppinger, S., Probst, H. C., Tian, B., Schaefer, M., Lackner, K. J., Westermann, F., & Danckwardt, S. (2018). Transcriptome 3′end organization by PCF11 links alternative polyadenylation to formation and neuronal differentiation of neuroblastoma. *Nature Communications*, *9*(1), 5331. https://doi.org/10.1038/s41467-018-07580-5

Oh, J. M., Venters, C. C., Di, C., Pinto, A. M., Wan, L., Younis, I., Cai, Z., Arai, C., So, B. R., Duan, J., & Dreyfuss, G. (2020). U1 snRNP regulates cancer cell migration and invasion in vitro. *Nature Communications*, *11*(1), 1. https://doi.org/10.1038/s41467-019-13993-7

Orkin, S. H., Cheng, T. C., Antonarakis, S. E., & Kazazian, H. H., Jr. (1985). Thalassemia due to a mutation in the cleavage-polyadenylation signal of the human beta-globin gene. *The EMBO Journal*, *4*(2), 453–456.

Park, H. J., Ji, P., Kim, S., Xia, Z., Rodriguez, B., Li, L., Su, J., Chen, K., Masamha, C. P., Baillat, D., Fontes-Garfias, C. R., Shyu, A. B., Neilson, J. R., Wagner, E. J., & Li, W. (2018). 3′ UTR shortening represses tumor-suppressor genes in trans by disrupting ceRNA crosstalk. *Nature Genetics*, *50*(6), 783–789. https://doi.org/10.1038/s41588-018-0118-8

Park, J. Y., Li, W., Zheng, D., Zhai, P., Zhao, Y., Matsuda, T., Vatner, S. F., Sadoshima, J., & Tian, B. (2011). Comparative analysis of mRNA isoform expression in cardiac hypertrophy and development reveals multiple post-transcriptional regulatory modules. *PLoS One*, *6*(7), e22391. https://doi.org/10.1371/journal.pone.0022391

Park, S. M., Ou, J., Chamberlain, L., Simone, T. M., Yang, H., Virbasius, C. M., Ali, A. M., Zhu, L. J., Mukherjee, S., Raza, A., & Green, M. R. (2016). U2AF35(S34F) promotes transformation by directing aberrant ATG7 pre-mRNA 3′ end formation. *Molecular Cell*, *62*(4), 479–490. https://doi.org/10.1016/j.molcel.2016.04.011

Passacantilli, I., Panzeri, V., Bielli, P., Farini, D., Pilozzi, E., Fave, G. D., Capurso, G., & Sette, C. (2017). Alternative polyadenylation of ZEB1 promotes its translation during genotoxic stress in pancreatic cancer cells. *Cell Death & Disease*, *8*(11), e3168. https://doi.org/10.1038/cddis.2017.562

Patel, R., Brophy, C., Hickling, M., Neve, J., & Furger, A. (2019). Alternative cleavage and polyadenylation of genes associated with protein turnover and mitochondrial function are deregulated in Parkinson's, Alzheimer's and ALS disease. *BMC Medical Genomics*, *12*(1), 60. https://doi.org/10.1186/s12920-019-0509-4

Pendurthi, U. R., Alok, D., & Rao, L. V. (1997). Binding of factor VIIa to tissue factor induces alterations in gene expression in human fibroblast cells: Up-regulation of poly(A) polymerase. *Proceedings of the National Academy of Sciences of the United States of America*, *94*(23), 12598–12603. https://doi.org/10.1073/pnas.94.23.12598

Perez Canadillas, J. M., & Varani, G. (2003). Recognition of GU-rich polyadenylation regulatory elements by human CstF-64 protein. *The EMBO Journal*, *22*(11), 2821–2830. https://doi.org/10.1093/emboj/cdg259

Plass, M., Rasmussen, S. H., & Krogh, A. (2017). Highly accessible AU-rich regions in 3′ untranslated regions are hotspots for binding of regulatory factors. *PLoS Computational Biology*, *13*(4), e1005460. https://doi.org/10.1371/journal.pcbi.1005460

Prasad, M. K., Bhalla, K., Pan, Z. H., O'Connell, J. R., Weder, A. B., Chakravarti, A., Tian, B., & Chang, Y. P. (2013). A polymorphic 3'UTR element in ATP1B1 regulates alternative polyadenylation and is associated with blood pressure. *PLoS One*, *8*(10), e76290. https://doi.org/10.1371/journal.pone.0076290

Prior, J. F., Lim, E., Lingam, N., Raven, J. L., & Finlayson, J. (2007). A moderately severe alpha-thalassemia condition resulting from a combination of the alpha2 polyadenylation signal (AATAAA→AATA- -) mutation and a 3.7 kb alpha gene deletion in an Australian family. *Hemoglobin*, *31*(2), 173–177. https://doi.org/10.1080/03630260701288997

Prudencio, M., Belzil, V. V., Batra, R., Ross, C. A., Gendron, T. F., Pregent, L. J., Murray, M. E., Overstreet, K. K., Piazza-Johnston, A. E., Desaro, P., Bieniek, K. F., DeTure, M., Lee, W. C., Biendarra, S. M., Davis, M. D., Baker, M. C., Perkerson, R. B., van Blitterswijk, M., Stetler, C. T., … Petrucelli, L. (2015). Distinct brain transcriptome profiles in C9orf72-associated and sporadic ALS. *Nature Neuroscience*, *18*(8), 1175–1182. https://doi.org/10.1038/nn.4065

Raabe, T., Bollum, F. J., & Manley, J. L. (1991). Primary structure and expression of bovine poly(A) polymerase. *Nature*, *353*(6341), 229–234. https://doi.org/10.1038/353229a0

Rani, A. Q. M., Yamamoto, T., Kawaguchi, T., Maeta, K., Awano, H., Nishio, H., & Matsuo, M. (2020). Intronic alternative polyadenylation in the middle of the DMD gene produces half-size N-terminal dystrophin with a potential implication of ECG abnormalities of DMD patients. *International Journal of Molecular Sciences*, *21*(10), 3555. https://doi.org/10.3390/ijms21103555

Raz, V., Dickson, G., & 'tHoen, P. A. C. (2017). Dysfunctional transcripts are formed by alternative polyadenylation in OPMD. *Oncotarget*, *8*(43), 73516–73528. https://doi.org/10.18632/oncotarget.20640

Raz, V., Routledge, S., Venema, A., Buijze, H., van der Wal, E., Anvar, S., Straasheijm, K. R., Klooster, R., Antoniou, M., & van der Maarel, S. M. (2011). Modeling oculopharyngeal muscular dystrophy in myotube cultures reveals reduced accumulation of soluble mutant PABPN1 protein. *The American Journal of Pathology*, *179*(4), 1988–2000. https://doi.org/10.1016/j.ajpath.2011.06.044

Rehfeld, A., Plass, M., Dossing, K., Knigge, U., Kjaer, A., Krogh, A., & Friis-Hansen, L. (2014). Alternative polyadenylation of tumor suppressor genes in small intestinal neuroendocrine tumors. *rontiers in Endocrinology (Lausanne)*, *5*, 46. https://doi.org/10.3389/fendo.2014.00046

Ren, F., Zhang, N., Zhang, L., Miller, E., & Pu, J. J. (2020). Alternative polyadenylation: A new frontier in post transcriptional regulation. *Biomarker Research*, *8*(1), 67. https://doi.org/10.1186/s40364-020-00249-6

Renton, A. E., Majounie, E., Waite, A., Simón-Sánchez, J., Rollinson, S., Gibbs, J. R., Schymick, J. C., Laaksovirta, H., van Swieten, J. C., Myllykangas, L., Kalimo, H., Paetau, A., Abramzon, Y., Remes, A. M., Kaganovich, A., Scholz, S. W., Duckworth, J., Ding, J., Harmer, D. W., … Traynor, B. J. (2011). A Hexanucleotide Repeat Expansion in C9ORF72 Is the Cause of Chromosome 9p21-Linked ALS-FTD. *Neuron*, *72*(2), 257–268. https://doi.org/10.1016/j.neuron.2011.09.010

Rhinn, H., Qiang, L., Yamashita, T., Rhee, D., Zolin, A., Vanti, W., & Abeliovich, A. (2012). Alternative alpha-synuclein transcript usage as a convergent mechanism in Parkinson's disease pathology. *Nature Communications*, *3*, 1084. https://doi.org/10.1038/ncomms2032

Riaz, M., Raz, Y., van Putten, M., Paniagua-Soriano, G., Krom, Y. D., Florea, B. I., & Raz, V. (2016). PABPN1-dependent mRNA processing induces muscle wasting. *PLoS Genetics*, *12*(5), e1006031. https://doi.org/10.1371/journal.pgen.1006031

Richard, P., Trollet, C., Gidaro, T., Demay, L., Brochier, G., Malfatti, E., Tom, F. M. S., Fardeau, M., Lafor, P., Romero, N., Martin-N, M. L., Sol, G., Ferrer-Monasterio, X., Saint-Guily, J. L., & Eymard, B. (2015). PABPN1 (GCN)11 as a dominant allele in oculopharyngeal muscular dystrophy -consequences in clinical diagnosis and genetic counselling. *Journal of Neuromuscular Diseases*, *2*(2), 175–180. https://doi.org/10.3233/JND-140060

Romo, L., Ashar-Patel, A., Pfister, E., & Aronin, N. (2017). Alterations in mRNA 3′ UTR isoform abundance accompany gene expression changes in human Huntington's disease brains. *Cell Reports*, *20*(13), 3057–3070. https://doi.org/10.1016/j.celrep.2017.09.009

Ross, N. T., Lohmann, F., Carbonneau, S., Fazal, A., Weihofen, W. A., Gleim, S., Salcius, M., Sigoillot, F., Henault, M., Carl, S. H., Rodríguez-Molina, J. B., Miller, H. R., Brittain, S. M., Murphy, J., Zambrowski, M., Boynton, G., Wang, Y., Chen, A., Molind, G. J., … Beckwith, R. E. J. (2020). CPSF3-dependent pre-mRNA processing as a druggable node in AML and Ewing's sarcoma. *Nature Chemical Biology*, *16*(1), 50–59. https://doi.org/10.1038/s41589-019-0424-1

Roy, J., & Mallick, B. (2018). Investigating piwi-interacting RNA regulome in human neuroblastoma. *Genes, Chromosomes & Cancer*, *57*(7), 339–349. https://doi.org/10.1002/gcc.22535

Rozenblatt-Rosen, O., Nagaike, T., Francis, J. M., Kaneko, S., Glatt, K. A., Hughes, C. M., LaFramboise, T., Manley, J. L., & Meyerson, M. (2009). The tumor suppressor Cdc73 functionally associates with CPSF and CstF 3′ mRNA processing factors. *Proceedings of the National Academy of Sciences*, *106*(3), 755–760.

Ruegsegger, U., Beyer, K., & Keller, W. (1996). Purification and characterization of human cleavage factor Im involved in the 3′ end processing of messenger RNA precursors. *The Journal of Biological Chemistry*, *271*(11), 6107–6113.

Ruepp, M. D., Aringhieri, C., Vivarelli, S., Cardinale, S., Paro, S., Schumperli, D., & Barabino, S. M. (2009). Mammalian pre-mRNA 3′ end processing factor CF I m 68 functions in mRNA export. *Molecular Biology of the Cell*, *20*(24), 5211–5223. https://doi.org/10.1091/mbc.E09-05-0389

Rund, D., Dowling, C., Najjar, K., Rachmilewitz, E. A., Kazazian, H. H., Jr., & Oppenheim, A. (1992). Two mutations in the beta-globin polyadenylylation signal reveal extended transcripts and new RNA polyadenylylation sites. *Proceedings of the National Academy of Sciences of the United States of America*, *89*(10), 4324–4328. https://doi.org/10.1073/pnas.89.10.4324

Ryan, K., Calvo, O., & Manley, J. L. (2004). Evidence that polyadenylation factor CPSF-73 is the mRNA 3′ processing endonuclease. *RNA*, *10*(4), 565–573.

Sandberg, R., Neilson, J. R., Sarma, A., Sharp, P. A., & Burge, C. B. (2008). Proliferating cells express mRNAs with shortened 3′ untranslated regions and fewer microRNA target sites. *Science*, *320*(5883), 1643–1647. https://doi.org/10.1126/science.1155390

Schönemann, L., Kühn, U., Martin, G., Schäfer, P., Gruber, A. R., Keller, W., Zavolan, M., & Wahle, E. (2014). Reconstitution of CPSF active in polyadenylation: Recognition of the polyadenylation signal by WDR33. *Genes & Development*, *250985*(250114), 2381–2393.

Schroder, J. M., Klossok, T., & Weis, J. (2011). Oculopharyngeal muscle dystrophy: Fine structure and mRNA expression levels of PABPN1. *Clinical Neuropathology*, *30*(3), 94–103. https://doi.org/10.5414/npp30094

Scott, G. K., Robles, R., Park, J. W., Montgomery, P. A., Daniel, J., Holmes, W. E., Lee, J., Keller, G. A., Li, W. L., & Fendly, B. M. (1993). A truncated intracellular HER2/neu receptor produced by alternative RNA processing affects growth of human carcinoma cells. *Molecular and Cellular Biology*, *13*(4), 2247–2257. https://doi.org/10.1128/mcb.13.4.2247

Shafik, A. M., Zhang, F., Guo, Z., Dai, Q., Pajdzik, K., Li, Y., Kang, Y., Yao, B., Wu, H., He, C., Allen, E. G., Duan, R., & Jin, P. (2021). N6-methyladenosine dynamics in neurodevelopment and aging, and its potential role in Alzheimer's disease. *Genome Biology*, *22*(1), 17. https://doi.org/10.1186/s13059-020-02249-z

Shankarling, G. S., Coates, P. W., Dass, B., & Macdonald, C. C. (2009). A family of splice variants of CstF-64 expressed in vertebrate nervous systems. *BMC Molecular Biology*, *10*, 22. https://doi.org/10.1186/1471-2199-10-22

Shao, J., Zhang, J., Zhang, Z., Jiang, H., Lou, X., Huang, B., Foltz, G., Lan, Q., Huang, Q., & Lin, B. (2013). Alternative polyadenylation in glioblastoma multiforme and changes in predicted RNA binding protein profiles. *OMICS*, *17*(3), 136–149. https://doi.org/10.1089/omi.2012.0098

Shell, S. A., Hesse, C., Morris, S. M., Jr., & Milcarek, C. (2005). Elevated levels of the 64-kDa cleavage stimulatory factor (CstF-64) in lipopolysaccharide-stimulated macrophages influence gene expression and induce alternative poly(A) site selection. *The Journal of Biological Chemistry*, *280*(48), 39950–39961. https://doi.org/10.1074/jbc.M508848200

Shen, T., Li, H., Song, Y., Li, L., Lin, J., Wei, G., & Ni, T. (2019). Alternative polyadenylation dependent function of splicing factor SRSF3 contributes to cellular senescence. *Aging (Albany NY)*, *11*(5), 1356–1388. https://doi.org/10.18632/aging.101836

Shi, Y., Di Giammartino, D. C., Taylor, D., Sarkeshik, A., Rice, W. J., Yates, J. R., 3rd, Frank, J., & Manley, J. L. (2009). Molecular architecture of the human pre-mRNA 3′ processing complex. *Molecular Cell*, *33*(3), 365–376. https://doi.org/10.1016/j.molcel.2008.12.028

Shi, Y., & Manley, J. L. (2015). The end of the message: Multiple protein-RNA interactions define the mRNA polyadenylation site. *Genes & Development*, *29*(9), 889–897. https://doi.org/10.1101/gad.261974.115

Shibata, E., Rajakumar, A., Powers, R. W., Larkin, R. W., Gilmour, C., Bodnar, L. M., Crombleholme, W. R., Ness, R. B., Roberts, J. M., & Hubel, C. A. (2005). Soluble fms-like tyrosine kinase 1 is increased in preeclampsia but not in normotensive pregnancies with small-for-gestational-age neonates: Relationship to circulating placental growth factor. *The Journal of Clinical Endocrinology and Metabolism*, *90*(8), 4895–4903. https://doi.org/10.1210/jc.2004-1955

Shimberg, G. D., Michalek, J. L., Oluyadi, A. A., Rodrigues, A. V., Zucconi, B. E., Neu, H. M., Ghosh, S., Sureschandra, K., Wilson, G. M., Stemmler, T. L., & Michel, S. L. (2016). Cleavage and polyadenylation specificity factor 30: An RNA-binding zinc-finger protein with an unexpected 2Fe-2S cluster. *Proceedings of the National Academy of Sciences of the United States of America*, *113*(17), 4700–4705. https://doi.org/10.1073/pnas.1517620113

Shin, J. H., Janer, M., McNeney, B., Blay, S., Deutsch, K., Sanjeevi, C. B., Kockum, I., Lernmark, Å., Graham, J., Arnqvist, H., Björck, E., Eriksson, J., Nyström, L., Ohlson, L. O., Scherstén, B., Ostman, J., Aili, M., Bååth, L. E., & Aman, J. (2007). Swedish Childhood Diabetes Study Group, & Diabetes Incidence in Sweden Study Group. IA-2 autoantibodies in incident type I diabetes patients are associated with a polyadenylation signal polymorphism in GIMAP5. *Genes & Immunity*, *8*(6), 503–512. https://doi.org/10.1038/sj.gene.6364413

Shulman, E. D., & Elkon, R. (2019). Cell-type-specific analysis of alternative polyadenylation using single-cell transcriptomics data. *Nucleic Acids Research*, *47*(19), 10027–10039. https://doi.org/10.1093/nar/gkz781

Singh, I., Lee, S. H., Sperling, A. S., Samur, M. K., Tai, Y. T., Fulciniti, M., Munshi, N. C., Mayr, C., & Leslie, C. S. (2018). Widespread intronic polyadenylation diversifies immune cell transcriptomes. *Nature Communications*, *9*(1), 1716. https://doi.org/10.1038/s41467-018-04112-z

Singh, P., Alley, T. L., Wright, S. M., Kamdar, S., Schott, W., Wilpan, R. Y., Mills, K. D., & Graber, J. H. (2009). Global changes in processing of mRNA 3′ untranslated regions characterize clinically distinct cancer subtypes. *Cancer Research*, *69*, 9422–9430.

Soetanto, R., Hynes, C. J., Patel, H. R., Humphreys, D. T., Evers, M., Duan, G., Parker, B. J., Archer, S. K., Clancy, J. L., Graham, R. M., Beilharz, T. H., Smith, N. J., & Preiss, T. (2016). Role of miRNAs and alternative mRNA 3′-end cleavage and polyadenylation of their mRNA targets in cardiomyocyte hypertrophy. *Biochimica et Biophysica Acta*, *1859*(5), 744–756. https://doi.org/10.1016/j.bbagrm.2016.03.010

Solnestam, B. W., Stranneheim, H., Hallman, J., Kaller, M., Lundberg, E., Lundeberg, J., & Akan, P. (2012). Comparison of total and cytoplasmic mRNA reveals global regulation by nuclear retention and miRNAs. *BMC Genomics*, *13*, 574. https://doi.org/10.1186/1471-2164-13-574

Sommer, J., Garbers, C., Wolf, J., Trad, A., Moll, J. M., Sack, M., Fischer, R., Grötzinger, J., Waetzig, G. H., Floss, D. M., & Scheller, J. (2014). Alternative intronic polyadenylation generates the interleukin-6 trans-signaling inhibitor sgp130-E10. *The Journal of Biological Chemistry*, *289*(32), 22140–22150. https://doi.org/10.1074/jbc.M114.560938

Sowd, G. A., Serrao, E., Wang, H., Wang, W., Fadel, H. J., Poeschla, E. M., & Engelman, A. N. (2016). A critical role for alternative polyadenylation factor CPSF6 in targeting HIV-1 integration to transcriptionally active chromatin. *Proceedings of the National Academy of Sciences of the United States of America*, *113*(8), E1054–E1063. https://doi.org/10.1073/pnas.1524213113

Spies, N., Nielsen, C. B., Padgett, R. A., & Burge, C. B. (2009). Biased chromatin signatures around polyadenylation sites and exons. *Molecular Cell*, *36*(2), 245–254. https://doi.org/10.1016/j.molcel.2009.10.008

Stacey, S.N., Sulem, P., Jonasdottir, A., Masson, G., Gudmundsson, J., Gudbjartsson, D.F., Magnusson, O.T., Gudjonsson, S.A., Sigurgeirsson, B., Thorisdottir, K., Ragnarsson, R., Benediktsdottir, K.R., Nexø, B.A., Tjønneland, A., Overvad, K., Rudnai, P., Gurzau, E., Koppova, K., Hemminki, K., … Stefansson, K. (2011). A germline variant in the TP53 polyadenylation signal confers cancer susceptibility. *Nature Genetics*, *43*(11), 1098–1103. https://doi.org/10.1038/ng.926

Stagg, B. C., Uehara, H., Lambert, N., Rai, R., Gupta, I., Radmall, B., Bates, T., & Ambati, B. K. (2014). Morpholino-mediated isoform modulation of vascular endothelial growth factor Receptor-2 (VEGFR2) reduces colon cancer xenograft growth. *Cancers (Basel)*, *6*(4), 2330–2342. https://doi.org/10.3390/cancers6042330

Sudheesh, A., Mohan, N., Francis, N., Laishram, R. S., & Anderson, R. A. (2019). Star-PAP controlled alternative polyadenylation coupled poly (A) tail length regulates protein expression in hypertrophic heart. *Nucleic Acids Research*, *47*(20), 10771–10787.

Sudheesh, A. P., & Laishram, R. S. (2017). Nuclear phosphatidyl-inositol-phosphate type I kinase alpha coupled Star-PAP polyadenylation regulates cell invasion. *Molecular and Cellular Biology*, *38*(5), e00457-17. https://doi.org/10.1128/MCB.00457-17

Sui, W., Zheng, C., Yang, M., Ou, M., Chen, J., Dong, L., Chen, P., Hou, X., Liu, F., Wei, X., & Dai, Y. (2016). Study on 3′-UTR length polymorphism in peripheral blood mononuclear cells of uremia patient. *Renal Failure*, *38*(1), 96–99. https://doi.org/10.3109/0886022X.2015.1104989

Sun, M., Ding, J., Li, D., Yang, G., Cheng, Z., & Zhu, Q. (2017). NUDT21 regulates 3′-UTR length and microRNA-mediated gene silencing in hepatocellular carcinoma. *Cancer Letters*, *410*, 158–168. https://doi.org/10.1016/j.canlet.2017.09.026

Sun, Y., Chen, H., Ye, H., Liang, W., Lam, K. K., Cheng, B., Lu, Y., & Jiang, C. (2020). Nudt21-mediated alternative polyadenylation of HMGA2 3′-UTR impairs stemness of human tendon stem cell. *Aging (Albany NY)*, *12*(18), 18436–18452. https://doi.org/10.18632/aging.103771

Sun, Y., Zhang, Y., Hamilton, K., Manley, J. L., Shi, Y., Walz, T., & Tong, L. (2018). Molecular basis for the recognition of the human AAUAAA polyadenylation signal. *Proceedings of the National Academy of Sciences of the United States of America*, *115*(7), E1419–E1428. https://doi.org/10.1073/pnas.1718723115

Sung, T. Y., Kim, M., Kim, T. Y., Kim, W. G., Park, Y., Song, D. E., Park, S. Y., Kwon, H., Choi, Y. M., Jang, E. K., Jeon, M. J., Shong, Y. K., Hong, S. J., & Kim, W. B. (2015). Negative expression of CPSF2 predicts a poorer clinical outcome in patients with papillary thyroid carcinoma. *Thyroid*, *25*(9), 1020–1025.

Szkop, K. J., Cooke, P. I. C., Humphries, J. A., Kalna, V., Moss, D. S., Schuster, E. F., & Nobeli, I. (2017). Dysregulation of alternative polyadenylation as a potential player in autism spectrum disorder. *Frontiers in Molecular Neuroscience*, *10*, 279. https://doi.org/10.3389/fnmol.2017.00279

Takagaki, Y., MacDonald, C. C., Shenk, T., & Manley, J. L. (1992). The human 64-kDa polyadenylylation factor contains a ribonucleoprotein-type RNA binding domain and unusual auxiliary motifs. *Proceedings of the National Academy of Sciences of the United States of America*, *89*(4), 1403–1407.

Takagaki, Y., & Manley, J. L. (1994). A polyadenylation factor subunit is the human homologue of the Drosophila suppressor of forked protein. *Nature*, *372*(6505), 471–474. https://doi.org/10.1038/372471a0

Takagaki, Y., & Manley, J. L. (1997). RNA recognition by the human polyadenylation factor CstF. *Molecular and Cellular Biology*, *17*(7), 3907–3914.

Takagaki, Y., & Manley, J. L. (2000). Complex protein interactions within the human polyadenylation machinery identify a novel component. *Molecular and Cellular Biology*, *20*(5), 1515–1525.

Takagaki, Y., Seipelt, R. L., Peterson, M. L., & Manley, J. L. (1996). The polyadenylation factor CstF-64 regulates alternative processing of IgM heavy chain pre-mRNA during B cell differentiation. *Cell*, *87*(5), 941–952.

Tamaddon, M., Shokri, G., Hosseini Rad, S. M. A., Rad, I., Emami Razavi, A., & Kouhkan, F. (2020). Involved microRNAs in alternative polyadenylation intervene in breast cancer via regulation of cleavage factor "CFIm25". *Scientific Reports*, *10*(1), 11608. https://doi.org/10.1038/s41598-020-68406-3

Tan, S., Ding, K., Chong, Q. Y., Zhao, J., Liu, Y., Shao, Y., Zhang, Y., Yu, Q., Xiong, Z., Zhang, W., Zhang, M., Li, G., Li, X., Kong, X., Ahmad, A., Wu, Z., Wu, Q., Zhao, X., Lobie, P. E., & Zhu, T. (2017). Post-transcriptional regulation of ERBB2 by miR26a/b and HuR confers resistance to tamoxifen in estrogen receptor-positive breast cancer cells. *The Journal of Biological Chemistry*, *292*(33), 13551–13564. https://doi.org/10.1074/jbc.M117.780973

Tan, S., Li, H., Zhang, W., Shao, Y., Liu, Y., Guan, H., Wu, J., Kang, Y., Zhao, J., Yu, Q., Gu, Y., Ding, K., Zhang, M., Qian, W., Zhu, Y., Cai, H., Chen, C., Lobie, P. E., Zhao, X., … Zhu, T. (2018). NUDT21 negatively regulates PSMB2 and CXXC5 by alternative polyadenylation and contributes to hepatocellular carcinoma suppression. *Oncogene*, *37*(35), 4887–4900. https://doi.org/10.1038/s41388-018-0280-6

Tassone, F., De Rubeis, S., Carosi, C., La Fata, G., Serpa, G., Raske, C., Willemsen, R., Hagerman, P. J., & Bagni, C. (2011). Differential usage of transcriptional start sites and polyadenylation sites in FMR1 premutation alleles. *Nucleic Acids Research*, *39*(14), 6172–6185. https://doi.org/10.1093/nar/gkr100

Thivierge, C., Tseng, H. W., Mayya, V. K., Lussier, C., Gravel, S. P., & Duchaine, T. F. (2018). Alternative polyadenylation confers Pten mRNAs stability and resistance to microRNAs. *Nucleic Acids Research*, *46*(19), 10340–10352. https://doi.org/10.1093/nar/gky666

Thomas, C. P., Andrews, J. I., & Liu, K. Z. (2007). Intronic polyadenylation signal sequences and alternate splicing generate human soluble Flt1 variants and regulate the abundance of soluble Flt1 in the placenta. *The FASEB Journal*, *21*(14), 3885–3895. https://doi.org/10.1096/fj.07-8809com

Tian, B., Hu, J., Zhang, H., & Lutz, C. S. (2005). A large-scale analysis of mRNA polyadenylation of human and mouse genes. *Nucleic Acids Research*, *33*(1), 201–212. https://doi.org/10.1093/nar/gki158

Tian, B., & Manley, J. L. (2013). Alternative cleavage and polyadenylation: The long and short of it. *Trends in Biochemical Sciences*, *38*(6), 312–320. https://doi.org/10.1016/j.tibs.2013.03.005

Tian, B., & Manley, J. L. (2017). Alternative polyadenylation of mRNA precursors. *Nature Reviews. Molecular Cell Biology*, *18*(1), 18–30. https://doi.org/10.1038/nrm.2016.116

Tian, P., Li, J., Liu, X., Li, Y., Chen, M., Ma, Y., Zheng, Y. Q., Fu, Y., & Zou, H. (2014). Tandem alternative polyadenylation events of genes in non-eosinophilic nasal polyp tissue identified by high-throughput sequencing analysis. *International Journal of Molecular Medicine*, *33*(6), 1423–1430. https://doi.org/10.3892/ijmm.2014.1734

To, K. K., Robey, R. W., Knutsen, T., Zhan, Z., Ried, T., & Bates, S. E. (2009). Escape from hsa-miR-519c enables drug-resistant cells to maintain high expression of ABCG2. *Molecular Cancer Therapeutics*, *8*(10), 2959–2968. https://doi.org/10.1158/1535-7163.MCT-09-0292

To, K. K., Zhan, Z., Litman, T., & Bates, S. E. (2008). Regulation of ABCG2 expression at the 3′ untranslated region of its mRNA through modulation of transcript stability and protein translation by a putative microRNA in the S1 colon cancer cell line. *Molecular and Cellular Biology*, *28*(17), 5147–5161. https://doi.org/10.1128/MCB.00331-08

Topalian, S. L., Kaneko, S., Gonzales, M. I., Bond, G. L., Ward, Y., & Manley, J. L. (2001). Identification and functional characterization of neo-poly(A) polymerase, an RNA processing enzyme overexpressed in human tumors. *Molecular and Cellular Biology*, *21*(16), 5614–5623. https://doi.org/10.1128/MCB.21.16.5614-5623.2001

Turner, R. E., Henneken, L. M., Liem-Weits, M., Harrison, P. F., Swaminathan, A., Vary, R., Nikolic, I., Simpson, K. J., Powell, D. R., Beilharz, T. H., & Dichtl, B. (2020). Requirement for cleavage factor IIm in the control of alternative polyadenylation in breast cancer cells. *RNA*, *26*(8), 969–981. https://doi.org/10.1261/rna.075226.120

Van Etten, J. L., Nyquist, M., Li, Y., Yang, R., Ho, Y., Johnson, R., Ondigi, O., Voytas, D. F., Henzler, C., & Dehm, S. M. (2017). Targeting a single alternative polyadenylation site coordinately blocks expression of androgen receptor mRNA splice variants in prostate cancer. *Cancer Research*, *77*(19), 5228–5235. https://doi.org/10.1158/0008-5472.CAN-17-0320

Van Peer, G., Mets, E., Claeys, S., De Punt, I., Lefever, S., Ongenaert, M., Rondou, P., Speleman, F., Mestdagh, P., & Vandesompele, J. (2018). A high-throughput 3′ UTR reporter screening identifies microRNA interactomes of cancer genes. *PLoS One*, *13*(3), e0194017. https://doi.org/10.1371/journal.pone.0194017

Venkat, S., Tisdale, A. A., Schwarz, J. R., Alahmari, A. A., Maurer, H. C., Olive, K. P., Eng, K. H., & Feigin, M. E. (2020). Alternative polyadenylation drives oncogenic gene expression in pancreatic ductal adenocarcinoma. *Genome Research*, *30*(3), 347–360. https://doi.org/10.1101/gr.257550.119

Vorlova, S., Rocco, G., Lefave, C. V., Jodelka, F. M., Hess, K., Hastings, M. L., Henke, E., & Cartegni, L. (2011). Induction of antagonistic soluble decoy receptor tyrosine kinases by intronic polyA activation. *Molecular Cell*, *43*(6), 927–939. https://doi.org/10.1016/j.molcel.2011.08.009

Wahle, E. (1991). Purification and characterization of a mammalian polyadenylate polymerase involved in the 3′ end processing of messenger RNA precursors. *The Journal of Biological Chemistry*, *266*(5), 3131–3139.

Wahle, E., Martin, G., Schiltz, E., & Keller, W. (1991). Isolation and expression of cDNA clones encoding mammalian poly(A) polymerase. *The EMBO Journal*, *10*(13), 4251–4257.

Wallace, A. M., Dass, B., Ravnik, S. E., Tonk, V., Jenkins, N. A., Gilbert, D. J., Copeland, N. G., & MacDonald, C. C. (1999). Two distinct forms of the 64,000 Mr protein of the cleavage stimulation factor are expressed in mouse male germ cells. *Proceedings of the National Academy of Sciences of the United States of America*, *96*(12), 6763–6768. https://doi.org/10.1073/pnas.96.12.6763

Wang, E. T., Sandberg, R., Luo, S., Khrebtukova, I., Zhang, L., Mayr, C., Kingsmore, S. F., Schroth, G. P., & Burge, C. B. (2008). Alternative isoform regulation in human tissue transcriptomes. *Nature*, *456*(7221), 470–476. https://doi.org/10.1038/nature07509

Wang, L., Chen, M., Fu, H., Ni, T., & Wei, G. (2020). Tempo-spatial alternative polyadenylation analysis reveals that 3′ UTR lengthening of Mdm2 regulates p53 expression and cellular senescence in aged rat testis. *Biochemical and Biophysical Research Communications*, *523*(4), 1046–1052. https://doi.org/10.1016/j.bbrc.2020.01.061

Wang, L., Hu, X., Wang, P., & Shao, Z. M. (2016). The 3′UTR signature defines a highly metastatic subgroup of triple-negative breast cancer. *Oncotarget*, *7*(37), 59834–59844. https://doi.org/10.18632/oncotarget.10975

Wang, L., Lang, G. T., Xue, M. Z., Yang, L., Chen, L., Yao, L., Li, X. G., Wang, P., Hu, X., & Shao, Z. M. (2020). Dissecting the heterogeneity of the alternative polyadenylation profiles in triple-negative breast cancers. *Theranostics*, *10*(23), 10531–10547. https://doi.org/10.7150/thno.40944

Wang, Q., He, G., Hou, M., Chen, L., Chen, S., Xu, A., & Fu, Y. (2018). Cell cycle regulation by alternative polyadenylation of CCND1. *Scientific Reports*, *8*(1), 6824. https://doi.org/10.1038/s41598-018-25141-0

Wang, R., Zheng, D., Wei, L., Ding, Q., & Tian, B. (2019). Regulation of Intronic polyadenylation by PCF11 impacts mRNA expression of long genes. *Cell Reports*, *26*(10), 2766–2778 e2766. https://doi.org/10.1016/j.celrep.2019.02.049

Wang, X., Li, M., Yin, Y., Li, L., Tao, Y., Chen, D., Li, J., Han, H., Hou, Z., Zhang, B., Wang, X, Ding, Y., Cui, H., & Zhang, H. (2015). Profiling of alternative polyadenylation sites in luminal B breast cancer using the SAPAS method. *International Journal of Molecular Medicine*, *35*(1), 39–50. https://doi.org/10.3892/ijmm.2014.1973

Wang, Y., Loomis, P. A., Zinkowski, R. P., & Binder, L. I. (1993). A novel tau transcript in cultured human neuroblastoma cells expressing nuclear tau. *The Journal of Cell Biology*, *121*(2), 257–267. https://doi.org/10.1083/jcb.121.2.257

Wang, Y., Wu, X. S., He, J., Ma, T., Lei, W., & Shen, Z. Y. (2016). A novel TP53 variant (rs78378222 A > C) in the polyadenylation signal is associated with increased cancer susceptibility: Evidence from a meta-analysis. *Oncotarget*, *7*(22), 32854–32865. https://doi.org/10.18632/oncotarget.9056

Weng, T., Ko, J., Masamha, C. P., Xia, Z., Xiang, Y., Chen, N. Y., Molina, J. G., Collum, S., Mertens, T. C., Luo, F., Philip, K., Davies, J., Huang, J., Wilson, C., Thandavarayan, R. A., Bruckner, B. A., Jyothula, S. S. K., Volcik, K. A., Li, L., … Blackburn, M. R. (2019). Cleavage factor 25 deregulation contributes to pulmonary fibrosis through alternative polyadenylation. *The Journal of Clinical Investigation*, *129*(5), 1984–1999. https://doi.org/10.1172/JCI122106

West, S., & Proudfoot, N. J. (2008). Human Pcf11 enhances degradation of RNA polymerase II-associated nascent RNA and transcriptional termination. *Nucleic Acids Research*, *36*(3), 905–914. https://doi.org/10.1093/nar/gkm1112

Whyteside, A. R., Turner, A. J., & Lambert, D. W. (2014). Endothelin-converting enzyme-1 (ECE-1) is post-transcriptionally regulated by alternative polyadenylation. *PLoS One*, *9*(1), e83260. https://doi.org/10.1371/journal.pone.0083260

Wiestner, A., Tehrani, M., Chiorazzi, M., Wright, G., Gibellini, F., Nakayama, K., Liu, H., Rosenwald, A., Muller-Hermelink, H. K., Ott, G., Chan, W. C., Greiner, T. C., Weisenburger, D. D., Vose, J., Armitage, J. O., Gascoyne, R. D., Connors, J. M., Campo, E., Montserrat, E., … Staudt, L. M. (2007). Point mutations and genomic deletions in CCND1 create stable truncated cyclin D1 mRNAs that are associated with increased proliferation rate and shorter survival. *Blood*, *109*(11), 4599–4606. https://doi.org/10.1182/blood-2006-08-039859

Wood, A. J., Schulz, R., Woodfine, K., Koltowska, K., Beechey, C. V., Peters, J., Bourc'his, D., & Oakey, R. J. (2008). Regulation of alternative polyadenylation by genomic imprinting. *Genes & Development*, *22*(9), 1141–1146. https://doi.org/10.1101/gad.473408

Wu, X., Gardashova, G., Lan, L., Han, S., Zhong, C., Marquez, R. T., Wei, L., Wood, S., Roy, S., Gowthaman, R., Karanicolas, J., Gao, F. P., Dixon, D. A., Welch, D. R., Li, L., Ji, M., Aubé, J., & Xu, L. (2020). Targeting the interaction between RNA-binding protein HuR and FOXQ1 suppresses breast cancer invasion and metastasis. *Communications Biology*, *3*(1), 193. https://doi.org/10.1038/s42003-020-0933-1

Wu, Y., Chen, H., Chen, Y., Qu, L., Zhang, E., Wang, Z., Wu, Y., Yang, R., Mao, R., Lu, C., & Fan, Y. (2019). HPV shapes tumor transcriptome by globally modifying the pool of RNA binding protein-binding motif. *Aging (Albany NY)*, *11*(8), 2430–2446. https://doi.org/10.18632/aging.101927

Xia, Z., Donehower, L. A., Cooper, T. A., Neilson, J. R., Wheeler, D. A., Wagner, E. J., & Li, W. (2014). Dynamic analyses of alternative polyadenylation from RNA-seq reveal a 3′-UTR landscape across seven tumour types. *Nature Communications*, *5*, 5274. https://doi.org/10.1038/ncomms6274

Xiang, K., Nagaike, T., Xiang, S., Kilic, T., Beh, M. M., Manley, J. L., & Tong, L. (2010). Crystal structure of the human symplekin-Ssu72-CTD phosphopeptide complex. *Nature*, *467*(7316), 729–733. https://doi.org/10.1038/nature09391

Xiang, Y., Ye, Y., Lou, Y., Yang, Y., Cai, C., Zhang, Z., Mills, T., Chen, N. Y., Kim, Y., Muge Ozguc, F., Diao, L., Karmouty-Quintana, H., Xia, Y., Kellems, R. E., Chen, Z., Blackburn, M. R., Yoo, S. H., Shyu, A. B., Mills, G. B., & Han, L. (2018). Comprehensive characterization of alternative polyadenylation in human cancer. *Journal of the National Cancer Institute*, *110*(4), 379–389. https://doi.org/10.1093/jnci/djx223

Xie, F., Ye, L., Chang, J. C., Beyer, A. I., Wang, J., Muench, M. O., & Kan, Y. W. (2014). Seamless gene correction of beta-thalassemia mutations in patient-specific iPSCs using CRISPR/Cas9 and piggyBac. *Genome Research*, *24*(9), 1526–1533. https://doi.org/10.1101/gr.173427.114

Xing, Y., Chen, L., Gu, H., Yang, C., Zhao, J., Chen, Z., Xiong, M., Kazobinka, G., Liu, Y., & Hou, T. (2021). Downregulation of NUDT21 contributes to cervical cancer progression through alternative polyadenylation. *Oncogene*, *40*(11), 2051–2064. https://doi.org/10.1038/s41388-021-01693-w

Xiong, M., Chen, L., Zhou, L., Ding, Y., Kazobinka, G., Chen, Z., & Hou, T. (2019). NUDT21 inhibits bladder cancer progression through ANXA2 and LIMK2 by alternative polyadenylation. *Theranostics*, *9*(24), 7156–7167. https://doi.org/10.7150/thno.36030

Xu, Y. F., Li, Y. Q., Liu, N., He, Q. M., Tang, X. R., Wen, X., Yang, X. J., Sun, Y., Ma, J., & Tang, L. L. (2018). Differential genome-wide profiling of alternative polyadenylation sites in nasopharyngeal carcinoma by high-throughput sequencing. *Journal of Biomedical Science*, *25*(1), 74. https://doi.org/10.1186/s12929-018-0477-6

Xu, Y. Z., Di Marco, S., Gallouzi, I., Rola-Pleszczynski, M., & Radzioch, D. (2005). RNA-binding protein HuR is required for stabilization of SLC11A1 mRNA and SLC11A1 protein expression. *Molecular and Cellular Biology*, *25*(18), 8139–8149. https://doi.org/10.1128/MCB.25.18.8139-8149.2005

Xue, Z., Warren, R. L., Gibb, E. A., MacMillan, D., Wong, J., Chiu, R., Hammond, S. A., Yang, C., Nip, K. M., Ennis, C. A., Hahn, A., Reynolds, S., & Birol, I. (2018). Recurrent tumor-specific regulation of alternative polyadenylation of cancer-related genes. *BMC Genomics*, *19*(1), 536. https://doi.org/10.1186/s12864-018-4903-7

Yan, H., Tian, R., Wang, W., Zhang, M., Wu, J., & He, J. (2018). Aberrant Ki-67 expression through 3′UTR alternative polyadenylation in breast cancers. *FEBS Open Bio*, *8*(3), 332–338. https://doi.org/10.1002/2211-5463.12364

Yang, Q., Coseno, M., Gilmartin, G. M., & Doublie, S. (2011). Crystal structure of a human cleavage factor CFI(m)25/CFI(m)68/RNA complex provides an insight into poly(A) site recognition and RNA looping. *Structure*, *19*(3), 368–377. https://doi.org/10.1016/j.str.2010.12.021

Yang, S. W., Li, L., Connelly, J. P., Porter, S. N., Kodali, K., Gan, H., Park, J. M., Tacer, K. F., Tillman, H., Peng, J., Pruett-Miller, S. M., Li, W., & Potts, P. R. (2020). A cancer-specific ubiquitin ligase drives mRNA alternative polyadenylation by ubiquitinating the mRNA 3′ end processing complex. *Molecular Cell*, *77*(6), 1206–1221. https://doi.org/10.1016/j.molcel.2019.12.022

Yang, X., Wu, J., Xu, W., Tan, S., Chen, C., Wang, X., Sun, J., & Kang, Y. (2018). Genome-wide profiling reveals cancer-related genes with switched alternative polyadenylation sites in colorectal cancer. *Oncotargets and Therapy*, *11*, 5349–5357. https://doi.org/10.2147/OTT.S164233

Yang, Z., & Kaye, D. M. (2009). Mechanistic insights into the link between a polymorphism of the 3′UTR of the SLC7A1 gene and hypertension. *Human Mutation*, *30*(3), 328–333. https://doi.org/10.1002/humu.20891

Yang, Z., Venardos, K., Jones, E., Morris, B. J., Chin-Dusting, J., & Kaye, D. M. (2007). Identification of a novel polymorphism in the 3′UTR of the L-arginine transporter gene SLC7A1: Contribution to hypertension and endothelial dysfunction. *Circulation*, *115*(10), 1269–1274. https://doi.org/10.1161/CIRCULATIONAHA.106.665836

Yao, C., Biesinger, J., Wan, J., Weng, L., Xing, Y., Xie, X., & Shi, Y. (2012). Transcriptome-wide analyses of CstF64-RNA interactions in global regulation of mRNA alternative polyadenylation. *Proceedings of the National Academy of Sciences of the United States of America*, *109*(46), 18773–18778. https://doi.org/10.1073/pnas.1211101109

Yao, C., Choi, E. A., Weng, L., Xie, X., Wan, J., Xing, Y., Moresco, J. J., Tu, P. G., Yates, J. R., & Shi, Y. (2013). Overlapping and distinct functions of CstF64 and CstF64tau in mammalian mRNA 3′ processing. *RNA*, *19*(12), 1781–1790. https://doi.org/10.1261/rna.042317.113

Yasuda, M., Shabbeer, J., Osawa, M., & Desnick, R. J. (2003). Fabry disease: Novel alpha-galactosidase A 3′-terminal mutations result in multiple transcripts due to aberrant 3′-end formation. *American Journal of Human Genetics*, *73*(1), 162–173. https://doi.org/10.1086/376608

Ye, C., Zhou, Q., Hong, Y., & Li, Q. Q. (2019). Role of alternative polyadenylation dynamics in acute myeloid leukaemia at single-cell resolution. *RNA Biology*, *16*(6), 785–797. https://doi.org/10.1080/15476286.2019.1586139

Yi, C., Wang, Y., Zhang, C., Xuan, Y., Zhao, S., Liu, T., Hao, J., Gao, Y., Yu, W., Chen, Y., Zhang, C., Guo, W., & Tang, B. (2016). Cleavage and polyadenylation specific factor 4 targets NF-κB/cyclooxygenase-2 signaling to promote lung cancer growth and progression. *Cancer Letters*, *381*(1), 1–13.

Yonaha, M., & Proudfoot, N. J. (2000). Transcriptional termination and coupled polyadenylation in vitro. *The EMBO Journal*, *19*(14), 3770–3777. https://doi.org/10.1093/emboj/19.14.3770

Yoon, Y., McKenna, M. C., Rollins, D. A., Song, M., Nuriel, T., Gross, S. S., Xu, G., & Glatt, C. E. (2013). Anxiety-associated alternative polyadenylation of the serotonin transporter mRNA confers translational regulation by hnRNPK. *Proceedings of the National Academy of Sciences of the United States of America*, *110*(28), 11624–11629. https://doi.org/10.1073/pnas.1301485110

Young, L. E., & Dixon, D. A. (2010). Posttranscriptional regulation of cyclooxygenase 2 expression in colorectal Cancer. *Current Colorectal Cancer Reports*, *6*(2), 60–67. https://doi.org/10.1007/s11888-010-0044-3

Young, L. E., Moore, A. E., Sokol, L., Meisner-Kober, N., & Dixon, D. A. (2012). The mRNA stability factor HuR inhibits microRNA-16 targeting of COX-2. *Molecular Cancer Research*, *10*(1), 167–180. https://doi.org/10.1158/1541-7786.MCR-11-0337

Young, L. E., Sanduja, S., Bemis-Standoli, K., Pena, E. A., Price, R. L., & Dixon, D. A. (2009). The mRNA binding proteins HuR and tristetraprolin regulate cyclooxygenase 2 expression during colon carcinogenesis. *Gastroenterology*, *136*(5), 1669–1679. https://doi.org/10.1053/j.gastro.2009.01.010

Yu, C., Gong, Y., Zhou, H., Wang, M., Kong, L., Liu, J., An, T., Zhu, H., & Li, Y. (2017). Star-PAP, a poly (A) polymerase, functions as a tumor suppressor in an orthotopic human breast cancer model. *Cell Death & Disease*, *8*(2), e2582.

Zhang, H., Lee, J. Y., & Tian, B. (2005). Biased alternative polyadenylation in human tissues. *Genome Biology*, *6*(12), R100. https://doi.org/10.1186/gb-2005-6-12-r100

Zhang, J., Sun, W., Ren, C., Kong, X., Yan, W., & Chen, X. (2019). A PolH transcript with a short 3′UTR enhances PolH expression and mediates cisplatin resistance. *Cancer Research*, *79*(14), 3714–3724. https://doi.org/10.1158/0008-5472.CAN-18-3928

Zhang, S., Zhang, X., Lei, W., Liang, J., Xu, Y., Liu, H., & Ma, S. (2019). Genome-wide profiling reveals alternative polyadenylation of mRNA in human non-small cell lung cancer. *Journal of Translational Medicine*, *17*(1), 257. https://doi.org/10.1186/s12967-019-1986-0

Zhang, X., Dudek, E. J., Liu, B., Ding, L., Fernandes, A. F., Liang, J. J., Horwitz, J., Taylor, A., & Shang, F. (2007). Degradation of C-terminal truncated alpha A-crystallins by the ubiquitin-proteasome pathway. *Investigative Ophthalmology & Visual Science*, *48*(9), 4200–4208. https://doi.org/10.1167/iovs.07-0196

Zhang, Y., Liu, L., Qiu, Q., Zhou, Q., Ding, J., Lu, Y., & Liu, P. (2021). Alternative polyadenylation: Methods, mechanism, function, and role in cancer. *Journal of Experimental & Clinical Cancer Research*, *40*(1), 51. https://doi.org/10.1186/s13046-021-01852-7

Zhang, Y., Wang, Y., Li, C., & Jiang, T. (2020). Systemic analysis of the prognosis-associated alternative polyadenylation events in breast Cancer. *Frontiers in Genetics*, *11*, 590770. https://doi.org/10.3389/fgene.2020.590770

Zhao, D., Duan, H., Kim, Y. C., & Jefcoate, C. R. (2005). Rodent StAR mRNA is substantially regulated by control of mRNA stability through sites in the 3′-untranslated region and through coupling to ongoing transcription. *The Journal of Steroid Biochemistry and Molecular Biology*, *96*(2), 155–173. https://doi.org/10.1016/j.jsbmb.2005.02.011

Zhao, J., Hyman, L., & Moore, C. (1999). Formation of mRNA 3′ ends in eukaryotes: Mechanism, regulation, and interrelationships with other steps in mRNA synthesis. *Microbiology and Molecular Biology Reviews*, *63*(2), 405–445.

Zheng, D., Wang, R., Ding, Q., Wang, T., Xie, B., Wei, L., Zhong, Z., & Tian, B. (2018). Cellular stress alters 3′UTR landscape through alternative polyadenylation and isoform-specific degradation. *Nature Communications*, *9*(1), 2268. https://doi.org/10.1038/s41467-018-04730-7

Zhong, J., Cao, R. X., Hong, T., Yang, J., Zu, X. Y., Xiao, X. H., Liu, J. H., & Wen, G. B. (2011). Identification and expression analysis of a novel transcript of the human PRMT2 gene resulted from alternative polyadenylation in breast cancer. *Gene*, *487*(1), 1–9. https://doi.org/10.1016/j.gene.2011.06.022

Zhou, L., Yuan, Q., & Yang, M. (2012). A functional germline variant in the P53 polyadenylation signal and risk of esophageal squamous cell carcinoma. *Gene*, *506*(2), 295–297. https://doi.org/10.1016/j.gene.2012.07.007

Zhu, H., Zhou, H. L., Hasman, R. A., & Lou, H. (2007). Hu proteins regulate polyadenylation by blocking sites containing U-rich sequences. *The Journal of Biological Chemistry*, *282*(4), 2203–2210. https://doi.org/10.1074/jbc.M609349200

Zhu, Y., Wang, X., Forouzmand, E., Jeong, J., Qiao, F., Sowd, G. A., Engelman, A. N., Xie, X., Hertel, K. J., & Shi, Y. (2018). Molecular mechanisms for CFIm-mediated regulation of mRNA alternative polyadenylation. *Molecular Cell*, *69*(1), 62–74 e64. https://doi.org/10.1016/j.molcel.2017.11.031

SUPPORTING INFORMATION

Additional supporting information may be found in the online version of the article at the publisher's website.

How to cite this article: Mohanan, N. K., Shaji, F., Koshre, G. R., & Laishram, R. S. (2021). Alternative polyadenylation: An enigma of transcript length variation in health and disease. *Wiley Interdisciplinary Reviews: RNA*, e1692. https://doi.org/10.1002/wrna.1692

International Journal of
Molecular Sciences

MDPI

Article

Star-PAP RNA Binding Landscape Reveals Novel Role of Star-PAP in mRNA Metabolism That Requires RBM10-RNA Association

Ganesh R. Koshre [1,2], Feba Shaji [1,3], Neeraja K. Mohanan [1,2], Nimmy Mohan [1], Jamshaid Ali [4] and Rakesh S. Laishram [1,*]

1 Cardiovascular Diseases & Diabetes Biology, Rajiv Gandhi Centre for Biotechnology, Trivandrum 695014, India; ganeshram@rgcb.res.in (G.R.K.); febashaji@rgcb.res.in (F.S.); neerajakm@rgcb.res.in (N.K.M.); nimmym@rgcb.res.in (N.M.)
2 Manipal Academy of Higher Education, Manipal 576104, India
3 Regional Centre for Biotechnology, Faridabad 121001, India
4 Bioinformatics Facility, Rajiv Gandhi Centre for Biotechnology, Trivandrum 695585, India; jam@rgcb.res.in
* Correspondence: laishram@rgcb.res.in; Tel.: +91-0471-2529592

Abstract: Star-PAP is a non-canonical poly(A) polymerase that selects mRNA targets for polyadenylation. Yet, genome-wide direct Star-PAP targets or the mechanism of specific mRNA recognition is still vague. Here, we employ HITS-CLIP to map the cellular Star-PAP binding landscape and the mechanism of global Star-PAP mRNA association. We show a transcriptome-wide association of Star-PAP that is diminished on Star-PAP depletion. Consistent with its role in the 3′-UTR processing, we observed a high association of Star-PAP at the 3′-UTR region. Strikingly, there is an enrichment of Star-PAP at the coding region exons (CDS) in 42% of target mRNAs. We demonstrate that Star-PAP binding de-stabilises these mRNAs indicating a new role of Star-PAP in mRNA metabolism. Comparison with earlier microarray data reveals that while UTR-associated transcripts are down-regulated, CDS-associated mRNAs are largely up-regulated on Star-PAP depletion. Strikingly, the knockdown of a Star-PAP coregulator RBM10 resulted in a global loss of Star-PAP association on target mRNAs. Consistently, RBM10 depletion compromises 3′-end processing of a set of Star-PAP target mRNAs, while regulating stability/turnover of a different set of mRNAs. Our results establish a global profile of Star-PAP mRNA association and a novel role of Star-PAP in the mRNA metabolism that requires RBM10-mRNA association in the cell.

Keywords: 3′-end processing; polyadenylation; Star-PAP; RBM10; HITS-CLIP; mRNA metabolism; RNA-turnover

Citation: Koshre, G.R.; Shaji, F.; Mohanan, N.K.; Mohan, N.; Ali, J.; Laishram, R.S. Star-PAP RNA Binding Landscape Reveals Novel Role of Star-PAP in mRNA Metabolism That Requires RBM10-RNA Association. *Int. J. Mol. Sci.* **2021**, *22*, 9980. https://doi.org/10.3390/ijms22189980

Academic Editor: Naoyuki Kataoka

Received: 17 July 2021
Accepted: 19 August 2021
Published: 15 September 2021

1. Introduction

Pre-mRNA 3′-end processing is an essential step in eukaryotic gene expression that involves two coupled steps-endonucleolytic cleavage followed by the addition of a poly(A) tail (polyadenylation) [1–4]. 3′-end processing is carried out by a cleavage and polyadenylation complex (CPA) that is associated with >85 protein components [3,5,6]. The CPA complex is comprised of subunits of cleavage and polyadenylation specificity factor (CPSF), cleavage stimulatory factor (CstF), cleavage factors Im (CFIm) and IIm (CFIIm), scaffolding protein symplekin, poly(A) polymerase (PAP), and poly(A) binding protein (PABPN1) as core components [3,4]. Cleavage and polyadenylation at the pre-mRNA 3′-end involve recognition of a poly(A) signal (PA-signal) by CPSF-30 and WDR33 subunits of CPSF complex [7–10]. CstF (CSTF2) interacts with the GU/U-rich downstream sequence (DSE) and cooperates with CPSF to assemble a stable CPA complex [11,12]. CPSF3 then cleaves pre-mRNA at the PA-site followed by PA-tail addition by a PAP on the upstream fragment, whereas the downstream fragment is rapidly degraded [13,14]. PABPN1 then binds and stabilises the PA-tail and controls PA-tail length [15–17]. Canonical PAPα/γ is the primary

PAP for mRNA polyadenylation in the nucleus [18,19]. The discovery of a variant of PAP, Star-PAP, reveals the existence of alternative PAP for nuclear polyadenylation [1,20,21]. Star-PAP selectively polyadenylates mRNAs involved in oxidative stress, apoptosis, cancer and cardiac hypertrophy [21–27]. In addition to the polyadenylation activity, Star-PAP has a confirmed uridylation activity [21,28,29], and has been implicated in the regulation of miRNA biogenesis and stability [30,31].

Approximately, 70% of human genes have multiple PA-sites that are alternately used (alternative polyadenylation, APA) generating diversity of mRNA isoforms [32,33]. Recently, we showed a genome-wide mechanism of APA wherein canonical PAPα and γ, and Star-PAP selects distinct PA-sites on target mRNAs [18]. Star-PAP primarily selects the PA-distal site resulting in a predominant 3′-UTR shortening on Star-PAP knockdown [18]. Yet, the mechanism of how Star-PAP selects target PA-site and assembles specific CPA complex is unclear. We identified a Star-PAP recognition element on the target mRNA 3′-UTRs (*HMOX1*, *BIK* and *NQO1*) and demonstrated that canonical PAPα/γ is excluded from Star-PAP targets enabling selective polyadenylation of target mRNA [20,25,34]. Mass spectrometry analysis of Star-PAP associated proteins identified RNA binding motif 10 (RBM10) as a unique Star-PAP complex component absent in the canonical PAPα/γ complex [24]. RBM10 is an RNA binding protein that recognises homopolymers of G or U ribonucleotides in vitro [35–38]. A mutational defect in RBM10 was reported to cause an X-linked recessive disorder (TARP syndrome) and lung adenocarcinoma [39,40]. RBM10 has high homology with other RBMs such as RBM5 involved in apoptosis [41,42]. Studies have demonstrated the role of RBM10 in alternative splicing and 3′-end processing [24,42,43]. RBM10 associates with different spliceosome complexes, hnRNPs, and U2 snRNPs and controls alternative splicing of apoptosis-related genes *FAS* and *BclX* [43–48]. Genome-wide RNA-Seq demonstrated significant skipped exons upon depletion of RBM10 in HEK 293 cells [42]. We show a splicing independent function of RBM10 that regulates 3′-end processing of Star-PAP target mRNAs involved in hypertrophy gene program [24]. Yet the global role of RBM10 on Star-PAP 3′-UTR association is unclear.

In this study, we carried out a HITS-CLIP experiment to map the Star-PAP binding landscape and to define the mechanism of Star-PAP target 3′-end PA-site selection. We observed a genome-wide association of Star-PAP in all the chromosomes that was lost on Star-PAP depletion. Consistent with its role in the 3′-UTR processing, we observed a high association of Star-PAP at the 3′-UTR region. Using 3′-RACE assay and RNA immunoprecipitation, we confirmed that Star-PAP global 3′-UTR association regulates 3′-end processing of target mRNAs. Strikingly, there was an enrichment of Star-PAP at the coding region exons (CDS) in more than 40% of target mRNA that was independent of the Star-PAP 3′-end processing function. We demonstrated that Star-PAP binding regulates the half-life of these mRNA targets indicating a new role of Star-PAP in mRNA metabolism. To further define the mechanism of the Star-PAP RNA association, we depleted RBM10 and carried out the Star-PAP HITS-CLIP experiment. Strikingly, we observed global loss of Star-PAP association (over 70% target mRNAs) on target RNAs on RNAi mediated RBM10 depletion. This includes both mRNAs where Star-PAP was associated at the 3′-UTR and CDS regions. Consistently, RBM10 depletion compromises 3′-end processing of a set of Star-PAP target mRNAs, whereas it regulates the stability and turnover of a different set of Star-PAP target mRNAs. Together, our results established a new role of Star-PAP in mRNA metabolism that is controlled through RBM10-RNA association.

2. Results

2.1. Genome-Wide Star-PAP RNA Binding Landscape Reveals Star-PAP Direct mRNA Targets

Star-PAP is a variant PAP that controls the expression of mRNAs involved in multiple cellular functions. Genome-wide microarray analysis after Star-PAP knockdown demonstrated both up-regulated and down-regulated sets of mRNAs [21,49]. Yet, how many of such altered mRNAs are directly controlled by Star-PAP or the mechanism of Star-PAP target PA-site/3′-UTR selection is still undefined. To assess this, we performed

HITS-CLIP sequencing after pull-down of Star-PAP in the presence and absence of RBM10 depletion with IgG as a reference control. HITS-CLIP of Star-PAP was further confirmed after Star-PAP depletion in a similar HITS-CLIP experiment.

HITS-CLIP sequencing raw data of each Star-PAP sample had approximately 10 million reads. After filtering for quality reads, removing adapter sequences and identical reads from PCR amplification, we obtained ~8 million sequencing reads that were used for aligning to the reference genome. Further, parsing the alignment to obtain uniquely mapped reads, and a minimal mapping size of 18 nucleotides, we generated about 4.2 million distinct sequencing reads that uniquely mapped to the human reference genome (hg19). The association of identified reads was observed in all chromosomes with a varying number of mapped reads (Figure 1a). The highest mapped reads were observed on chromosomes 1, 8 and 19 and the lowest reads were observed on Chromosome Y (Supplementary Figures S1a and S2a). After peak calling and subtraction for reference IgG HITS-CLIP, we identified 420,000 read clusters corresponding to ~14,000 distinct transcripts in Star-PAP HITS-CLIP. To confirm the specificity of Star-PAP binding, we employed siRNA-mediated depletion of Star-PAP and a similar HITS-CLIP experiment was carried out. Interestingly, depletion of Star-PAP resulted in the loss of 65% of the mapped regions on the reference genome (Figure 1a, Supplementary Figure S2a). The loss of read clusters was observed in almost all chromosomes with varying degrees (Supplementary Figure S2a). Reduced maps on Star-PAP knockdown in some of the chromosomes (chromosome 2, 4, 7, 17, 13, 19, and 20) and percent reductions in respective chromosomes are shown in Figure 1a, Supplementary Figures S1a and S2a. To further assess the difference in the Star-PAP associated clusters between control and Star-PAP depletion on specific mRNAs, we enlarged a region of 17-kb at *CHGB* mRNA and a 7-kb region around *CST4* mRNA from chromosome 20 (Figure 1a). We also enlarged a 200-bp region around the peak cluster that shows Star-PAP associated nucleotide sequence on the mRNA (Supplementary Figure S2c). Together, these results reveal different binding regions of Star-PAP on different mRNAs that were lost on siStar-PAP depletion.

Mapping of the genetic regions of Star-PAP association showed Star-PAP binding sites were primarily associated with protein-coding RNAs (>70%) with less than 15% in the non-coding RNAs (miRNA, snRNA, lncRNA and snoRNA), and ~10% in the intronic RNAs (Figure 1b). For the analysis of Star-PAP specific target protein-coding mRNAs, we considered transcripts that had high read detection (>10-read tags per cluster) and those absent from the HITS-CLIP experiment after Star-PAP depletion. With this stringent condition, we obtained 4200 specific mRNAs directly associated with Star-PAP (Supplementary Table S1). Among the specific protein-coding mRNAs, significant Star-PAP association was detected at the CDS (exons) region, 3′-UTR and terminal exons, and in the 5′-UTR regions (Figure 1c). Overall, Star-PAP detection was high at the 3′-UTR regions (46%) consistent with its primary role in the 3′-UTR processing. Interestingly, the detection in the CDS region was equally high (42%) (Figure 1c) indicating a distinct role of Star-PAP in mRNA metabolism. Moreover, in many of the transcripts, Star-PAP was detected at both CDS and 3′-UTR regions. Three mRNAs with Star-PAP association at the 3′-UTR and CDS regions are shown in Figure 1a and Supplementary Figure S2c. Yet, how Star-PAP binding at the CDS region alters gene expression is not understood (detailed in the following sections). Consistent with earlier studies of the Star-PAP target mRNAs, our in silico analysis of nucleotide composition of these Star-PAP specific reads confirms a biased GC content over AU in the Star-PAP bound regions in both 3′-UTR and CDS regions (Supplementary Figure S1b). Analysis of consensus sequence motif of 12-mers using MEME-Chip software confirmed an -AUA- containing consensus motif at the target mRNAs (Supplementary Figure S2b). An enlarged region of the Star-PAP read cluster at the 3′-UTR of target mRNA also shows a similar motif with an -AUA- sequence (Supplementary Figure S2c). This is in line with our earlier in vitro footprinting data and in silico target analysis reinforcing the earlier role of Star-PAP in the 3′-end processing of target mRNAs [20,25].

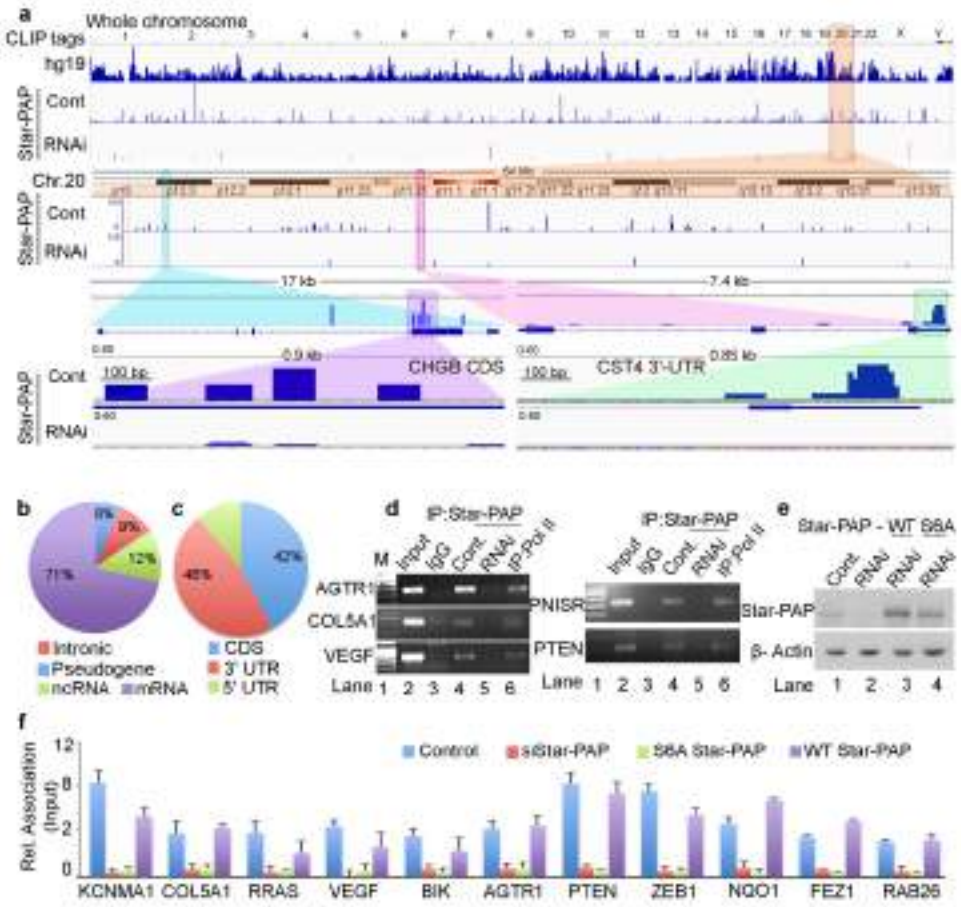

Figure 1. Star-PAP genome-wide binding landscape across the human genome shows a variety of mRNA targets. (**a**) HITS-CLIP signals of Star-PAP distribution across human genome showing whole chromosomal association of Star-PAP in control and siRNA Star-PAP depletion in HEK 293 cells. Star-PAP HITS-CLIP tag distribution in one example chromosome (chromosome 20) and the loss of the mapped tags on siStar-PAP is shown below. Similar distribution on 6 selected chromosomes is shown in Supplementary Figure S1a. The CLIP tags here and in the supplementary figures were counted after peak calling. Enlarged 17-kb region of *CHGB* mRNA and 7.4-kb *CST4* mRNA along with mapped cluster region in the *CHGB*-CDS and *CST4*-UTR regions is shown below. (**b**) Distribution Star-PAP associations among different RNA species (protein-coding (mRNA), non-coding RNAs (ncRNA), pseudo genes, and intronic RNA regions are indicated). (**c**) Distribution of Star-PAP associated nucleotide positions of mRNAs among coding exons (CDS), 3′-UTR and terminal exon, and the 5′-UTR regions. (**d**) RNA immunoprecipitation (RIP) analysis of Star-PAP in control and siRNA treated cells and the control Pol II on various Star-PAP targets as indicated. Input, 10% of the IP lysate. M, marker lane. (**e**) Western blot analysis of Star-PAP and control β-actin in control and Star-PAP depleted HEK 293 cells in the presence and absence of rescue with wild type and S6A mutant Star-PAP. (**f**) Quantitative RIP (qRIP) analysis of various Star-PAP target mRNAs detected in the HITS-CLIP experiment as indicated, showing the relative association of Star-PAP in control, Star-PAP knockdown and Star-PAP RNA binding mutant (S6A) Star-PAP expressed cells. (S6A Star-PAP carrying silent mutations that render siRNA ineffective was ectopically expressed in the cell after endogenous Star-PAP knockdown). Error bar represents SEM (standard error mean) of three independent experiments.

2.2. Star-PAP Associated mRNA Targets Show Wide Roles of Star-PAP in Human Diseases and Signaling Pathways

To validate our HITS-CLIP experiments, we performed qualitative RNA immunoprecipitation (RIP) and quantitative RIP (qRIP) analysis of selected Star-PAP target mRNAs. We observed the association of Star-PAP with mRNAs including the earlier established targets (*AGTR1*, *COL5A1*, *VEGF*, *PTEN*, *PNISR*, *IFRD1*) by qualitative RIP analysis (Figure 1d). Star-PAP knockdown resulted in the loss of association. Control RNA Pol II was associated with all mRNAs tested (Figure 1d). Similarly, in the qRIP analysis as well, we observed the

association of Star-PAP on mRNAs (*KCNMA1*, *COL5A1*, *RRAS*, *VEGF*, *BIK*, *AGTR1*, *PTEN*, *ZEB1*, *NQO1*, *FEZ1*, *RAB26*) that was lost on Star-PAP knockdown (Figure 1f). In addition, Star-PAP RNA binding mutant (S6A Star-PAP) [50] but not wild type Star-PAP also resulted in the loss of binding to target mRNAs (Figure 1f). Western analysis of siRNA Star-PAP depletion and rescue with wild type and S6A Star-PAP is shown in Figure 1e. To gain further insight into cellular functions of Star-PAP target mRNAs, we analysed Star-PAP bound mRNAs from HITS-CLIP sequencing for functional pathways in different human diseases and cellular signals (Supplementary Figure S1c–d). We observed enrichment of mRNAs involved in cancer, heart disease, metabolic diseases, immunity and infection among the Star-PAP bound targets (Supplementary Figure S1c). Among the signalling pathways, RTK-MAPK, PI3K-Akt, GPCR, Interleukin and Wnt signalling pathways were enriched among the target mRNAs (Supplementary Figure S1d) indicating a wide function of Star-PAP in the cell.

2.3. Star-PAP RNA Binding Can Both Down Regulate and Up-Regulate Target mRNA Expression

Interestingly, qRT-PCR analysis indicated the down-regulation of a number of Star-PAP-associated mRNAs on Star-PAP depletion consistent with Star-PAPs role in the 3′-end processing (Figure 2a, Supplementary Figure S2d). However, a number of mRNAs (*BPNT1*, *CTSO*, *SSX2*) that were bound by Star-PAP were up-regulated on Star-PAP knockdown (Figure 2a) suggesting a distinct function of Star-PAP in mRNA metabolism in addition to the 3′-end processing. These mRNAs were equally up-regulated in the presence of S6A Star-PAP RNA binding mutation. There was no effect of Star-PAP knockdown on the control non-target *GCLC* mRNA (Figure 2a). To gain further mechanistic insight into the role of Star-PAP in RNA metabolism, we compared mRNAs detected in our HITS-CLIP Star-PAP with that of earlier microarray analysis that showed altered expression on Star-PAP depletion (~1500 genes up-regulated and ~2400 genes down-regulated) [49]. Around 55% of the mRNAs whose expression was significantly altered on Star-PAP knockdown in microarray analysis were detected in our Star-PAP HITS-CLIP (Figure 2b) indicating that the expression of these set of mRNAs is directly regulated by Star-PAP-RNA association. Interestingly, there was a higher occurrence of down-regulated mRNAs than that of up-regulated mRNAs in the Star-PAP HITS-CLIP. There was ~60% of the down-regulated genes on Star-PAP depletion was detected in the Star-PAP HITS-CLIP (Figure 2c). Consistently, Star-PAP was primarily detected at the 3′-UTR and the terminal exon among these mRNAs (Figure 2d). Moreover, among the mRNA from the HITS-CLIP data where Star-PAP was detected at the 3′-UTR region, the majority were down-regulated on Star-PAP depletion in the microarray data (Supplementary Figure S2e). The Association of Star-PAP on a select mRNA at the 3′-UTR is shown in Supplementary Figure S2c. Together these results reveal that the Star-PAP association at the 3′-UTR region regulates the 3′-end processing of target mRNAs.

Further, qRIP analysis of 6 select mRNAs that were down-regulated on Star-PAP depletion (*COL5A1*, *KCNMA1*, *WIF1*, *NQO1*, *FEZ1*, *RRAS2*) demonstrated a biased association of Star-PAP at the 3′-UTR compared to the CDS regions (Figure 2e). Consistently, qRT-PCR analysis of selected mRNAs among those of UTR associated demonstrated a loss of expression (*RAB26*, *ASCC3*, *CAMK2B*, *NQO1*, *IGF2*, *HMOX1*, *ALDH2*, *PTBP2*, *RGS4*, *STC1*, *STY1*, *RTN1*) (Supplementary Figure S2d). Western analysis confirms down-regulation of corresponding protein expression of target mRNAs (*HMOX1*, *NQO1* and *CDH1*) on Star-PAP depletion (Figure 2g) consistent with the loss of Star-PAP association on the depletion. Further, 3′-RACE assay confirms the role of Star-PAP in the cleavage and polyadenylation of these mRNAs (*IGF2*, *COL5A1*, *BIK*, *KCNMA1*, *HMOX1*, *NQO1*) (Figure 2f). There was a loss of 3′-RACE product on Star-PAP depletion as reported earlier (Figure 2f). These results were further corroborated with cleavage assay where we observed increased accumulation of uncleaved pre-mRNAs (*KCNMA1*, *NQO1*, *COL5A1*, *WIF1*, *FEZ1*) while the expression levels were reduced on Star-PAP depletion (Figure 2h). Together, HITS-CLIP data confirm the global role of Star-PAP in the 3′-end processing of target mRNAs by the association

at the 3′-UTR region. Interestingly, analysis of the polyadenylation site usage (PA-site choice) of these mRNAs revealed a higher distal PA-sites usage (~40%) consistent with earlier genome-wide Star-PAP APA analysis (Supplementary Figure S2f) [18]. We also observed proximal PA-site selection in around 30% of mRNAs whereas ~20% of mRNAs have single PA-sites (Supplementary Figure S2f). Functional analysis of these UTR-associated mRNAs shows a higher prevalence in cellular functions including cell cycle, apoptosis, myocyte hypertrophy, cell invasion, metastasis and metabolic pathways (Supplementary Figure S2g).

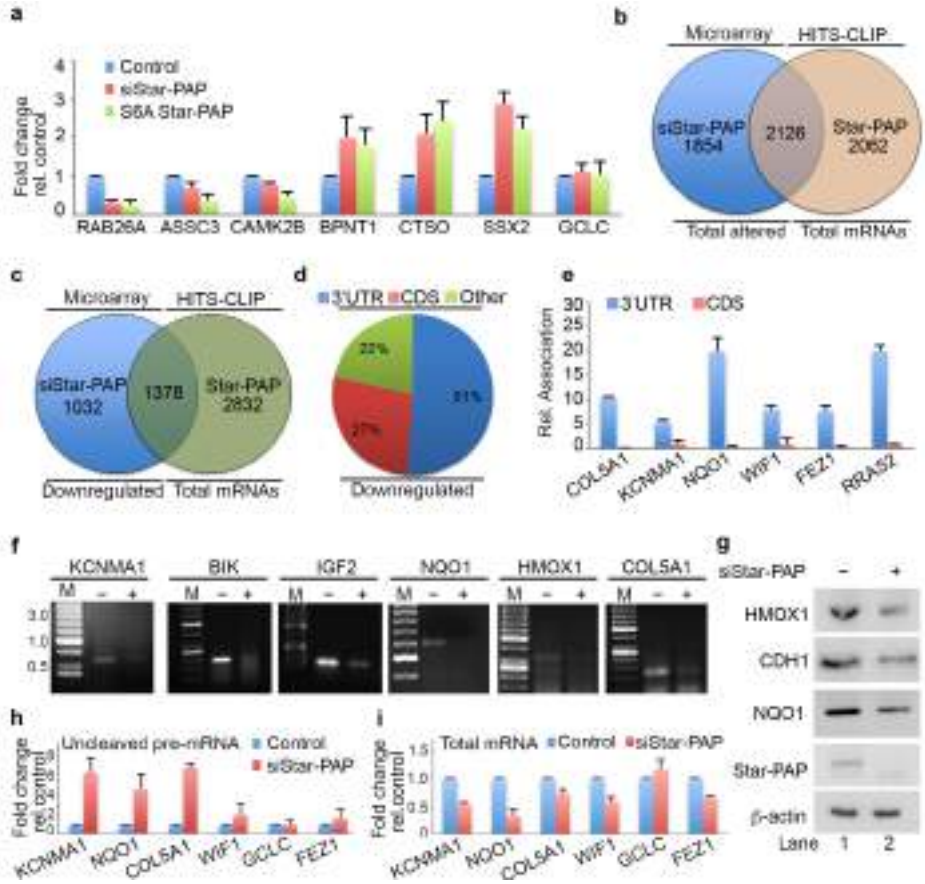

Figure 2. Star-PAP global mRNA association regulates the 3′-end processing of target mRNAs. (**a**) qRT-PCR analysis of select Star-PAP associated mRNAs from HITS-CLIP experiment with total RNA isolated from HEK 293 cells with control, Star-PAP, and with exogenous S6A Star-PAP expression after silencing of endogenous Star-PAP in HEK 293 cells, as in Figure 1e. The error bars indicate standard errors of the mean (SEM). (**b**) Venn diagram showing overlapped mRNA targets detected in Star-PAP HITS-CLIP and significantly altered (both down-regulated and up-regulated) mRNAs on Star-PAP depletion from earlier microarray analysis. (**c**) Venn diagram showing overlapped mRNA targets between down-regulated genes on Star-PAP depletion from earlier microarray analysis and mRNAs associated with Star-PAP detected in Star-PAP HITS-CLIP. (**d**) Distribution of Star-PAP associated nucleotide positions in the coding region and 3′-UTR region among overlapped down-regulated mRNAs on Star-PAP knockdown that is detected in Star-PAP HITS-CLIP experiment. (**e**) qRIP analysis showing the relative association of Star-PAP in the coding region and 3′-UTR region on select Star-PAP target mRNAs as indicated. Error bar represents SEM of three independent experiments. (**f**) 3′-RACE assay of various Star-PAP target mRNAs (*KCNMA1*, *IGF2*, *HMOX1*, *BIK*, *COL5A1*, *NQO1*) from total RNA isolated from HEK 293 cells after Star-PAP knockdown. The absence of siRNA (-siRNA) indicates that control-scrambled siRNA was used. (**g**) Western blot analysis of Star-PAP, target proteins, and control actin from control and Star-PAP knockdown HEK 293 cells. (**h**,**i**) Measurement of uncleaved pre-mRNA levels (**h**) expressed relative to total mRNA (**i**) after Star-PAP knockdown or control cells as indicated.

2.4. Star-PAP mRNA Binding Regulates Stability and Turnover Rate of Target mRNAs

Among the up-regulated genes on Star-PAP depletion in our microarray, only around 50% of the genes were detected in Star-PAP HITS-CLIP (Figure 3b). These mRNAs represent the set of mRNAs whose expression is negatively regulated by Star-PAP binding. The other set of up-regulated mRNAs in the microarray (not detected in our Star-PAP HITS-CLIP) is likely controlled indirectly. Interestingly, among the Star-PAP targets detected in HITS-CLIP that are up-regulated on Star-PAP depletion (708 mRNAs), Star-PAP was mapped primarily at the CDS exonic regions (~70%), while a minority (<20%) was mapped in the 3′-UTR region (Figure 3b) suggesting a novel function of Star-PAP independent of 3′-end processing. Consistently, there was an overall higher coverage of the CDS region compared to the 3′-UTR region among these mRNAs (Supplementary Figure S3a). Further, qRIP analysis on select mRNAs (*PNISR*, *IRFD1*, *LHX9*, *TP73*, *RRAS2*) demonstrated primary association of Star-PAP at the CDS region over the 3′-UTR region on these mRNAs (Figure 3c). Consistently, 3′-RACE and cleavage assay show no effect of Star-PAP knockdown on the cleavage and polyadenylation of this set of mRNAs (Figure 3d,e).

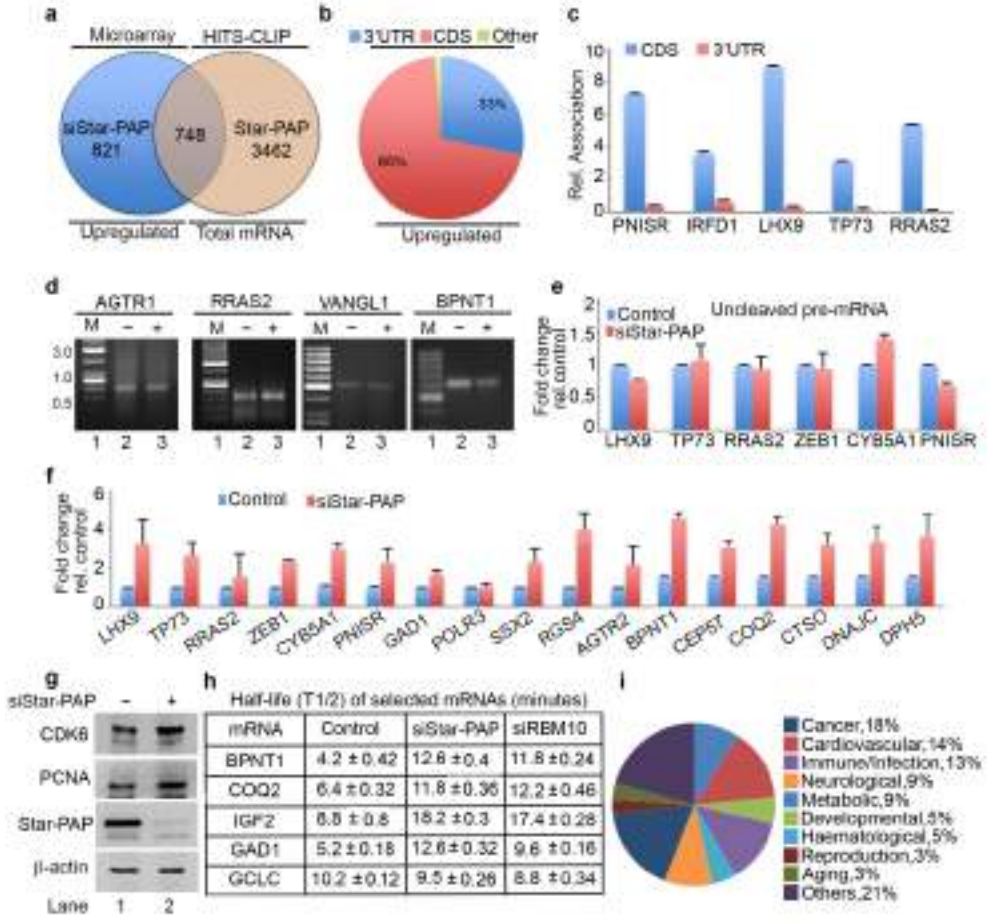

mRNA	Control	siStar-PAP	siREM10
BPNT1	4.2 ± 0.42	12.6 ± 0.4	11.8 ± 0.24
COQ2	6.4 ± 0.32	11.8 ± 0.36	12.2 ± 0.46
IGF2	6.8 ± 0.8	18.2 ± 0.3	17.4 ± 0.28
GAD1	5.2 ± 0.18	12.6 ± 0.32	9.6 ± 0.16
GCLC	10.2 ± 0.12	9.5 ± 0.26	8.8 ± 0.34

Figure 3. Star-PAP mRNA association regulates mRNA half-life in a novel Star-PAP-mediated mRNA metabolism pathway. (**a**) Venn diagram showing overlapped mRNA targets between up-regulated genes on siStar-PAP from earlier microarray analysis and mRNAs associated with Star-PAP detected in the Star-PAP HITS-CLIP experiment. (**b**) Distribution of Star-PAP associated nucleotide positions in the coding region and 3′-UTR region among up-regulated mRNAs on Star-PAP knockdown that is also common with that in Star-PAP HITS-CLIP experiment. (**c**) qRIP analysis showing the relative association of Star-PAP in the coding region and 3′-UTR region on select Star-PAP target mRNAs as indicated. Error bar represents SEM of three independent experiments. (**d**) 3′-RACE assay of various Star-PAP target mRNAs (*AGTR1*, *PNISR*, *VANGL1*, *BPNT1*) from total RNA isolated from HEK 293 cells from control or after Star-PAP knockdown as indicated. (**e**) Measurement of uncleaved pre-mRNA levels expressed relative to total mRNA after Star-PAP knockdown or control cells as indicated. (**f**) qRT-PCR analysis of select Star-PAP target mRNAs primarily associated at the coding region from

HITS-CLIP experiment with total RNA isolated from HEK 293 cells with control and Star-PAP knockdown. (**g**) Western blot analysis of Star-PAP, target proteins, and control actin from control and Star-PAP knockdown HEK 293 cells. (**h**) Half-life (T1/2) measurement of various Star-PAP target mRNAs after transcription inhibition with actinomycin D under conditions as indicated. T1/2 is expressed in hours. Data are mean ± SEM of $n = 3$ independent experiments. (**i**) A schematic pie chart showing functional pathway analysis of Star-PAP target mRNAs obtained from HITS-CLIP experiment that were up-regulated on siStar-PAP microarray.

To understand the mechanism of how Star-PAP binding negatively regulates the expression of these of mRNAs, we carried out the qRT-PCR analysis of select mRNAs (*LHX9*, *TP73*, *RRAS2*, *ZEB1*, *CYB5A1*, *PNISR*, *GAD1*, *POLR3*, *SSX2*, *RGS4*, *AGTR2*, *BPNT1*, *CEP57*, *COQ2*, *CTSO*, *DNAJC* and *DPH5*) (Figure 3f). We observed increased mRNA levels on Star-PAP depletion consistent with our microarray analysis. Western blot also showed increased protein levels on Star-PAP depletion (Figure 3g) suggesting Star-PAP's role as a negative regulator of mRNA stability (Figure 3f,g). To further understand the mechanism, we measured mRNA stability and turnover by measuring half-life (*BPNT1*, *COQ2*, *IGF2*, *GAD1* and control non-target *GCLC*) after inactivating transcription with actinomycin D in the presence and absence of Star-PAP knockdown (Figure 3h). Strikingly, there was an increase in the half-life (2 to 3-fold) of mRNAs with no effect on the non-target *GCLC* mRNA (Figure 3h). These results demonstrate that Star-PAP binding on the CDS region de-stabilises mRNA and as a result a depletion of Star-PAP results in both increased mRNA and protein expressions. A list of Star-PAP-associated mRNAs down-regulated on siStar-PAP is shown in Supplementary Table S2. Functional pathway analysis of these mRNAs showed enrichment of genes involved in diseases including cardiovascular, metabolic, infection, and cancer (Figure 3i). A list of Star-PAP associated mRNAs up-regulated on Star-PAP knockdown is shown in Supplementary Table S2.

2.5. Transcriptome-Wide Star-PAP Binding Analysis after RBM10 Depletion Indicates Global Role of RBM10 in Star-PAP Target mRNA Association

RBM10 is a Star-PAP-associated protein that is required for the regulation of mRNAs involved in cardiac hypertrophy [24]. Therefore, we investigated the genome-wide role of RBM10 in the Star-PAP recognition of target mRNAs. We carried out a similar HITS-CLIP experiment of Star-PAP after siRNA-mediated depletion of RBM10 in HEK 293 cells (Figure 4a). Strikingly, RBM10 depletion resulted in a loss of >60% of mapped read clusters associated with different chromosomes (Figure 4a, Supplementary Figure S3b). Relative reductions of Star-PAP association on six select chromosomes on RBM10 depletion are shown in Supplementary Figure S3b. Among the 4200 protein-coding genes bound by Star-PAP detected in our HITS-CLIP, ~70% of the mRNAs were not detected after RBM10 knockdown (Figure 4b). Interestingly, among the down-regulated genes on Star-PAP knockdown (UTR regulated), the majority (around 950) of mRNAs were not detected after RBM10 depletion (Figure 4d) indicating that RBM10 is required for Star-PAP association on target PA-sites. Moreover, among the >700 up-regulated genes on siStar-PAP that are detected on HITS-CLIP (negative regulation by Star-PAP), the majority (~540 mRNAs) were not detected after the RBM10 depletion (Figure 4c). This indicates the role of RBM10 on an overall Star-PAP target mRNA association. A list of mRNAs in Star-PAP HITS-CLIP lost on RBM10 depletion is tabulated in Supplementary Table S3. Four select mRNAs where there was a loss of Star-PAP association on RBM10 depletion are shown in Figure 4e,f and Supplementary Figure S3c,d. Together, these results indicate that Star-PAP target mRNA association requires RBM10 in the cell.

Figure 4. Star-PAP global mRNA association requires co-regulator RBM10. (**a**) HITS-CLIP signals of Star-PAP distribution across human genome showing loss of whole chromosomal association of Star-PAP on RBM10 knockdown in HEK 293 cells. Reference genome hg19 is indicated on top. Star-PAP HITS-CLIP tag distribution in one of the chromosome (chromosome 20) and the loss of the mapped tags on siRBM10 is shown below. The CLIP tags were counted after peak calling. (**b**) Doughnut plots showing the total number of Star-PAP target mRNAs that were not detected after RBM10 depletion. (**c**,**d**) Doughnut plots showing up-regulated and down-regulated mRNAs on Star-PAP depletion that were not detected in the Star-PAP HITS-CLIP after RBM10 depletion. (**e**,**f**) Star-PAP HITS-CLIP read cluster association on select target mRNAs in the presence and absence of RBM10 knockdown as indicated. (**g**) qRT-PCR analysis of Star-PAP target mRNAs that are detected in our HITS-CLIP in the presence and absence of Star-PAP and RBM10 knockdowns. (**h**) Western blot analysis of RBM10 in control and RBM10 knockdown in HEK 293 cells.

2.6. RBM10-RNA Association Regulates Star-PAP-Mediated mRNA Metabolism

The genome-wide loss of Star-PAP association on RBM10 depletion was further tested using qRIP experiment using 10 select mRNAs (*COQ2*, *AGTR1*, *DPH5*, *GAD1*, *BPNT1*, *PAK1*, *LMNB1*, *NGEF*, *RAB26*, *BRCA1*, *NOS2*) (Figure 4g). We selected both sets of mRNAs that were up-regulated or down-regulated on Star-PAP depletion. We observed a clear loss of Star-PAP association in all mRNAs investigated upon RBM10 depletion (Figure 4g). There was no effect of RBM10 knockdown on RBM10 independent Star-PAP target mRNAs. Western analysis for siRNA depletion of RBM10 is shown in Figure 4h. This confirms the requirement of RBM10 for Star-PAP target mRNA binding. Similarly, in a RIP analysis, we observed the association of both RBM10 and Star-PAP on Star-PAP target mRNAs (*AGTR1*, *BPNT1*, *NOS2*) and that Star-PAP association was a loss on RBM10 depletion (Figure 5a) indicating that RBM10 RNA binding is required for Star-PAP association with the target mRNA. To confirm this, we tested Star-PAP association with target RNAs with RBM10 RNA binding motif deletion (that compromised RBM10 RNA binding) (Figure 5b). For this purpose, we ectopically expressed wild type and RNA binding motif deleted RBM10

that has silent mutations on the targeting siRNA sites. We observed a significant loss of Star-PAP association with target RNAs (*BPNT1*, *PAK1*, *AGTR1*) on Star-PAP knockdown as well as RRM motif deletion RBM10 revealing that RBM10 binding is required for the Star-PAP association with the target RNA (Figure 5b). RBM10 is a U-rich or G-rich sequence binding protein and therefore, we tested the nucleotide sequence on mRNAs with Star-PAP mapped regions that were lost on RBM10 depletion. We observed a higher U-content and G-content of Star-PAP reads on mRNAs where Star-PAP was not detected on RBM10 depletion (Supplementary Figure S4a). Moreover, analysis of motif at these reads by CentriMo software indicates the potential association of 6U binding motif with a frequency of 48%, 7U with 33% and 8U with 18%, respectively, but a marginal possibility of G-motifs with 10% for 6G, 5% for 7G and <3% for 8G, respectively (Supplementary Figure S4b). Together, these results indicate that the RBM10 RNA association regulates Star-PAP target mRNA binding.

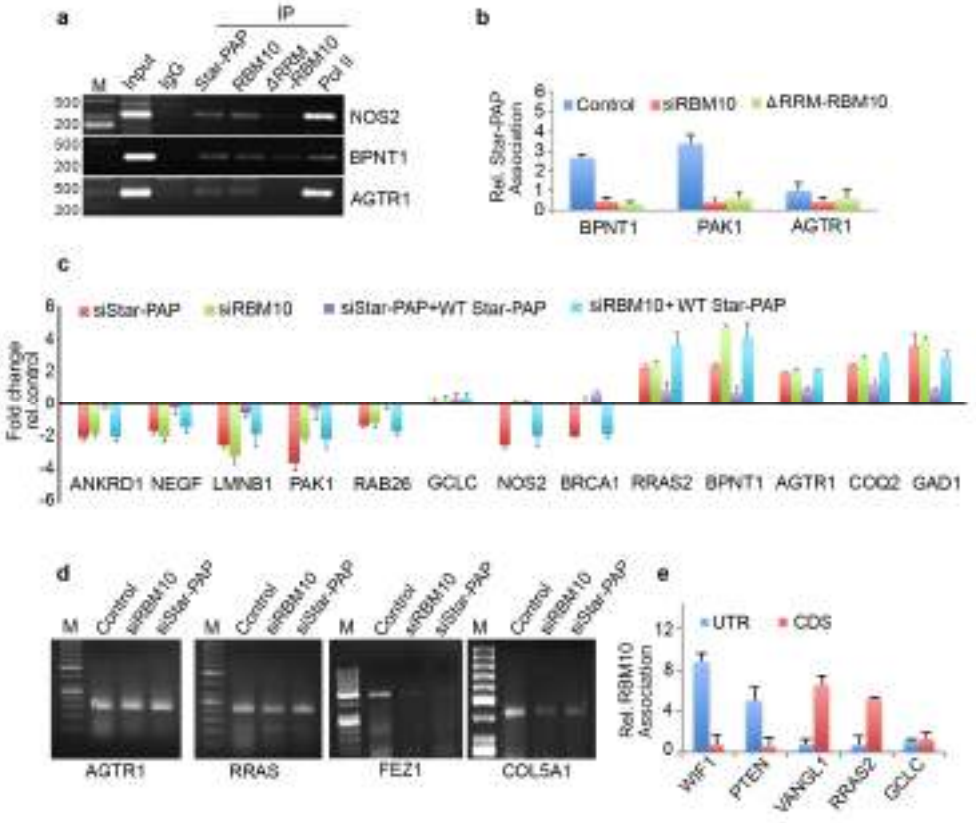

Figure 5. RBM10 regulates Star-PAP mediated mRNA metabolism. (**a**) RIP analysis of Star-PAP, RBM10, and RBM10 RNA binding motif deletion along with control RNA pol II on various Star-PAP targets in control and siRNA treated HEK 293 cells as indicated. Input, 10% of the IP lysate. M, marker lane. (**b**) qRIP analysis of Star-PAP association with various altered mRNAs as indicated in the presence of control or RBM10 siRNA and RRM deleted RBM10 in HEK 293 cells. (**c**) qRT-PCR analysis of various Star-PAP target mRNAs in the presence of Star-PAP or RBM10 depletion with the rescue with wild type Star-PAP ectopic expression in HEK 293 cells. (**d**) 3′-RACE assay of various Star-PAP target mRNAs from total mRNAs isolated after siStar-PAP or siRBM10 in HEK 293 cells. (**e**) qRIP analysis showing the relative association of RBM10 in the coding region and 3′-UTR region on select Star-PAP target mRNAs as indicated. Error bar represents SEM of three independent experiments.

Therefore, we tested mRNA metabolism from both sets of mRNAs (down-regulated and up-regulated on Star-PAP depletion from our microarray analysis). First, RBM10 knockdown resulted in a differential expression of Star-PAP target mRNAs—a loss of expression of a set of mRNAs (*ANKRD1*, *NEGF*, *LMNB1*, *PAK1*, *RAB26*, *NOS2*) (UTR-associated) whereas an increased expression for another set of RNAs (*RRAS2*, *BPNT1*,

AGTR1, *COQ2*, *GAD1*) (CDS-associated) (Figure 5c). The altered expression on RBM10 depletion was not rescued by Star-PAP ectopic expression (Figure 5c). This indicates that RBM10 is involved in the Star-PAP-mediated mRNA metabolism. Since the UTR-associated mRNAs were regulated through 3′-end processing and the CDS-associated group through RNA turnover and stability, we tested both 3′-UTR RNA processing (by cleavage assay and 3′-RACE assay) and RNA half-life measurement. In a 3′-RACE assay, there was compromised mRNA maturation on RBM10 depletion on *FEZ1* and *COL5A1*, whereas, there was no effect of RBM10 depletion on *AGTR1* or RRAS (up-regulated on the knockdown) (Figure 5d). Similarly, in the cleavage assay, RBM10 knockdown affected specifically mRNAs that were compromised on Star-PAP knockdown with no effect on the RNAs that were up-regulated on Star-PAP depletion (Supplementary Figure S4c,d). Concomitantly, measurement of half-life after RBM10 knockdown indicated increased half-life of target mRNAs similar to Star-PAP depletion (Figure 3h). Consistently, there was an overall higher RBM10 association at the 3′-UTR of down-regulated mRNAs whereas CDS association was prominent for the up-regulated mRNAs (Figure 5e). Together, these results indicate that RBM10 is required for Star-PAP mediated mRNA metabolism in both 3′-end processing and RNA destabilisation. Interestingly, among the RBM10-independent mRNAs (mRNAs where Star-PAP association was not affected by RBM10 depletion), Star-PAP was largely associated with the CDS region (~66% of the mRNAs) compared to the UTR region (~24% of the mRNAs) (Supplementary Figure S4e). Similarly, these mRNAs also exhibited higher proximal PA-site (40%) usage than the distal PA-site (25%) usage as opposed to the RBM10 dependent mRNAs (Supplementary Figure S4f) suggesting a role of RBM10 in Star-PAP mediated APA. Functionally, these mRNAs show enrichment of signalling pathways including RTK-MAPK, PI3K-Akt, JAK-STAT, mTOR and TGF-β in the cell (Supplementary Figure S4g).

3. Discussion

Star-PAP is a variant PAP that plays a critical role in the 3′-end processing of select mRNAs [20,21,25]. Star-PAP follows a distinct processing mechanism that is dispensable of important canonical components including CstF-64. Star-PAP instead requires additional associated factors including kinases and RNA binding proteins [1,34]. Star-PAP binds to target mRNA UTR and helps recruit the cleavage and polyadenylation factors [20,34]. However, the role of Star-PAP-associated factors in the Star-PAP UTR/PA-site selection or in the processing reaction is unclear. From mass spectrometry analysis, we established RBM10 as a unique Star-PAP coregulator required for specific mRNA regulation involved in myocyte hypertrophy [24]. In this study, we showed that RBM10 regulates global Star-PAP association on target mRNAs. This is consistent with the ubiquitous expression patterns of both the proteins where RBM10 will be required for Star-PAP mediated 3′-end processing [21,24]. Nevertheless, our study strongly indicates the role of RBM10 in determining Star-PAP specificity. There are two aspects of Star-PAP specificity: first, the selection of a PA-site, and second, the exclusion of canonical PAP from the target PA-site to have an exclusive/specific control of targets by Star-PAP [1]. RBM10 can have roles in both these aspects of specificity. In the first aspect, the RBM10-RNA association would recruit Star-PAP in a sequence-specific manner to help assemble a stable Star-PAP cleavage complex. In line with this, a loss of RBM10 would compromise Star-PAP binding on the RNA as observed in our study. Second, RBM10 binding at the vicinity of the Star-PAP binding region could exclude canonical PAPα or other components of canonical machinery that are absent from the Star-PAP processing complex. This supports our earlier hypothesis that Star-PAP requires a co-regulator for the function and specificity of its cellular activities [1]. Such specificity driven by associated factors will have important ramifications in the regulation of Star-PAP mediated alternative polyadenylation [18,23]. Yet, the role of RBM10 in APA is yet to be defined.

We reported a GC-rich sequence with an -AUA- motif for Star-PAP recognition, and a suboptimal downstream region with a U-depleted sequence on Star-PAP targets [20]. We

confirmed from our HITS-CLIP experiment that Star-PAP-associated regions have a biased GC over AU composition in addition to a motif containing AUA on global Star-PAP targets. While sequence specificity for Star-PAP is critical, earlier reports indicate the signalling regulations are critical for the Star-PAP specificity [23,25,50,51]. Such signalling influence on specificity may operate through associated proteins such as RBM10. At least three agonists-oxidative stress, hypertrophic signal, and the toxin dioxin are known to regulate Star-PAP target mRNA selection [21,23,24,50]. It is still unclear how these signals drive the Star-PAP functions. Our finding of the RBM10 requirement for Star-PAP association shows the potential involvement of RBM10 in transducing the signal-mediated specificity of Star-PAP targets. This is consistent with RBM10′s role in the regulation of Star-PAP target anti-hypertrophy regulators in the heart [24]. Similarly, kinases CKIα/ε and PKCδ are also shown to modulate Star-PAP mRNA selection [25,50,51]. This could occur through either direct Star-PAP phosphorylation or indirectly via RBM10 phosphorylation that affects the sequence-specific binding of Star-PAP on distinct mRNAs. One of the phosphorylations at the ZF region on Star-PAP (Serine 6) was shown to regulate the specificity of Star-PAP regulation of some mRNAs involved in stress response and cell invasion [49,51]. Yet, the overall sequence-specific changes for Star-PAP induced by signalling conditions or by different phosphorylation statuses are yet to be defined.

Star-PAP has an established role in the 3′-end RNA processing that controls the expression of a large number of mRNAs that regulate various cellular functions [23,25–27,49,51]. In addition to its adenylation function, Star-PAP has a confirmed uridylation activity [28,52]. The substrate preference of Star-PAP (U vs. A) in the cell is likely driven by associated factors or co-regulators such as RBM10 [20,21,24]. Additionally, Star-PAP has also been shown to regulate the stability and processing of miRNAs [26,30,31,53]. The depletion of Star-PAP resulted in a decrease in the levels of a large number of miRNAs, yet how Star-PAP regulates miRNA expression is unclear [30]. Star-PAP can be immunoprecipitated with specific miRNAs and also along with the RISC complex proteins indicating a potential post-transcriptional role on miRNA biogenesis [26,31]. Consistent with this, we also detected a number of miRNA associations with Star-PAP in our HIT-CLIP experiment. Together, these findings show a diverse role of Star-PAP in different RNA processing events. In this study, we show a new function of Star-PAP in the mRNA metabolism that regulates mRNA stability and/or turnover. A model of how RBM10 regulates Star-PAP-RNA association and mRNA metabolism is shown in Figure 6. Here, Star-PAP acts as a negative regulator and its binding destabilises target mRNAs. This function is independent of Star-PAP polyadenylation of target mRNAs, uridylation of U6 snRNA, and miRNA regulations [21,30,52]. Nevertheless, this affects more than 1000 mRNA targets involved in multiple cellular functions and signaling pathways. RNA binding proteins are known to regulate the stability of the bound RNA (e.g., ARE binding proteins HNRNPD, ZFP36, TTP, KSRP or BRF5) that can promote mRNA turnover via recruiting decapping enzyme at the 5′-end or recruiting deadenylating enzyme at the 3′-end [54–58]. Alternatively, Star-PAP could promote mRNA silencing by binding near AGO2 sites and contributing to its loading with miRNAs as in the case of AUF1 protein [59–61]. Star-PAP is known to interact with AGO2 and also pull down miRNA [26,31]. Therefore, Star-PAP binding could also promote miRNA-mediated silencing on the Star-PAP-associated target mRNAs by recruiting targeting miRNAs.

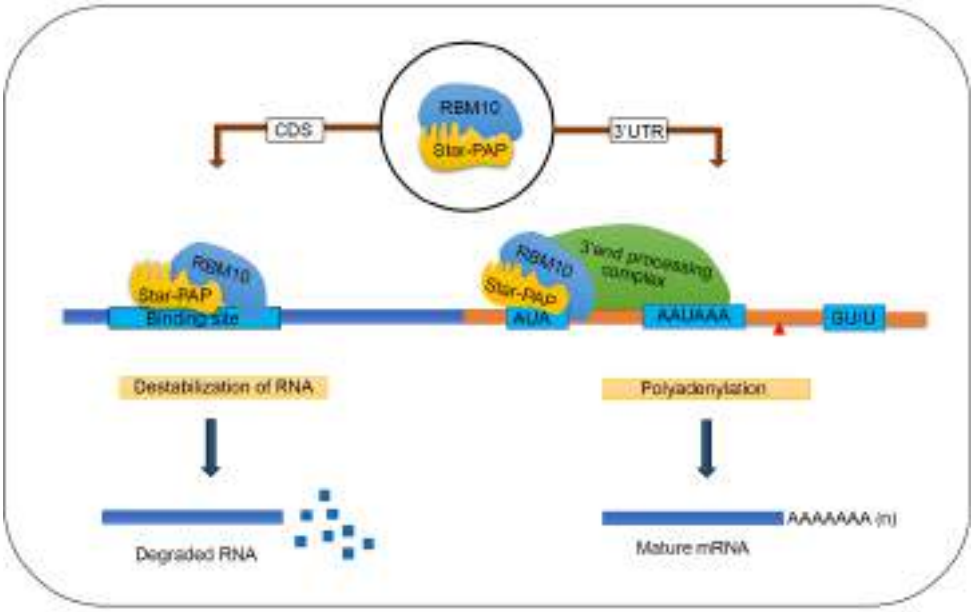

Figure 6. A model showing how RBM10 regulates Star-PAP-RNA association and mRNA metabolism (mRNA 3′-end processing and mRNA de-stabilisation).

4. Materials and Methods

4.1. Cell Culture, Transfections and Treatment

HEK 293 cells were obtained from American Type Cell Culture Collection. HEK 293 cells were maintained in Dulbecco's Modified Eagle's Medium (Himedia, Mumbai, India) with 10% Foetal Bovine Serum (Gibco Biosciences, Dublin, Ireland) and 50 U/mL Penicillin Streptomycin (Gibco) at 37 °C in 5% CO_2. Transient knockdown experiments were carried out using custom-made siRNAs (Eurogenetec, Seraing, Belgium) by calcium phosphate method as described earlier [23]. Transient overexpression of Star PAP and RBM10 were performed using pCMV Tag2A constructs expressing FLAG-epitope tagged Star-PAP and RBM10 that has silent mutations rendering the siRNA used for the knockdown ineffective as described earlier [24,50]. Whenever required, cells were treated with actinomycin D (5 µg/mL in DMSO) and DMSO treatment was used as solvent control.

4.2. RNA Isolation

Cultured HEK 293 cells from 10 cm dishes (1 mL/1 × 10^6 cells) were harvested in 2 mL epi tubes. Harvested cells were then washed with PBS and total RNA was isolated using RNase easy mini Kit (Qiagen, Germantown, MD, USA) as per the instruction of the manufacturer.

4.3. Quantitative Real-Time PCR (qRT-PCR)

qRT-PCR was carried out in a CFX96 multi-colour system (Bio-Rad, Hercules, CA, USA) using iTaq SYBR Green Supermix (Bio-Rad, Hercules, CA, USA) as described previously [23]. Then, 2 µg of total RNA was reverse transcribed using MMLV reverse transcriptase (Invitrogen, Waltham, MA, USA) with oligodT primer. Real-time primers were designed using Primer3 software and the difference in the melting temperature of corresponding forward and reverse primers were less than 1. Melt-curve analysis was used to check for single-product amplification and primer efficiency was near 100% in all experiments. Quantifications were expressed in arbitrary units, and target mRNA abundance was normalised to the expression of *GAPDH* with the Pfaffl method [62]. All qRT-PCR results are representative of at least three independent experiments ($n > 3$).

4.4. Cleavage Assay

To determine the cleavage efficiency of mRNA, the accumulation of non-cleaved mRNA levels was measured by quantitative real-time PCR (qRT-PCR). Total RNA was reverse transcribed using random hexamers and qRT-PCR was carried out using a pair of primers across the cleavage site to amplify non-cleaved mRNAs as described earlier [21]. Non-cleaved messages were expressed as fold-change over the total spliced mRNA.

4.5. HITS-CLIP Sequencing and Analysis

HITS-CLIP experiments were carried out as described earlier [63,64]. Briefly, HEK 293 cells grown on 15 cm plates were UV irradiated (400 mJ/cm^2) three times for 15 min each before harvesting. Cells were then harvested and lysed in 1X PXL buffer (1× PBS, 0.1% SDS, 0.5% deoxycholate, 0.5% NP-40, and protease inhibitor Cocktail) by sonication. The lysate was then treated with DNase I followed by partial RNAse digestion. Debris was then separated by high ultracentrifugation at 30,000 rpm for 40 min at 4 °C. Next, immunoprecipitation was carried out from the supernatant using anti-Star-PAP antibody [50] conjugated with pre-incubated Dynabeads Protein A (Invitrogen, Waltham, MA, USA) in the presence of bridging anti-rabbit IgG antibody, overnight at 4 °C. IP samples were washed twice with 1X PXL, followed by 5× PXL high salt wash buffer (5× PBS, 0.1% SDS, 0.5% deoxycholate, 0.5% NP40) and three times with 1× PNK buffer (50 mMTris-HCl, pH 7.4, 10 mM $MgCl_2$, 0.5% NP40). Washed IP samples were further treated with PNK (80 µL PNK reaction) with 10× PNK buffer, 4 µL of PNK enzyme and 1 µL of ATP) in a thermomixer at 37 °C for 20 min. It was further washed with 1× PXL and 5× PXL and twice with 1× PNK buffer. The efficiency and specificity of IP were confirmed by Western blot analysis and denaturing acrylamide gel. Protein–RNA complexes were subjected to Proteinase K (Sigma-Aldrich, St. Louis, MO, USA) digestion at 37 °C, 20 min in 1× PK/urea buffer and the released RNA fragments were extracted by acid Phenol:Chloroform:Isoamyl alcohol. It was followed by overnight precipitation using 3 M sodium acetate and 0.75 µL glycogen and 1:1 of ethanol: isopropanol. CLIP RNA fragments were finally resuspended in 10 mM Tris-HCl pH 7.5. Library preparation and sequencing were carried out at the commercially available facility at Genotypic Technologies (http://www.genotypic.co.in, accessed on 7 September 2017). The library was prepared using NEBNext Ultra Directional RNA Library Prep kit as per the manufacturer's instruction and sequenced on an Illumina platform.

The raw data generated was checked for quality using FastQC (https://www.bioinformatics.babraham.ac.uk/projects/trim_galore/, accessed on 20 May 2019). Low-quality sequences, artifacts sequences, contaminated sequences and low-quality reads were filtered using Clip tool kit (fastq_filter.pl, 20 May 2019) (mean score 20 from 0–24) [65]. Cutadapt was used to trim low-quality sequences from the ends before the adapters and to remove universal adapter sequences (DOI:10.14806/ej.17.1.200). Filtered and trimmed sequences were then subjected to duplicate removal using Cliptool Kit (fastq2collapse.pl, 20 May 2019) [65]. Reads were then mapped to the human reference genome (hg19) using Burrows–Wheeler Aligner (BWA) tool [66]. The MAPQ score and the minimal mapping size (in parseAlignment.pl program of Cliptool kit) were set to 1 and 18 nt, respectively, so that a single read in alignment file should map to a single locus in genome [65]. The duplicate tags with the same start coordinates mapped on chromosomes at the 5′ end of RNA tags were collapsed together using Clip tool kit (tag2collapse.pl, 20 May 2019) [65]. Peak calling was then performed using Model-based Analysis of ChIP-Seq (MACS2) using IgG as control with the parameter set of high confidence enrichment ratio against a background with an mFold range of minimum 5 and maximum 50 against and fragment size of 500 and filtered the peaks using *p*-value 0.05 [67]. After processing with this parameter and IgG subtraction, we identified more than 420,000 read clusters. Genomic annotations were further obtained by extracting co-ordinates of the read clusters with reference human genome hg19 using Bedtools intersect [68]. Basic unix utilities (sort, uniq, awk and sed, etc.) were used for parsing and sorting based on genomic features. Next, the Integrative Genomics Viewer tool was used to visualize the genome-wide analysis, complete chromosomal visualisation

peak and specific binding peaks in various regions of a gene [69]. Nucleotide compositions were then extracted using Galaxy (https://usegalaxy.org/, 10 October 2020) and plotted % nucleotide content as box plot. Motif detection software MEME-Chip was used to identify the binding motifs from the read sequences with E-value cut off of 0.05 [70].

4.6. RNA Immunoprecipitation (RIP)

RIP analysis was carried out as described earlier [21,71]. Briefly, HEK 293 cells were cross-linked with 1% formaldehyde for 10 min followed by the addition of 0.125 M glycine for 5 min to halt crosslinking. Washed cells were lysed by incubating for 10 min in 300 µL of cell lysis buffer (10 mM Tris-HCl pH 8.0, 10 mM NaCl, 0.2% NP-40, 1× EDTA free Proteinase Inhibitor, 1000 U RNaseI (Promega, Madison, WI, USA). Crude Nuclei pelleted (5 min, 2500 rpm at 4 °C) and 400 µL nuclei lysis buffer (50 mM Tris-HCl pH 8.0, 10 mM EDTA, 1% SDS, 1× EDTA free Proteinase Inhibitor, 1000 U RNaseI (Promega, Madison, WI, USA)) added to the pellet and sonicated at 22% amplitude 20 s pulse for 5 min. The nuclear lysate was centrifuged at 15,000 rpm for 10 min, supernatant collected and treated with DNase1 for 20 min at 37 °C followed by the addition of EDTA to 20 mM to stop the digestion. Supernatant incubated overnight at 4 °C with respective antibodies for Star-PAP, RBM10, RNA Pol II, FLAG and Rabbit IgG. Further, the mixture was incubated with Protein G beads which were equilibrated with IP dilution buffer (20 mM Tris-HCl pH 8, 150 mM NaCl, 2 mM EDTA, 1% Triton X-100, 0.01% SDS, 1× EDTA free Proteinase Inhibitor, 1000 U RNaseI (Promega, Madison, WI, USA) for 2 h at 4 °C. Further, the complex was pelleted down at 5000 rpm for 5 min at 4 °C and washed with IP dilution buffer (3× 5000 rpm for 5 min at 4 °C). Immunoprecipitates were eluted with 300 µL elution buffer (1% SDS, 100 mM Sodium bicarbonate) and NaCl added to 200 mM followed by proteinase K for 2 h. Reverse crosslinking was then carried out by incubating the mixture at 67 °C for 4 h. RNA was isolated from the mixture using Trizol (Invitrogen, Waltham, MA, USA) reagent according to the manufacturer's protocol. cDNA was then synthesised using Random Hexamers (Invitrogen, Waltham, MA, USA) by MMLV RT (Invitrogen, Waltham, MA, USA). PCR amplification was carried out and visualised on agarose gel.

For quantitative RIP, the immunoprecipitated RNA samples were diluted at 1:10. These samples along with input RNA were quantified using CFX multi colour system (Bio-Rad, Hercules, CA, USA) as described above. Values from each sample were corrected using reactions lacking reverse transcriptase. Quantifications were expressed in arbitrary units, and IgG immunoprecipitation product levels were used as controls for normalisation of the abundance of the target messages. The quantitative association was then expressed relative to the input RNA signal as described [72,73] using the method of Pfaffl [62]. The primers used for qRIP are listed in the Supplementary Text.

For determining UTR and CDS association on different mRNAs, we carried out qRIP analysis using specific primers designed at the 3′-UTR and CDS regions as described above.

4.7. Half-Life ($T_{1/2}$) Measurement

HEK 293 cells were transfected with RNAi specific to Star-PAP and RBM10. Cells were then treated with actinomycin D (5 µg/mL in DMSO) for different time points (0, 2, 4, 6, 8, 12, 18, 24, 30, 36, 42 and 48 h) post-transfection. Cells were then harvested for total RNA was isolated from cells from each time point. cDNA was synthesised by oligodT primer followed by qRT-PCR as described above. mRNA half-life ($T_{\frac{1}{2}}$) was measured as described earlier by following the decrease in % mRNA level over time with 0 time point taken as 100% of each mRNA expression [74].

4.8. 3′-RACE

3′-RACE assay was carried out as described previously [50]. Briefly, 2 µg of total RNA isolated from HEK 293 cell was used for cDNA synthesis using an engineered oligodT primer with a unique sequence at the 5′-end (Adapter primer) and MMLV-RT (Invitrogen, Waltham, MA, USA). This was followed by PCR amplification using a gene-specific forward

primer and a universal adapter primer that is complementary to the unique sequence on the engineered oligodT primer (AUAP primer). The RACE products analysed on a 2% agarose gel and confirmed by sequencing.

4.9. Immunoblotting

Cell lysates were prepared in 1× SDS-PAGE loading buffer (0.06 M Tris, 25% Gylcerol, 2% SDS, 0.002% Bromophenol blue, 1% β-mercapto ethanol). Denaturation was carried out by heating the mixture at 95 °C for 20 min. Proteins were separated in SDS PAGE gel in 1× Tris Glycine Buffer (25 mM Tris pH 8.0, 190 mM Glycine, 0.1% SDS pH 8.3). Transfer of proteins to the PVDF was performed in a transfer buffer (25 mM Tris pH 8.0, 190 mM Glycine, 20% Methanol). PVDF membrane after transfer was blocked in 5% skimmed milk in 1× TBST (20 mM Tris pH 7.4, 150 mM NaCl, 0.1% Tween-20) for 45 min at room temperature. Primary antibodies were diluted in TBST as per the manufacturer's instruction and incubated in a shaking platform overnight at 4 °C. The blots were washed in TBST 3 times for 10 min followed by incubation in HRP conjugated secondary antibody (Jackson Immuno Research Laboratory, West Grove, PA, USA). Further, imaging of the blots was carried out using chemiluminescent substrate (Bio-Rad, Hercules, CA, USA) in an iBright FL1500 platform (Invitrogen, Waltham, MA, USA).

4.10. Statistics

All data were obtained from at least three independent experiments and are represented as mean ± standard error mean, SEM. The statistical significance of the differences in the mean is calculated using ANOVA with statistical significance at a *p*-value of less than 0.05. All Western blots show representations of at least three independent blotting experiments.

4.11. Primers and Antibodies

A list of all the primers and antibodies employed in the study is shown in the Supplementary Data.

Supplementary Materials: The following are available online at https://www.mdpi.com/article/10.3390/ijms22189980/s1.

Author Contributions: Conceptualization, R.S.L.; methodology, G.R.K., F.S., N.K.M., N.M. and R.S.L.; software, G.R.K. and J.A.; validation, F.S. and N.K.M.; formal analysis, R.S.L., F.S., N.K.M. and G.R.K.; investigation, G.R.K., F.S., N.K.M. and N.M.; resources, R.S.L.; writing—original draft preparation, F.S., N.K.M. and R.S.L.; writing, review and editing, R.S.L., F.S. and N.K.M.; project administration, R.S.L.; funding acquisition, R.S.L. All authors have read and agreed to the published version of the manuscript.

Funding: This work is supported by Swarnajayanti Fellowship (DST/SJF/LSA-03/2018-19) to R.S.L., and Senior Research Fellowships from Department of Biotechnology, Council of Scientific and Industrial Research, and University Grant Commission, Government of India to G.R.K., F.S. and N.K.M., respectively.

Institutional Review Board Statement: Not applicable.

Informed Consent Statement: Not applicable.

Data Availability Statement: The accession number for raw and processed HITS-CLIP data reported in this paper deposited at NCBI Gene Expression Omnibus (GEO) (https://www.ncbi.nlm.nih.gov/geo/) is GSE182643.

Acknowledgments: We thank RSL Lab members for carefully reading the manuscript.

Conflicts of Interest: Authors declare no conflict of interest.

References

1. Laishram, R.S. Poly(A) polymerase (PAP) diversity in gene expression–star-PAP vs canonical PAP. *FEBS Lett.* **2014**, *588*, 2185–2197. [CrossRef] [PubMed]
2. Proudfoot, N. New perspectives on connecting messenger RNA 3′ end formation to transcription. *Curr. Opin. Cell Biol.* **2004**, *16*, 272–278. [CrossRef] [PubMed]
3. Mandel, C.R.; Bai, Y.; Tong, L. Protein factors in pre-mRNA 3′-end processing. *Cell Mol. Life Sci.* **2008**, *65*, 1099–1122. [CrossRef] [PubMed]
4. Zhao, J.; Hyman, L.; Moore, C. Formation of mRNA 3′ ends in eukaryotes: Mechanism, regulation, and interrelationships with other steps in mRNA synthesis. *Microbiol. Mol. Biol. Rev.* **1999**, *63*, 405–445. [CrossRef]
5. Shi, Y.; Di Giammartino, D.C.; Taylor, D.; Sarkeshik, A.; Rice, W.J.; Yates, J.R., III; Frank, J.; Manley, J.L. Molecular architecture of the human pre-mRNA 3′ processing complex. *Mol. Cell* **2009**, *33*, 365–376. [CrossRef]
6. Wahle, E.; Keller, W. The biochemistry of polyadenylation. *Trends Biochem. Sci.* **1996**, *21*, 247–250. [CrossRef]
7. Chan, S.L.; Huppertz, I.; Yao, C.; Weng, L.; Moresco, J.J.; Yates, J.R., III; Ule, J.; Manley, J.L.; Shi, Y. CPSF30 and Wdr33 directly bind to AAUAAA in mammalian mRNA 3′ processing. *Genes Dev.* **2014**, *28*, 2370–2380. [CrossRef]
8. Clerici, M.; Faini, M.; Muckenfuss, L.M.; Aebersold, R.; Jinek, M. Structural basis of AAUAAA polyadenylation signal recognition by the human CPSF complex. *Nat. Struct. Mol. Biol.* **2018**, *25*, 135–138. [CrossRef]
9. Schönemann, L.; Kühn, U.; Martin, G.; Schäfer, P.; Gruber, A.R.; Keller, W.; Zavolan, M.; Wahle, E. Reconstitution of CPSF active in polyadenylation: Recognition of the polyadenylation signal by WDR33. *Genes Dev.* **2014**, *28*, 2381–2393.
10. Sun, Y.; Zhang, Y.; Hamilton, K.; Manley, J.L.; Shi, Y.; Walz, T.; Tong, L. Molecular basis for the recognition of the human AAUAAA polyadenylation signal. *Proc. Natl. Acad. Sci. USA* **2018**, *115*, E1419–E1428.
11. Perez Canadillas, J.M.; Varani, G. Recognition of GU-rich polyadenylation regulatory elements by human CstF-64 protein. *EMBO J.* **2003**, *22*, 2821–2830. [CrossRef] [PubMed]
12. Takagaki, Y.; Manley, J.L. RNA recognition by the human polyadenylation factor CstF. *Mol. Cell Biol.* **1997**, *17*, 3907–3914. [CrossRef] [PubMed]
13. Mandel, C.R.; Kaneko, S.; Zhang, H.; Gebauer, D.; Vethantham, V.; Manley, J.L.; Tong, L. Polyadenylation factor CPSF-73 is the pre-mRNA 3′-end-processing endonuclease. *Nature* **2006**, *444*, 953–956. [CrossRef]
14. Ryan, K.; Calvo, O.; Manley, J.L. Evidence that polyadenylation factor CPSF-73 is the mRNA 3′ processing endonuclease. *RNA* **2004**, *10*, 565–573. [CrossRef] [PubMed]
15. Deo, R.C.; Bonanno, J.B.; Sonenberg, N.; Burley, S.K. Recognition of polyadenylate RNA by the poly(A)-binding protein. *Cell* **1999**, *98*, 835–845. [CrossRef]
16. Kuhn, U.; Gundel, M.; Knoth, A.; Kerwitz, Y.; Rudel, S.; Wahle, E. Poly(A) tail length is controlled by the nuclear poly(A)-binding protein regulating the interaction between poly(A) polymerase and the cleavage and polyadenylation specificity factor. *J. Biol. Chem.* **2009**, *284*, 22803–22814. [CrossRef]
17. Kuhn, U.; Wahle, E. Structure and function of poly(A) binding proteins. *Biochim. Biophys. Acta* **2004**, *1678*, 67–84. [CrossRef] [PubMed]
18. Li, W.; Li, W.; Laishram, R.S.; Hoque, M.; Ji, Z.; Tian, B.; Anderson, R.A. Distinct regulation of alternative polyadenylation and gene expression by nuclear poly(A) polymerases. *Nucleic Acids Res.* **2017**, *45*, 8930–8942. [CrossRef]
19. Topalian, S.L.; Kaneko, S.; Gonzales, M.I.; Bond, G.L.; Ward, Y.; Manley, J.L. Identification and functional characterization of neo-poly(A) polymerase, an RNA processing enzyme overexpressed in human tumors. *Mol. Cell Biol.* **2001**, *21*, 5614–5623. [CrossRef]
20. Laishram, R.S.; Anderson, R.A. The poly A polymerase Star-PAP controls 3′-end cleavage by promoting CPSF interaction and specificity toward the pre-mRNA. *EMBO J.* **2010**, *29*, 4132–4145. [CrossRef]
21. Mellman, D.L.; Gonzales, M.L.; Song, C.; Barlow, C.A.; Wang, P.; Kendziorski, C.; Anderson, R.A. A PtdIns4,5P2-regulated nuclear poly(A) polymerase controls expression of select mRNAs. *Nature* **2008**, *451*, 1013–1017. [CrossRef]
22. Gonzales, M.L.; Mellman, D.L.; Anderson, R.A. CKIalpha is associated with and phosphorylates star-PAP and is also required for expression of select star-PAP target messenger RNAs. *J. Biol. Chem.* **2008**, *283*, 12665–12673. [CrossRef]
23. Sudheesh, A.; Mohan, N.; Francis, N.; Laishram, R.S.; Anderson, R.A. Star-PAP controlled alternative polyadenylation coupled poly (A) tail length regulates protein expression in hypertrophic heart. *Nucleic Acids Res.* **2019**, *47*, 10771–10787. [CrossRef] [PubMed]
24. Mohan, N.; Kumar, V.; Kandala, D.T.; Kartha, C.C.; Laishram, R.S. A Splicing-Independent Function of RBM10 Controls Specific 3′ UTR Processing to Regulate Cardiac Hypertrophy. *Cell Rep.* **2018**, *24*, 3539–3553. [CrossRef] [PubMed]
25. Li, W.; Laishram, R.S.; Ji, Z.; Barlow, C.A.; Tian, B.; Anderson, R.A. Star-PAP control of BIK expression and apoptosis is regulated by nuclear PIPKIalpha and PKCdelta signaling. *Mol. Cell* **2012**, *45*, 25–37. [CrossRef] [PubMed]
26. Duan, A.; Kong, L.; An, T.; Zhou, H.; Yu, C.; Li, Y. Star-PAP regulates tumor protein D52 through modulating miR-449a/34a in breast cancer. *Biol. Open* **2019**, *8*, bio045914. [CrossRef]
27. Yu, C.; Gong, Y.; Zhou, H.; Wang, M.; Kong, L.; Liu, J.; An, T.; Zhu, H.; Li, Y. Star-PAP, a poly (A) polymerase, functions as a tumor suppressor in an orthotopic human breast cancer model. *Cell Death Dis.* **2017**, *8*, e2582. [CrossRef]
28. Yamashita, S.; Takagi, Y.; Nagaike, T.; Tomita, K. Crystal structures of U6 snRNA-specific terminal uridylyltransferase. *Nat. Commun.* **2017**, *8*, 15788. [CrossRef] [PubMed]

29. Trippe, R.; Sandrock, B.; Benecke, B.J. A highly specific terminal uridylyl transferase modifies the 3′-end of U6 small nuclear RNA. *Nucleic Acids Res.* **1998**, *26*, 3119–3126. [CrossRef]
30. Knouf, E.C.; Wyman, S.K.; Tewari, M. The human TUT1 nucleotidyl transferase as a global regulator of microRNA abundance. *PLoS ONE* **2013**, *8*, e69630. [CrossRef] [PubMed]
31. Haas, G.; Cetin, S.; Messmer, M.; Chane-Woon-Ming, B.; Terenzi, O.; Chicher, J.; Kuhn, L.; Hammann, P.; Pfeffer, S. Identification of factors involved in target RNA-directed microRNA degradation. *Nucleic Acids Res.* **2016**, *44*, 2873–2887. [CrossRef]
32. Hoque, M.; Ji, Z.; Zheng, D.; Luo, W.; Li, W.; You, B.; Park, J.Y.; Yehia, G.; Tian, B. Analysis of alternative cleavage and polyadenylation by 3′ region extraction and deep sequencing. *Nat. Methods* **2013**, *10*, 133–139. [CrossRef] [PubMed]
33. Tian, B.; Manley, J.L. Alternative polyadenylation of mRNA precursors. *Nat. Rev. Mol. Cell Biol.* **2017**, *18*, 18–30. [CrossRef]
34. Divya, T.K.; Nimmy, M.; Vivekanand, A.; Sudheesh, A.P.; Reshmi, G.; Rakesh, S.L. CstF-64 and 3′-UTR cis-element determine Star-PAP specificity for target mRNA selection by excluding PAPalpha. *Nucleic Acids Res.* **2016**, *44*, 811–823.
35. Aravind, L.; Koonin, E.V. G-patch: A new conserved domain in eukaryotic RNA-processing proteins and type D retroviral polyproteins. *Trends Biochem. Sci.* **1999**, *24*, 342–344. [CrossRef]
36. Inoue, A.; Takahashi, K.P.; Kimura, M.; Watanabe, T.; Morisawa, S. Molecular cloning of a RNA binding protein, S1-1. *Nucleic Acids Res.* **1996**, *24*, 2990–2997. [CrossRef]
37. Nguyen, C.D.; Mansfield, R.E.; Leung, W.; Vaz, P.M.; Loughlin, F.E.; Grant, R.P.; Mackay, J.P. Characterization of a family of RanBP2-type zinc fingers that can recognize single-stranded RNA. *J. Mol. Biol.* **2011**, *407*, 273–283. [CrossRef]
38. Xiao, S.J.; Wang, L.Y.; Kimura, M.; Kojima, H.; Kunimoto, H.; Nishiumi, F.; Yamamoto, N.; Nishio, K.; Fujimoto, S.; Kato, T.; et al. S1-1/RBM10: Multiplicity and cooperativity of nuclear localisation domains. *Biol. Cell* **2013**, *105*, 162–174. [CrossRef]
39. Gripp, K.W.; Hopkins, E.; Johnston, J.J.; Krause, C.; Dobyns, W.B.; Biesecker, L.G. Long-term survival in TARP syndrome and confirmation of RBM10 as the disease-causing gene. *Am. J. Med. Genet. A* **2011**, *155*, 2516–2520. [CrossRef]
40. Imielinski, M.; Berger, A.H.; Hammerman, P.S.; Hernandez, B.; Pugh, T.J.; Hodis, E.; Cho, J.; Suh, J.; Capelletti, M.; Sivachenko, A.; et al. Mapping the hallmarks of lung adenocarcinoma with massively parallel sequencing. *Cell* **2012**, *150*, 1107–1120. [CrossRef]
41. Sutherland, L.C.; Rintala-Maki, N.D.; White, R.D.; Morin, C.D. RNA binding motif (RBM) proteins: A novel family of apoptosis modulators? *J. Cell Biochem.* **2005**, *94*, 5–24. [CrossRef]
42. Wang, Y.; Gogol-Doring, A.; Hu, H.; Frohler, S.; Ma, Y.; Jens, M.; Maaskola, J.; Murakawa, Y.; Quedenau, C.; Landthaler, M.; et al. Integrative analysis revealed the molecular mechanism underlying RBM10-mediated splicing regulation. *EMBO Mol. Med.* **2013**, *5*, 1431–1442. [CrossRef]
43. Inoue, A.; Yamamoto, N.; Kimura, M.; Nishio, K.; Yamane, H.; Nakajima, K. RBM10 regulates alternative splicing. *FEBS Lett.* **2014**, *588*, 942–947. [CrossRef]
44. Agafonov, D.E.; Deckert, J.; Wolf, E.; Odenwalder, P.; Bessonov, S.; Will, C.L.; Urlaub, H.; Luhrmann, R. Semiquantitative proteomic analysis of the human spliceosome via a novel two-dimensional gel electrophoresis method. *Mol. Cell Biol.* **2011**, *31*, 2667–2682. [CrossRef]
45. Glisovic, T.; Bachorik, J.L.; Yong, J.; Dreyfuss, G. RNA-binding proteins and post-transcriptional gene regulation. *FEBS Lett.* **2008**, *582*, 1977–1986. [CrossRef]
46. Keene, J.D. RNA regulons: Coordination of post-transcriptional events. *Nat. Rev. Genet.* **2007**, *8*, 533–543. [CrossRef]
47. Makarov, E.M.; Owen, N.; Bottrill, A.; Makarova, O.V. Functional mammalian spliceosomal complex E contains SMN complex proteins in addition to U1 and U2 snRNPs. *Nucleic Acids Res.* **2012**, *40*, 2639–2652. [CrossRef]
48. Rappsilber, J.; Ryder, U.; Lamond, A.I.; Mann, M. Large-scale proteomic analysis of the human spliceosome. *Genome Res.* **2002**, *12*, 1231–1245. [CrossRef] [PubMed]
49. Sudheesh, A.P.; Laishram, R.S. Nuclear phosphatidyl-inositol-phosphate type I kinase alpha coupled Star-PAP polyadenylation regulates cell invasion. *Mol. Cell Biol.* **2017**, *38*, e00457-17.
50. Mohan, N.; Sudheesh, A.P.; Francis, N.; Anderson, R.; Laishram, R.S. Phosphorylation regulates the Star-PAP-PIPKIalpha interaction and directs specificity toward mRNA targets. *Nucleic Acids Res.* **2015**, *43*, 7005–7020. [CrossRef]
51. Laishram, R.S.; Barlow, C.A.; Anderson, R.A. CKI isoforms alpha and epsilon regulate Star-PAP target messages by controlling Star-PAP poly(A) polymerase activity and phosphoinositide stimulation. *Nucleic Acids Res.* **2011**, *39*, 7961–7973. [CrossRef]
52. Trippe, R.; Guschina, E.; Hossbach, M.; Urlaub, H.; Luhrmann, R.; Benecke, B.J. Identification, cloning, and functional analysis of the human U6 snRNA-specific terminal uridylyl transferase. *RNA* **2006**, *12*, 1494–1504. [CrossRef] [PubMed]
53. Snoek, B.C.; Babion, I.; Koppers-Lalic, D.; Pegtel, D.M.; Steenbergen, R.D. Altered microRNA processing proteins in HPV-induced cancers. *Curr. Opin. Virol.* **2019**, *39*, 23–32. [CrossRef]
54. Chen, C.Y.; Gherzi, R.; Ong, S.E.; Chan, E.L.; Raijmakers, R.; Pruijn, G.J.; Stoecklin, G.; Moroni, C.; Mann, M.; Karin, M. AU binding proteins recruit the exosome to degrade ARE-containing mRNAs. *Cell* **2001**, *107*, 451–464. [CrossRef]
55. Fabian, M.R.; Frank, F.; Rouya, C.; Siddiqui, N.; Lai, W.S.; Karetnikov, A.; Blackshear, P.J.; Nagar, B.; Sonenberg, N. Structural basis for the recruitment of the human CCR4-NOT deadenylase complex by tristetraprolin. *Nat. Struct. Mol. Biol.* **2013**, *20*, 735–739. [CrossRef] [PubMed]
56. Gherzi, R.; Lee, K.Y.; Briata, P.; Wegmuller, D.; Moroni, C.; Karin, M.; Chen, C.Y. A KH domain RNA binding protein, KSRP, promotes ARE-directed mRNA turnover by recruiting the degradation machinery. *Mol. Cell* **2004**, *14*, 571–583. [CrossRef]
57. Loflin, P.; Chen, C.Y.; Shyu, A.B. Unraveling a cytoplasmic role for hnRNP D in the in vivo mRNA destabilization directed by the AU-rich element. *Genes Dev.* **1999**, *13*, 1884–1897. [CrossRef] [PubMed]

58. Sanduja, S.; Blanco, F.F.; Dixon, D.A. The roles of TTP and BRF proteins in regulated mRNA decay. *Wiley Interdiscip. Rev. RNA* **2011**, *2*, 42–57. [CrossRef]
59. Wu, X.; Chesoni, S.; Rondeau, G.; Tempesta, C.; Patel, R.; Charles, S.; Daginawala, N.; Zucconi, B.E.; Kishor, A.; Xu, G.; et al. Combinatorial mRNA binding by AUF1 and Argonaute 2 controls decay of selected target mRNAs. *Nucleic Acids Res.* **2013**, *41*, 2644–2658. [CrossRef]
60. Yoon, J.H.; Jo, M.H.; White, E.J.; De, S.; Hafner, M.; Zucconi, B.E.; Abdelmohsen, K.; Martindale, J.L.; Yang, X.; Wood, W.H., III; et al. AUF1 promotes let-7b loading on Argonaute 2. *Genes Dev.* **2015**, *29*, 1599–1604. [CrossRef]
61. Min, K.W.; Jo, M.H.; Shin, S.; Davila, S.; Zealy, R.W.; Kang, S.I.; Lloyd, L.T.; Hohng, S.; Yoon, J.H. AUF1 facilitates microRNA-mediated gene silencing. *Nucleic Acids Res.* **2017**, *45*, 6064–6073. [CrossRef]
62. Pfaffl, M.W. A new mathematical model for relative quantification in real-time RT-PCR. *Nucleic Acids Res.* **2001**, *29*, e45. [CrossRef]
63. Chi, S.W.; Zang, J.B.; Mele, A.; Darnell, R.B. Argonaute HITS-CLIP decodes microRNA-mRNA interaction maps. *Nature* **2009**, *460*, 479–486. [CrossRef]
64. Ule, J.; Jensen, K.; Mele, A.; Darnell, R.B. CLIP: A method for identifying protein-RNA interaction sites in living cells. *Methods* **2005**, *37*, 376–386. [CrossRef]
65. Shah, A.; Qian, Y.; Weyn-Vanhentenryck, S.M.; Zhang, C. CLIP Tool Kit (CTK): A flexible and robust pipeline to analyze CLIP sequencing data. *Bioinformatics* **2017**, *33*, 566–567. [CrossRef]
66. Li, H.; Durbin, R. Fast and accurate short read alignment with Burrows-Wheeler transform. *Bioinformatics* **2009**, *25*, 1754–1760. [CrossRef]
67. Zhang, Y.; Liu, T.; Meyer, C.A.; Eeckhoute, J.; Johnson, D.S.; Bernstein, B.E.; Nusbaum, C.; Myers, R.M.; Brown, M.; Li, W.; et al. Model-based analysis of ChIP-Seq (MACS). *Genome Biol.* **2008**, *9*, R137. [CrossRef]
68. Quinlan, A.R.; Hall, I.M. BEDTools: A flexible suite of utilities for comparing genomic features. *Bioinformatics* **2010**, *26*, 841–842. [CrossRef]
69. Thorvaldsdottir, H.; Robinson, J.T.; Mesirov, J.P. Integrative Genomics Viewer (IGV): High-performance genomics data visualization and exploration. *Brief. Bioinform.* **2013**, *14*, 178–192. [CrossRef]
70. Ma, W.; Noble, W.S.; Bailey, T.L. Motif-based analysis of large nucleotide data sets using MEME-ChIP. *Nat. Protoc.* **2014**, *9*, 1428–1450. [CrossRef]
71. Gilbert, C.; Kristjuhan, A.; Winkler, G.S.; Svejstrup, J.Q. Elongator interactions with nascent mRNA revealed by RNA immunoprecipitation. *Mol. Cell* **2004**, *14*, 457–464. [CrossRef]
72. Gilbert, C.; Svejstrup, J.Q. RNA immunoprecipitation for determining RNA-protein associations in vivo. *Curr. Protoc. Mol. Biol.* **2006**, *75*, 27.4.1–27.4.11. [CrossRef] [PubMed]
73. Selth, L.A.; Gilbert, C.; Svejstrup, J.Q. RNA immunoprecipitation to determine RNA-protein associations in vivo. *Cold Spring Harb. Protoc.* **2009**, *2009*, pdb-prot5234. [CrossRef]
74. Krishnan, M.; Singh, A.B.; Smith, J.J.; Sharma, A.; Chen, X.; Eschrich, S.; Yeatman, T.J.; Beauchamp, R.D.; Dhawan, P. HDAC inhibitors regulate claudin-1 expression in colon cancer cells through modulation of mRNA stability. *Oncogene* **2010**, *29*, 305–312. [CrossRef]